U.PORTO

INSTITUTO DE CIÊNCIAS BIOMÉDICAS ABEL SALAZAR
UNIVERSIDADE DO PORTO

U.PORTO

FACULDADE DE CIÊNCIAS
UNIVERSIDADE DO PORTO

MSc

2.º CICLO

FCUP
ICBAS
2020

U.PORTO

Development of new antibiotics for the current public health bacterial threats

Bárbara Raquel Soares Nunes

ICBAS

FC

U.PORTO

INSTITUTO DE CIÊNCIAS BIOMÉDICAS ABEL SALAZAR
UNIVERSIDADE DO PORTO

U.PORTO

FACULDADE DE CIÊNCIAS
UNIVERSIDADE DO PORTO

Development of new antibiotics for the current public health bacterial threats

Bárbara Raquel Soares Nunes

Master's thesis in Biochemistry presented to
Faculty of Sciences and
Abel Salazar's Institute of Biomedical Sciences
University of Porto

2020

Development of new antibiotics for the current public health bacterial threats

Bárbara Raquel Soares Nunes
Master's degree in Biochemistry
Faculty of Sciences and Abel Salazar's Institute of Biomedical Sciences
University of Porto
2020

Supervisor
Doctor Fernando Cagide-Fagín, Researcher
Faculty of Sciences of the University of Porto (FCUP)

Co-Supervisor
Doctor Ana Catarina Gomes Oliveira, Researcher
Faculty of Sciences of the University of Porto (FCUP)

U.PORTO

INSTITUTO DE CIÊNCIAS BIOMÉDICAS ABEL SALAZAR
UNIVERSIDADE DO PORTO

U.PORTO

FACULDADE DE CIÊNCIAS
UNIVERSIDADE DO PORTO

Todas as correções determinadas pelo júri, e só essas, foram efetuadas.

O Presidente do Júri,

Porto, _____/_____/_____

ACKNOWLEDGEMENTS

I would like to express my gratitude to all those that, knowingly or unknowingly, helped me in the successful completion of this Master's Thesis.

First of all, I would like to express my warm and sincerely gratitude to my supervisors, Dr. Fernando Cagide and Dr[a]. Catarina Oliveira, for their guidance and orientation through the development of this Thesis work. Their mentorship was exceedingly significant to my person as a scientist, in providing me a well-rounded experience in scientific research and stimulated me to grow as a critic biochemist and independent thinker. To Professor Fernanda Borges, I acknowledge for receiving me in her research group in Centre for Investigation in Chemistry (CIQUP), Faculty of Sciences of the University of Porto, where I had the opportunity to conduct an important part of my project.

To Professor Manuel Simões, thank you for receiving me in the Laboratory for Process Engineering, Environment, Biotechnology and Energy (LEPABE), Faculty of Engineering of the University of Porto, and for all the support shown during the length of this project. A special thank you to Diana Oliveira and Anabela Borges who kindly helped me whenever I needed. My appreciation also goes to the technicians from laboratory E-103, Carla and Sílvia, whose kindness and help were vital in several moments.

Moreover, I would like to express my gratitude to Professor Fernando Remião, for receiving me in the Toxicological Laboratory, Faculty of Pharmacy of the University of Porto, where I learned to work with cell culture. I wish to extend my warmest thanks to Dr. Carlos Fernandes, whose teaching and support were of huge importance to my project. I deeply appreciate all his efforts and availability in helping me and assisting me in the process.

To my lab colleagues, thank you for the good times shared and especially for the good mood and constant motivation over this year.

Finally, I want to acknowledge my parents, Paula and Eusébio, for the patience, support and encouragements at all times. To my brother, Gonçalo, I want to thank for his support and for his thoughtfulness towards my Thesis work period. To my great and good friends, Rita, João, Catarina and Ana, for their support and friendship that always make the most of everything. Also, I want to acknowledge Bruno, for his support and concern.

ABSTRACT

Nowadays, antibiotics are crucial to treat bacterial infections. However, bacterial resistance to commonly used antibiotics is actually one of the most relevant public health problems at global level, since it presents clinical and economic worrying consequences, and is associated with increase morbidity and mortality. To circumvent this issue, a quest for the development of new antimicrobial and therapeutic strategies has been widely recognized.

Due to their exclusive properties, ionic liquids (ILs) have attracted an increased academical and industrial attention in the last decades. The possibility of tailoring their properties for a specific task by selecting the appropriate cation, anion and substituent on the cationic constituent, makes these ionic compounds good candidates for a variety of applications. In this context, this Thesis focuses on the design and synthesis of a series of twenty-one alkyl cationic derivatives (ionic liquids) as potential antibiotics. The effects of these compounds in the control of planktonic bacterial growth of *Staphylococcus aureus* and in cytotoxicity in HK-2 and HepG2 human cell lines were studied, with the purpose of analysing the influence of the alkyl chain length and the type of cation head in their activity.

Alkyltriphenylphosphonium derivatives [C_nTPPBr] were found to be effective antimicrobial agents for *S. aureus* bacterium in planktonic state. Bacterial susceptibility to these triphenylphosphonium (TPP) derivatives was much superior to that observed for the other tested derivatives. The antimicrobial activity proved to be directly dependent on the lipophilicity, *i.e.*, on the length of the alkyl chain. Longer alkyl side chains showed superior results in inhibiting bacterial growth of *S. aureus*. All compounds decreased significantly the cell viability of HK-2 and HepG2 human cell lines. Based on its cytotoxicity/antimicrobial efficacy ratio, [C_{10}TPPBr] was proposed as a potential candidate for further lead optimization as antimicrobial agent, even though a noticeable *in vitro* cytotoxic effect on human cell lines was observed, a problem that limits its application for *in vivo* use.

***Keywords*:** bacterial infections, antibiotic resistance, antibiotics, ionic liquids, *Staphylococcus aureus*, antimicrobial activity, cytotoxicity

RESUMO

Os antibióticos são indispensáveis no tratamento de infeções bacterianas. No entanto, a resistência bacteriana aos antibióticos é atualmente um problemas sério de saúde pública, uma vez que é responsável por consequências clínicas e económicas graves, relacionadas com o aumento da morbilidade e mortalidade. Pelas razões apontadas, várias organizações nacionais e internacionais reconhecem a relevância do desenvolvimento de novos agentes antimicrobianos e estratégias terapêuticas para o controlo da resistência microbiana.

Nas últimas décadas, os líquidos iónicos (ILs) têm sido alvo de elevado interesse quer a nível académico quer a nível industrial. Esta magnitude deve-se em grande parte às suas propriedades físico-químicas únicas, assim como à possibilidade de, através de uma apropriada seleção do catião, anião ou substituinte do constituinte catiónico, ser possível ajustar as suas propriedades a uma dada aplicação. Neste contexto, esta Tese centra-se no desenho e síntese de uma série de vinte e um derivados alquil catiónicos, compostos por ILs, visando contribuir para o desenvolvimento de novos agentes antimicrobianos. Para tal, foram estudados os efeitos destes compostos no controlo do crescimento bacteriano de *Staphylococcus aureus* no estado planctónico, bem como o seu perfil de citotoxicidade em linhas celulares humanas HK-2 e HepG2, com o intuito de analisar a influência do comprimento da cadeia alquílica e do catião na atividade dos compostos.

Os derivados de alquil trifenilfosfónio [C_nTPPBr] revelaram ser eficazes como agentes antimicrobianos para a bactéria *S. aureus* no estado planctónico. A suscetibilidade bacteriana a estes derivados de trifenilfosfónio (TPP) foi superior à observada para os outros derivados testados. A atividade antimicrobiana foi diretamente dependente da lipofilicidade dos compostos, isto é, do comprimento da cadeia alquílica. Compostos com cadeias alquilo mais longas apresentaram melhores resultados na inibição do crescimento bacteriano de *S. aureus*. Porém todos os compostos mostraram efeitos tóxicos significativos em células humanas HK-2 e HepG2, em todas as concentrações testadas. Tendo como base o rácio citotoxicidade/eficácia antimicrobiana, propõe-se o composto [C_{10}TPPBr] como um candidato válido para a futura otimização e desenvolvimento de agentes antimicrobianos, e desta forma modelar o seu efeito tóxico em linhas celulares humanas *in vitro*, permitindo o seu possível uso *in vivo*.

***Palavras-chave*:** infeções bacterianas, resistência aos antibióticos, antibióticos, líquidos iónicos, *Staphylococcus aureus*, atividade antimicrobiana, citotoxicidade

THESIS ORGANIZATION

The development of this Master's Thesis was a collaborative process between three academic institutions of the University of Porto: CIQUP, Faculty of Sciences; LEPABE, Faculty of Engineering; and UCIBIO-REQUIMTE, Laboratory of Toxicology, Faculty of Pharmacy. This Thesis is organized in four chapters comprised by: Introduction (Chapter 1), Experimental Part (Chapter 2), Results and Discussion (Chapter 3), Concluding remarks and Future Perspectives (Chapter 4). A brief introduction to each chapter is made in Figure 1.

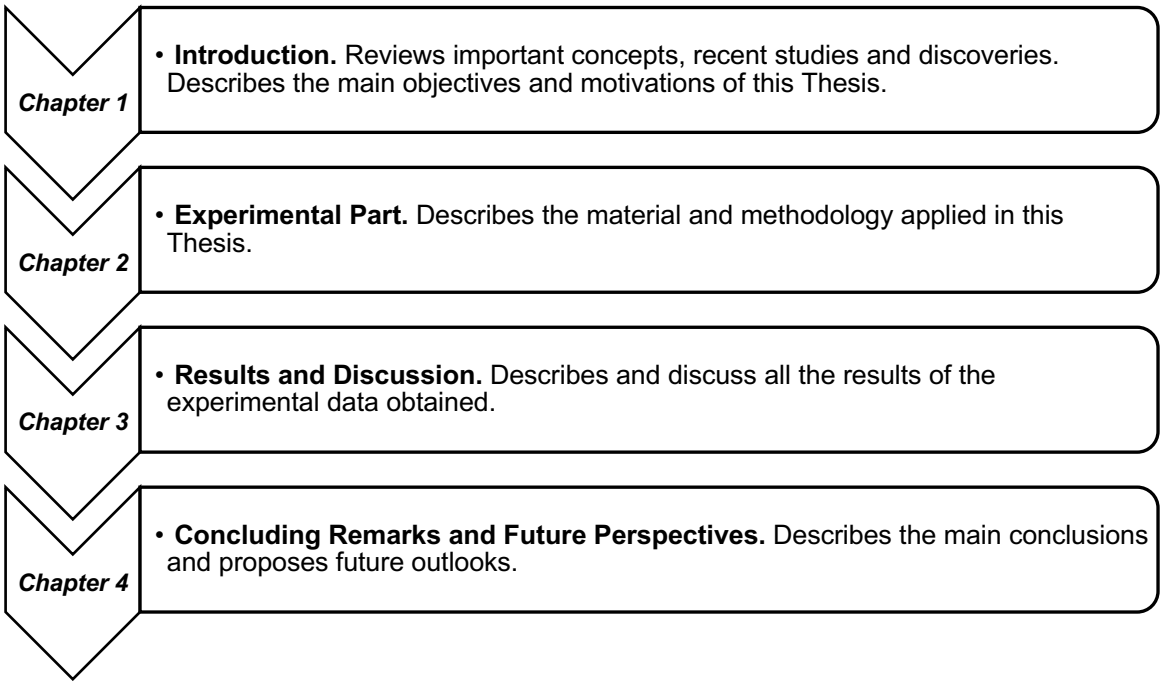

Figure 1. Schematic model of organization of this Thesis according to each chapter.

Chapter 1 deals with antibiotic resistance describing the current situation, the urgent need for new treatments and reiterating the priority of this problematic for research and development. It includes a literature review of antibiotics recently approved by FDA, in particular against *Staphylococcus aureus*. It also encloses the significance of ionic liquids for the design and development of new agents and the synthetic strategy followed to obtain these compounds. Finally, the main objectives to be achieved are also outlined.

In *Chapter 2*, the materials and methods used to perform all the experimental work are described, along with important observations necessary for their preparation. The experimental part is subdivided into three sections: Chemical, Microbiological, and Human cell Studies. In *Chapter 3*, the results are showed, analysed and discussed. The

organization of this chapter is done with the same logic sequence comprised by these three sections.

Finally, *Chapter 4* presents an overview of all the developed work, with a compilation of the leading conclusions withdrawn from this Thesis. Perspectives and suggestions for further research are also identified and described.

TABLE OF CONTENTS

LIST OF FIGURES

LIST OF TABLES

LIST OF ABBREVIATIONS AND SYMBOLS

Abbreviations

ABSSSI	Acute bacterial skin and skin structure infection
ACN	Acetonitrile
AME	Aminoglycoside-modifying enzymes
APIs	Active pharmaceutical ingredients
BLI	*β*-lactamase inhibitor
CA-MRSA	Community-acquired MRSA
CAP	Community-acquired pneumonia
CDAD	*Clostridioides difficile*-associated disease
CE	Clinical evaluable
CFU	Colony forming unit
cIAI	complicated intra-abdominal infection
CLSI	Clinical and laboratory standards institute
CRAB	Carbapenem-resistant *Acinetobacter baumannii*
CRE	Carbapenem-resistant *Enterobacteriaceae*
CRPA	Carbapenem-resistant *Pseudomonas aeruginosa*
cSSSI	complicated skin and skin structure infection
cUTI	complicated urinary tract infection
DBO	Diazabicyclooctane
DCF	2',7'-Dichlorofluorescein
DCFH	Dichlorodihydrofluorescein
DCFH-DA	2′,7′-Dichlorofluorescin diacetate
DEPT	Distortionless enhancement by polarization transfer
DMEM	Dulbecco's modified eagle's medium
DMSO	Dimethylsulfoxide
DNA	Deoxyribonucleic acid
e.g.	*Exempli gratia* from Latin, which means "for example"
EMA	European medicines agency
EOT	End of treatment
ESBL	Extended-spectrum *β*-lactamase

EtOAc	Ethyl acetate
EUCAST	European committee on antimicrobial susceptibility testing
FBS	Fetal bovine serum
FDA	Food and drug Administration
HA-MRSA	Healthcare-associated *Staphylococcus aureus*
HAP	Hospital-acquired pneumonia
HBSS	Hank's balanced salt solution
i.e.	*Id est* from Latin, which means “in other words”
ILs	Ionic liquids
ITT	Intent-to-treat
IV	Intravenous
KPC	*Klebsiella pneumoniae* carbapenemase
LA-MRSA	Livestock-associated MRSA
LPS	Lipopolysaccharide
MAA	Marketing authorization application
MBC	Minimum bactericidal concentration
MBL	Metallo-*β*-lactamase
MDR	Multidrug-resistant
ME	Microbiologically evaluable
MeOH	Methanol
MHB	Muller-hinton broth
MIC	Minimum inhibitory concentration
MITT	Modified intent-to-treat
MRSA	Methicillin-resistant *Staphylococcus aureus*
MSSA	Methicillin-sensitive *Staphylococcus aureus*
MTT	3-(4,5-dimethylthiazol-2-yl)-2,5-diphenyltetrazolium bromide
NDA	New drug application
NDMs	New Delhi metallo- *β*-lactamases
NMR	Nuclear magnetic resonance
NR	Neutral red
OD	Optical density
OXA	Oxacillinase
PBP	Penicillin-binding protein
PCA	Plate count agar

PO	Per oral
R&D	Research and development
RNS	Reactive nitrogen species
ROS	Reactive oxygen species
RS	Reactive species
SCC*mec*	Staphylococcal cassette chromosome *mec*
SD	Standard deviation
SRB	Sulforhodamine B
TLC	Thin-layer chromatography
TMS	Tetramethylsilane
TOC	Test-of-cure
URTI	Upper respiratory tract infection
UTI	Urinary tract infection
uUTI	Uncomplicated urinary tract infection
VAP	Ventilator-associated pneumonia
VISA	Vancomycin-intermediate *Staphylococcus aureus*
VRSA	Vancomycin-resistant *Staphylococcus aureus*
WHO	World health organization
XDR	Extremely drug resistant

Codes of synthesized ionic liquids

[C_6TPPBr]	Hexyltriphenylphosphonium bromide
[C_8TPPBr]	Octyltriphenylphosphonium bromide
[C_{10}TPPBr]	Decyltriphenylphosphonium bromide
[C_6mimBr]	3-Hexyl-1-methyl-1H-imidazol-3-ium bromide
[C_8mimBr]	1-Methyl-3-octyl-1H-imidazol-3-ium bromide
[C_{10}mimBr]	3-Decyl-1-methyl-1H-imidazol-3-ium bromide
[C_6IQBr]	2-Hexylisoquinolin-2-ium bromide
[C_8IQBr]	2-Octylisoquinolin-2-ium bromide
[C_{10}IQBr]	2-Decylisoquinolin-2-ium bromide
[C_6mPyrBr]	1-Hexyl-4-methylpyridin-1-ium bromide
[C_8mPyBr]	4-Methyl-1-octylpyridin-1-ium bromide
[C_{10}mPyrBr]	1-Decyl-4-methylpyridin-1-ium bromide

[C_6QBr]	1-Hexylquinolin-1-ium bromide
[C_8QBr]	1-Octylquinolin-1-ium bromide
[C_{10}QBr]	1-Decylquinolin-1-ium bromide
[C_6PyrBr]	1-Hexylpyridin-1-ium bromide
[C_8PyrBr]	1-Octylpyridin-1-ium bromide
[C_{10}PyrBr]	1-Decylpyridin-1-ium bromide
[C_6TEABr]	*N,N,N*-Triethylhexan-1-aminium bromide
[C_8TEABr]	*N,N,N*-Triethyloctan-1-aminium bromide
[C_{10}TEABr]	*N,N,N*-Triethyldecan-1-aminium bromide

Codes of bacteria

C. difficile	*Clostridium difficile*
E. faecalis	*Enterococcus faecalis*
E. coli	*Escherichia coli*
H. pylori	*Helicobacter pylori*
P. aeruginosa	*Pseudomonas aeruginosa*
P. fluorescens	*Pseudomonas fluorescens*
S. aureus	*Staphylococcus aureus*
S. epidermidis	*Staphylococcus epidermidis*
S. agalactiae	*Streptococcus agalactiae*
S. pneumoniae	*Streptococcus pneumoniae*
S. pyogenes	*Streptococcus pyogenes*

Symbols

λ	Detection wavelength
η	Yield
Hz	Hertz
Eq	Equivalent
δ	Chemical shift
J	Coupling constant
s	Singlet
bs	Broad singlet

d	Doublet
dd	Doublet of doublets
ddd	Doublet of doublet of doublets
t	Triplet
q	Quartet
m	Multiplet

Chapter 1

INTRODUCTION

This Chapter provides a review of subjects that are relevant for the Thesis project. First, the current concern about the emergence of multidrug-resistant (MDR) pathogens accompanied by the lack of effective therapeutic solutions is analysed. It includes a literature review of antibiotics recently approved by FDA, in particular against *Staphylococcus aureus*. Further, an insight of interesting properties of ionic liquids, as new scaffolds for the development of antimicrobial agents, including their highly tuneable nature is made. Several studies on the antimicrobial and cytotoxic properties of ionic liquids are mentioned, in a view of possible application as therapeutic agents. As some trends have been established to rule out the biological role against microorganisms and cytotoxicity of these compounds they are discussed in this chapter. A special emphasis will be given to the synthetic routes often used to obtain this type of compounds. In addition, the main Thesis objectives to be achieved are also outlined.

1.1. Antibiotics – historical overview

The discovery of antibiotics was a milestone in human history, since up to the early 1900's, infectious diseases were the leading cause of human mortality worldwide [1–3]. The discovery of penicillin in 1928 by Alexander Fleming, followed by the synthesis of the first sulfonamide "Prontosil" by Gerhard Domagk sparked a new era in the treatment of infectious diseases and paved away the modern medicine [2,3].

The term "antibiotic" was introduced by Selman Waksman, in 1941, as any small molecule, produced by a microorganism, that in dilute concentrations either effectively inhibit the growth of or effectively kill other microorganisms [4,5]. Nowadays, the term antibiotic is used more broadly to include any antimicrobial compound, either of natural or synthetic origin [6].

The majority of the antibiotics classes currently used as medicines were identified between the 1940's and 1960's (Figure 2), characterised as the golden era of the antibiotics drug discovery [4]. During this period, there was a continuing expansion of the antimicrobial arsenal. Alexander Fleming and Gerhard Domagk's work was followed by many pioneering scientists. Particularly, the work of Selman Waksman, for novel and systematic methodologies in antibiotic discovery and whom was accredited for the discovery of streptomycin, the first effective treatment for tuberculosis. After this discovery, Waksman was awarded the Nobel Prize and was heralded as "Father of Antibiotics" [7,8].

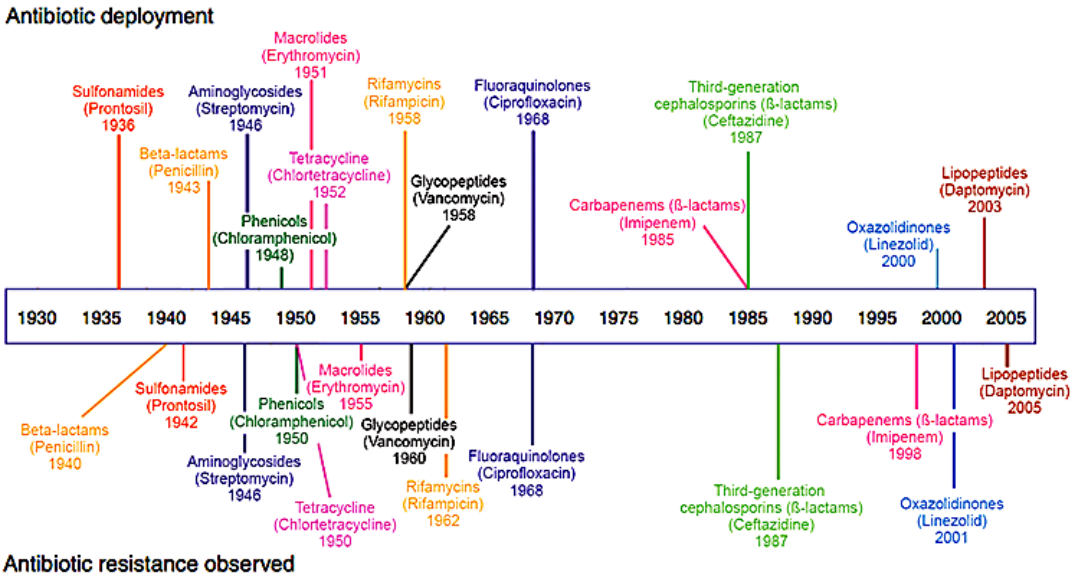

Figure 2. Timeline of antibiotic introduction in the clinical practice (top) and the emergence of antibiotic resistance (bottom) (Adapted from [9]).

During the 20th century, deaths from infectious diseases declined rapidly throughout the developed world [10]. With antibiotics covering some of history's most important human pathogens – *e.g.*, cholera, tuberculosis or malaria, many leaders in public health were confident that they were witnessing the end of infectious diseases as a major health threat [10–12]. For instance, in 1969, the US surgeon general, William Stewart, told Congress that it was time "to close the book on infectious diseases" [12]. This statement clearly illustrates the common assumption at the time, that infectious diseases would pose a problem no more. Without the work contribution of these pioneering microbiologists and their colleagues, modern medicine could not have developed to the point of today. Several medical procedures depend on the availability of effective antibiotic drugs – *e.g.*, organ transplantation, chemotherapy for cancer treatment, hip replacement surgery and many other activities [13]. Without effective antibiotics, clinical medicine, as we know it, could be compromised [2,8].

1.2. Antibiotic resistance

As soon as new antibiotics were discovered, a new problem was raised with the development and dissemination of resistance starting to be observed for all of them (Figure 2. bottom) [3,14]. In fact, it was reported that the resistance to penicillin even preceded their introduction into clinical use, due to emergence of penicillinase enzyme, which hydrolysis the antibiotic and makes it ineffective [15,16]. This could be the first warning towards eminent antibiotic resistance, that has culminated in one of the greatest threats to public health today, recognized by every international health organizations [2,3,17,18].

As of today, human pathogens have developed varied resistance mechanisms to practically all of the available medicines on the pharmaceutical market [19]. The impact of such resistances on treatment of infectious diseases is wide considering that available antibiotics therapies are now losing their effectiveness [20–23]. This global crisis can in part be attributed to the indiscriminate and uncontrolled overuse of antibiotics, in both clinical and non-clinical settings, as well as the antibiotic selective pressure [20,21,24]. Indeed, throughout evolution, the microorganisms have accumulated a huge diversity of remarkable mechanisms that can be mobilized in response to external aggression, including the presence of antibiotics that may jeopardize their existence [3,24]. Bacteria sharing the same environmental niche with antimicrobial-producing organisms have developed mechanisms to counteract the effect of antibiotic exposure, and consequently, their intrinsic resistance enables them to thrive in its presence [3,23,25].

Meanwhile, bacteria use two major genetic strategies to withstand the effect of the antibiotic: *(i)* acquisition of specific resistance mechanisms through horizontal gene transfer; and *(ii)* mutations in gene(s) often associated with the mechanism of action of the compound [2,25].

1.2.1. Horizontal gene transfer

Bacteria have a unprecedent ability to acquire new genetic material either as addition to their genomes or in the form of extrachromosomal genetic material such as *via* horizontal gene transfer (*e.g.*, plasmids). The ability of bacteria to adapt to new environments as a part of bacterial evolution most frequently results from the acquisition of new genetic material through horizontal gene transfer rather than by mutational resistance. This acquisition is accommodated through three main strategies, *(i)* transformation (incorporation of naked deoxyribonucleic acid (DNA) from the environment), *(ii)* transduction (phage mediated) or *(iii)* conjugation (transfer of DNA or plasmids between bacteria) [Figure 3] [2,3,25]. A crucial role in these processes is that acquired material can be added on the chromosome or plasmids *via* either integrons or transposons [26]. In addition, the acquired genetic material can be transmitted by horizontal transfer to other strains and species, but also vertically to the daughter cells [27].

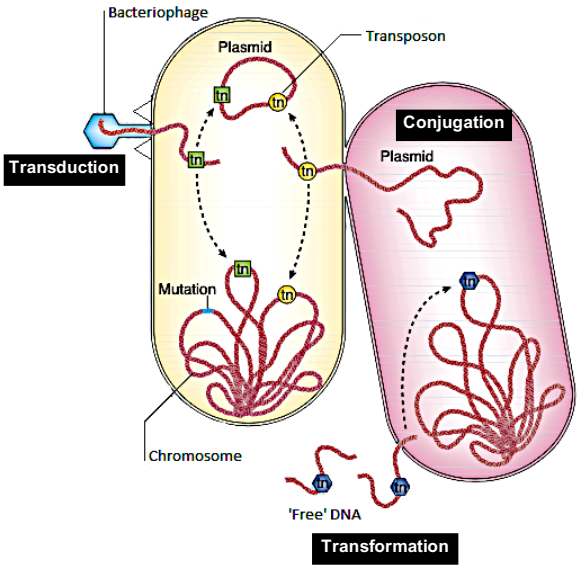

Figure 3. Schematic model illustrating the three main strategies through bacteria acquire external genetic material: phage transduction, transformation (uptake of DNA from environment) or conjugation (plasmid transfer from one species to another) (Adapted from [27]).

1.2.2. Mutational resistance

In this scenario, a subset of bacterial cells derived from a susceptible population develop mutations in genes that affect the activity of the antibiotic (Figure 4A). In the absence of antibiotics, the mutant cells will only exist as a tiny proportion of the bacterial population. However, in the presence of antibiotics, all bacterial cells except for the antibiotic-resistant mutants will be killed (Figure 4B). In this context, the antibiotic-resistant mutations are a powerful adaptative mechanism, which confer the antibiotic-resistant cells the ability to grow and multiply. Over time, such genotypes will become continually more prevalent throughout the bacterial population (Figure 4C) [25,28].

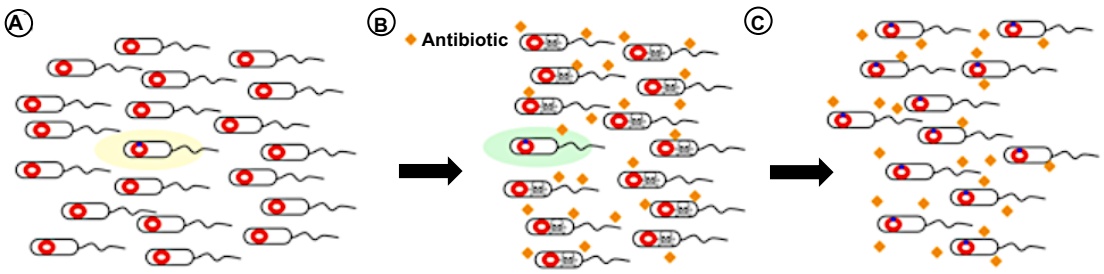

Figure 4. Schematic model illustrating the bacterial antibiotic mutational resistance acquisition mechanism (Adapted from [28]).

Generally, mutations result in antimicrobial resistance altering the antibiotic action *via* one of the following mechanisms: (i) modification of the antibiotic target site (reduced binding affinity); (ii) decreased uptake of the antibiotic into the cell; (iii) induced the overexpression of efflux pumps to actively pump the antibiotic out of the cell; or (iv) global changes in important metabolic pathways *via* modulation of regulatory networks [25]. Mutational changes are responsible for acquired resistance in certain bacterial species, such as *Helicobacter pylori* and *Mycobacterium tuberculosis*, or for particular antibiotics, especially for the synthetic agents such as fluoroquinolones and oxazolidinones [28,29].

1.3. Multidrug-resistance: a global public health crisis and security threat

Resistance development in so many human pathogens has been an unprecedented global problem, as resistance has evolved into multidrug resistance [3,22,24]. This has led to substantially increased the burden of both community-acquired and hospital-associated infections, raising the prospect of a post-antibiotic era [3,30]. A recent evaluation of this

crisis has estimated that, by 2050, 10 million people will die every year due to multidrug-resistance (MDR), leading to an economic loss of about US$ 100 trillion, if nothing is done to reverse the trend [2,31,32].

Within this context, in 2017, the World Health Organization (WHO) published a list of global priority pathogens – 12 species of bacteria with critical, high, and medium antibiotic-resistance – to help in prioritizing the research and development (R&D) of new and effective antibiotic treatments [22,33]. Table 1 shows the bacteria included for prioritization and the most alarming resistances they represent.

Table 1. World Health Organization (WHO) priority pathogens list for R&D of new antibiotics (Adapted from [33]).

Priority category	Pathogens	Antibiotic resistance
Critical	*Acinetobacter baumannii*	Carbapenem-resistant
	Pseudomonas aeroginosa	Carbapenem-resistant
	Enterobacteriaceae	Carbapenem-resistant
		Third generation cephalosporin-resistant
High	*Enterococcus faecium*	Vancomycin-resistant
	Staphylococcus aureus	Methicillin-resistant
		Vancomycin-resistant intermediate and resistant
	Helicobacter pylori	Clarithromycin-resistant
	Campylobacter	Fluoroquinolone-resistant
	Salmonella spp.	Fluoroquinolone-resistant
	Neisseria gonorrhoeae	Third generation cephalosporin-resistant
Medium	*Streptococcus pneumoniae*	Penicillin-non-susceptible
	Haemophilus influenzae	Ampicillin-resistant
	Shigella spp.	Fluoroquinolone-resistant

The most critical group includes MDR bacteria – *Acinetobacter*, *Pseudomonas* and various *Enterobacteriaceae* – that pose a particular threat in healthcare settings, and among patients whose care requires devices like ventilators and intravenous catheters [34]. These bacteria have the highest resistance rates to both carbapenems and third generation cephalosporin, which is the best available treatment [3].

In addition, based on the severity of the hazard, the WHO also listed *Staphylococcus aureus* as a “high priority” surveillance object (See Table 1), being an increasingly drug resistant bacteria. Therefore, in this Thesis project, the pathogen was chosen for the microbiological studies, as it is a globally established priority for which innovative new treatments are urgently needed.

1.3.1. Multidrug-resistant (MDR) *Staphylococcus aureus*

Staphylococcus aureus (*S. aureus*) is a Gram-positive bacterium and the causative agent of mainly skin and soft tissue infections, as well as invasive infections such as bacteremia, pneumonia and necrotizing fasciitis [14,35–37]. This bacterium has a double-faced lifestyle: on one hand, behaves as a harmless colonizer, and on the other hand is a potentially lethal opportunistic pathogen and an ultimately a leading cause of infectious worldwide [38]. Studies showed that about 30 % of the human population is asymptomatically colonized with *S. aureus* on either a transient or persistent basis [39,40].

Prior to the introduction of penicillin, the mortality rate associated to *S. aureus* infections was above 80 % [41]. The discovery of penicillin led to its widespread use against *S. aureus*, but by the mid-1940s penicillin resistance through plasmid borne penicillinase was widespread [42,43]. Penicillinase act by hydrolysing the amide bond present in the β-lactam ring of penicillin, rendering the antibiotic ineffective (Figure 5A). Reacting to the resistance trends, the semisynthetic penicillin (methicillin), resistant to enzymatic degradation, was marketed in 1959 [42,43]. Methicillin is resistant to cleavage by *S. aureus* penicillinase due to the presence of an orthodimethoxyphenyl side group, which prevents the enzyme access to its target amide bond by steric hindrance (Figure 5B) [44].

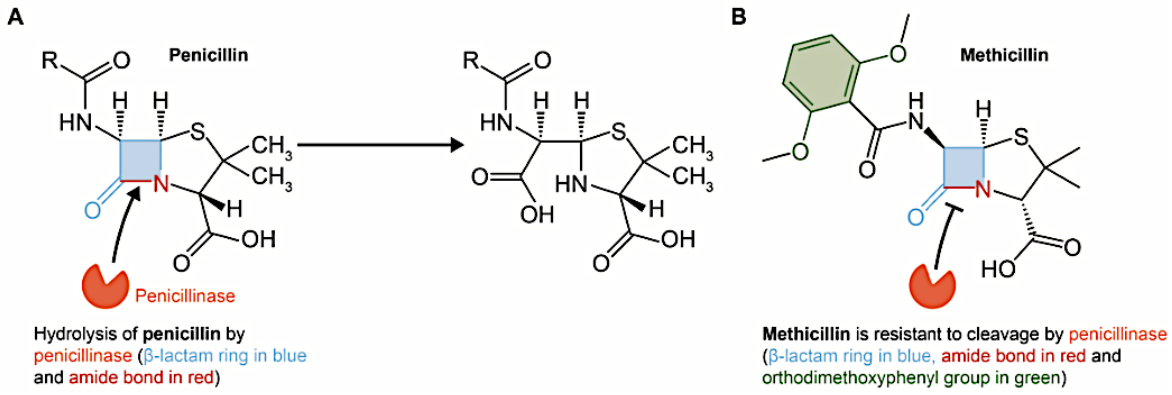

Figure 5. Penicillinase hydrolysis the amide bond of the β-lactam ring of penicillin, rendering the β-lactam antibiotic inactive **(A)**. Methicillin is resistant to cleavage by *S. aureus* penicillinase due to the presence of an orthodimethoxyphenyl side group, which prevents the enzyme access to its target amide bond by steric hindrance **(B)** (Adapted from [44]).

By 1961 methicillin-resistant *S. aureus* (MRSA) had been described in the United Kingdom [39,42,43,45,46]. Over the next few decades, increasing number of MRSA outbreaks were reported in different parts of the world [47]. Currently, MRSA accounts for a large prevalence of healthcare-associated *S. aureus* (HA-MRSA) and is associated with significant morbidity and mortality [48]. The recent occurrence of community-acquired MRSA (CA-MRSA) further

underscored *S. aureus* as a serious infectious disease threat. Remarkably, CA-MRSA is capable of causing infections in healthy individuals outside of healthcare settings [49]. More recently, livestock-associated MRSA (LA-MRSA), specifically sequence type (ST) 398, has emerged, mainly in individuals in contact with animals, in France and the Netherlands [50–52].

The methicillin resistance is related with the presence of an altered penicillin-binding protein (PBP), called PBP2a, with a decreased affinity to virtually all beta-lactams antibiotics [50,53–57]. In the presence of beta-lactams, transpeptidase domain of the four native PBPs (PBP1-4) of *S. aureus* is inactivated, and the PBP2a, a peptidoglycan transpeptidase, in cooperation with the transglycosylase domain of PBP2, catalysis the cell wall biosynthesis reactions (Figure 6) [37,55,58].

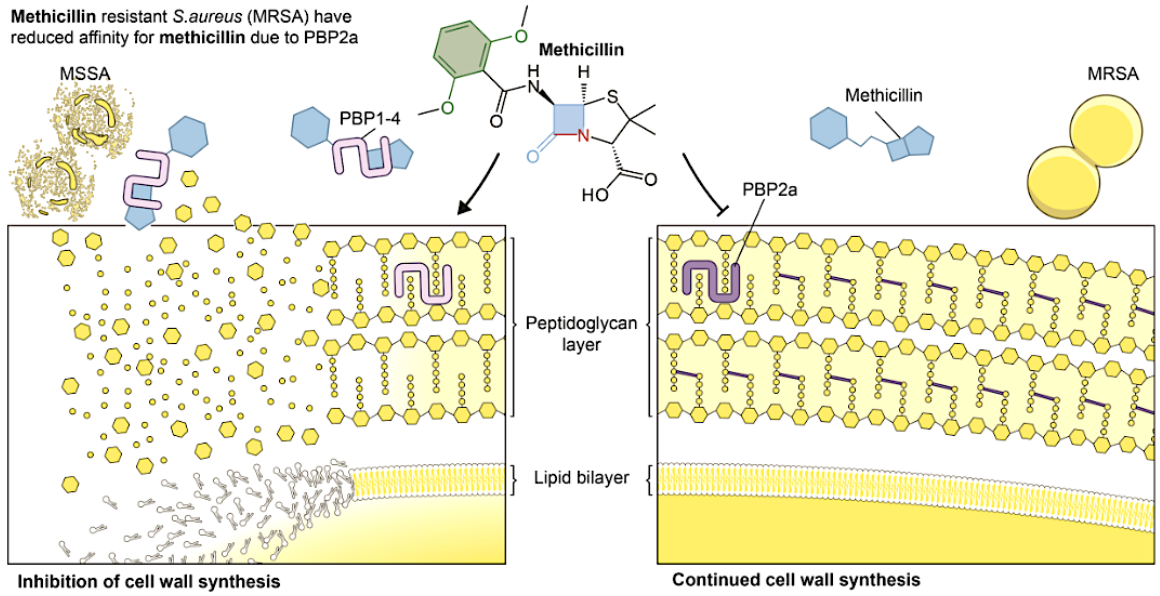

Figure 6. Methicillin-susceptible *S. aureus* (MSSA) (left) contains penicillin binding proteins 1-4 (PBP1-4) that are promptly bound by methicillin, a process that inhibits peptidoglycan and cell wall synthesis. *S. aureus* methicillin resistance is conferred by penicillin-binding protein 2a (PBP2a), which has a lower affinity for methicillin (right). Therefore, PBP2a can still crosslink peptidoglycan when *S. aureus* native PBPs are inhibited (Adapted from [44]).

PBP2a is encoded by the *mecA* gene, which is carried by a mobile genetic element named staphylococcal cassette chromosome *mec* (SCC*mec*) [36,50,54]. Till date, eleven SCC*mec* types (I-XI) have been described [59]. In 2007, a *mecA* homologue (*mecC*) was described in a *S. aureus* strain of animal origin (LGA251). This *mecA* homologue showing around 70 % nucleotide sequence homology with the classical *S. aureus mecA* gene, confers lower levels of resistance to methicillin than *mecA* [60]. Following 2010, several studies have

reported the presence of this gene in different *S. aureus* genetic backgrounds on both human and animal origin.

Treatment of MRSA infections usually include treatment with glycopeptide antibiotics (vancomycin) and oxazolidinones such as linezolid [8]. In particular, vancomycin has been considered the gold standard antimicrobial for the treatment of serious MRSA infections. However, the occurrence of vancomycin-intermediate resistance (VISA) and vancomycin-resistant (VRSA) in *S. aureus* has been reported within the past two decades [61]. The first VISA was identified in Japan in 1996, and several other strains were described afterwards in the USA, India, China and also in Portugal [14,38,57,62]. However, a fully resistant strain of *S. aureus* to vancomycin was firstly reported only in 2002 from Michigan, USA [14,38,57,63]. Since that time, a total of 52 VRSA isolates have been reported, namely in the USA (n=14), India (n=16), Iran (n=11), Pakistan (n=9), Brazil (n=1) and Portugal (n=1) [57].

Phenotypically, VISA strains all share common features: (i) increased cell wall thickness that prevents the access of vancomycin to its target; (ii) reduced autolytic activity; (iii) attenuated virulence allowing immune escape and long persistence [14,57,62,64–66]. While the phenotype of VISA strains is fairly consistent, their genetic characteristics have not been fully identified [62,64]. Recent advances in understanding the mechanisms underlying progression of vancomycin resistance in VISA reveal that mutations in genes encoding two-component systems (TCSs) such as vraSR, graSR and walKR, coupled with RNA polymerase β subunit (RpoB) mutation translate are strongly associated with a VISA phenotype [14,57,62,64,65]. However, additional studies are essential to clarify this association considering that only a small number of mutations in several genes have been experimentally examined [57,64].

The VRSA is predominantly mediated by horizontal gene transfer of the vanA gene cluster (Figure 7). Furthermore, the vanA cluster is often located on the Tn1546 transposon element, which was acquired from vancomycin resistant *Enterococcus* species (VRE) [14,57,63,67,68]. The vanA gene cluster encodes an epitope substitution of the D-alanyl-D-alanine dipeptide residue in the *S. aureus* cell wall precursor Lipid-II to D-alanyl-D-lactate, which drastically reduces the affinity of vancomycin for the cell wall precursor [14,57,63,67–69]. Induction of the vanA gene cluster is regulated by the VanS/VanR two-component system in response to extracellular glycopeptide [14,57,63,67,69]. Vancomycin bound to D-Ala-D-Ala termini is perceived by VanS sensor kinase, which phosphorylates the VanR

response regulator, which in turn induces the expression of the vanHAX genes responsible for the D-Ala-D-Lac dipeptide substitution [14,63,67,69].

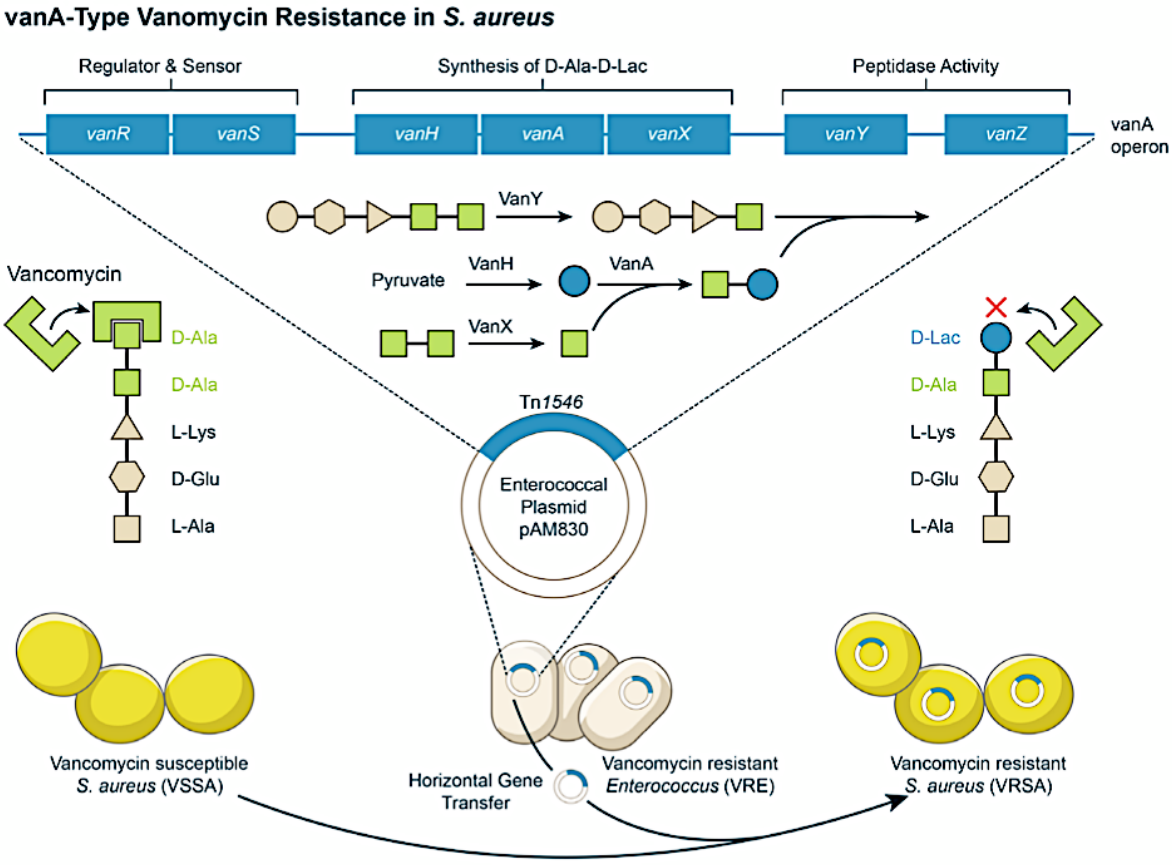

Figure 7. Schematic model illustrating the acquisition and molecular mechanism of vanA-type in VRSA strains (Adapted from [14]).

1.3.2. Antibiotics launched since 2017

The continuous rise and dissemination of resistant isolates is one emergent challenge in which the current drug discovery and development programs do not provide the needed solutions. In fact, recently WHO reports showed a serious lack of new antibacterial drugs and that more interventions are needed. Since 2017, eight new antibiotics have been approved, including one for treatment of tuberculosis (TB). Half of these are targeted to at least one of the “critical” priority pathogens and the other half are targeted to “high” and “medium” priority pathogens following the WHO priority pathogens list [70]. A general overview of these antibiotics can be seen in Table 2.

Table 2. Antibacterial agents that have been approved since 2017 by the FDA or EMA (modified according to the WHO report [70]).

Name	Approval Time	Antibiotic class	Company	Spectrum against Organisms	Indication	Administration
Delafloxacin	FDA (6/2017 ABSSSI, 10/2019 CAP) MAA	Fluoroquinolone	Melinta	MRSA, penicillin-sensitive, penicillin-resistant, and levofloxacin-resistant *S. pneumoniae*, *Streptococcus pyogenes* and enterococci. Gram-negative pathogens including quinolone-susceptible *P. aeruginosa*. Anaerobes [71]	ABSSSI, CAP	IV: 300 mg q12 h PO: 450 mg q12 h [71]
Vaborbactam + meropenem	FDA (8/2017) EMA (11/2018)	Boronate BLI + carbapenem	Melinta	Gram-negatives, including ESBL, KPC. No activity against MBL and OXA [71]	cUTI	IV: 2 g/2 g q8h [71]
Plazomicin	FDA (8/2018)	Aminoglycoside	Achaogen	Gram-positives (including MRSA) and Gram-negatives, including ESBL, CRE (most KPCs, OXA; no NDMs), MDR *Pseudomonas*, MDR *Acinetobacter*, and aminoglycosides resistant isolates [71]	cUTI	IV: 15 mg/kg q24h [71]
Eravacycline	FDA (8/2018) EMA (9/2018)	Tetracycline	Tetraphase	MRSA, *Enterococci* (including vancomycin-resistant) and *Enterobacteriaceae* expressing ESBL, KPC and OXA [71]	cIAI	IV: 1 mg/kg q12h [71]
Omadacycline	FDA (10/2018)	Tetracycline	Paratek	Gram-positive aerobes (including methicillin-resistant and penicillin-resistant strains), Gram-negative aerobes, anaerobes, and atypical bacterial pathogens [71]	CAP (IV), ABSSSI (IV, PO)	IV: 100 mg q12h for 2 doses, followed by 100 mg q24h PO: 300 mg q24 h [71]
Relebactam + imipenem/cilastatin	FDA (7/2019)	DBO-BLI + carbapenem/ degradation inhibitor	MSD	Gram-negatives, including AmpC, ESBL, KPC. No activity against MBL and OXA [71]	cUTI, cIAI	IV: 500 mg/250-125 mg q6h [71]
Lefamulin	FDA (8/2019)	Pleuromutilin	Nabriva	Gram-positive and atypical organisms, including MRSA and vancomycin-resistant *Enterococci* [71]	CAP	IV: 150 mg q12h PO: 600 mg q12h [71]
Pretomanid	FDA (8/2019)	Nitroimidazole	TB Alliance	*Mycobacterium tuberculosis*	XDR TB	PO: 200 mg q24h for 26 weeks [1] [72]

Abbreviations: ABSSSI (acute bacterial skin and skin structure infection), BLI (β-lactamase inhibitor), CAP (community-acquired pneumonia), cIAI (complicated intra-abdominal infection), CRE (carbapenem-resistant *Enterobacteriaceae*), cUTI (complicated urinary tract infection), DBO (diazabicyclooctane), EMA (European Medicines Agency), ESBL (extended-spectrum β-lactamase), FDA (Food and Drug Administration), KPC (*Klebsiella pneumoniae* carbapenemase), IV (intravenous), MBL (metallo-β-llactamase), MDR (multidrug-resistant), NDMs (New Delhi metallo- β-lactamases), OXA (oxacillinase), PO (oral), XDR (extremely drug resistant).

Bacteria abbreviations: MRSA (methicillin-resistant *Staphylococcus aureus*, *S. pneumoniae* (*Streptococcus pneumoniae*).

The bold names denote novel antibiotics for MDR *S. aureus*.

[1] Pretomanid tablets must be administered only as part of a regimen in combination with bedaquiline and linezolid.

In accordance with the goals of the Thesis project, a more detailed insight into the novel portfolio of drugs depicted in Table 2 with activity against MDR *S. aureus* will be provided. It includes a brief presentation of microbiological data and/or clinical data for each of the compounds including official information published by PubMed, Google Scholar, and the site of ClinicalTrials.gov.

Delafloxacin (Baxdela™, Table 2, Figure 8) is a recently approved fluoroquinolone with broad-spectrum against Gram-positive and Gram-negative organisms [73–78]. Its unique chemical properties (anion at physiological pH, uncharged at acidic pH) appear to be correlated with its enhance of potency in acidic environments, which are characteristic of sites of infection, and thus could be a benefit when treating infections [74,76,77,79,80]. In a phase II trial in 2008, comparing the efficacy and tolerability of delafloxacin *vs*. tigecycline in patients with complicated skin and skin-structure infections (cSSSIs), delafloxacin achieved similarly efficacy rates than tigecycline [77]. In another phase II trial in 2011, the clinical efficacy of delafloxacin was compared to linezolid and vancomycin in patients who had acute bacterial skin and skin structure infections (ABSSSIs) [77]. With complete resolution of signs and symptoms as the primary endpoint, delafloxacin demonstrated similar response compared with linezolid and greater cure rates compared with vancomycin in the treatment of ABSSSI [76,77]. [77]. Delafloxacin is highly active against *S. aureus* and exhibits a low probability for the selection of resistant mutants in MRSA (10^{-9}-10^{-11}) [75,77,79]. It demonstrates potent activity against MRSA although MICs are higher (MIC_{50}, 0.25 μg/mL) for fluoroquinolone-resistant isolates compared with fluoroquinolone-susceptible isolates (MIC_{50}, 0.004 μg/mL) [73,74,77–79]. It is also active against *S. aureus* biofilms [73,74,77].

Plazomicin (Zemdri™, Table 2, Figure 8) is a semisynthetic aminoglycoside derived from sisomicin [78,81,82]. It has been structurally modified to prevent inactivation by aminoglycoside-modifying enzymes (AME), which represent the main mechanism of aminoglycoside resistance in *S. aureus*, regardless of the methicillin-resistance phenotype and in MDR Gram-negatives [78,81,82]. Currently plazomicin is indicated for the treatment of complicated urinary tract infections (cUTIs) caused by extended spectrum β-lactamase (ESBL)-producing *Enterobacteriaceae* and carbapenem-resistant *Enterobacteriaceae* (CRE) with limited treatment options [78,81,82]. The role of plazomicin for MDR *S. aureus* infections was mainly based on *in vitro* studies [82]. Plazomicin displays a good *in vitro* activity against *S. aureus* (both MRSA and MSSA strains) and coagulase-negative staphylococci [78,81,82]. *In vitro* synergism was reported with daptomycin and ceftobiprole against MRSA and VISA, suggesting a potential role for plazomicin combination therapy for

the treatment of serious infections due to this pathogen [82,83]. Despite plazomicin has been approved by the FDA for the treatment of cUTI, there is uncertainty about its future as the development company (Achaogen) has filed for bankruptcy [78,84].

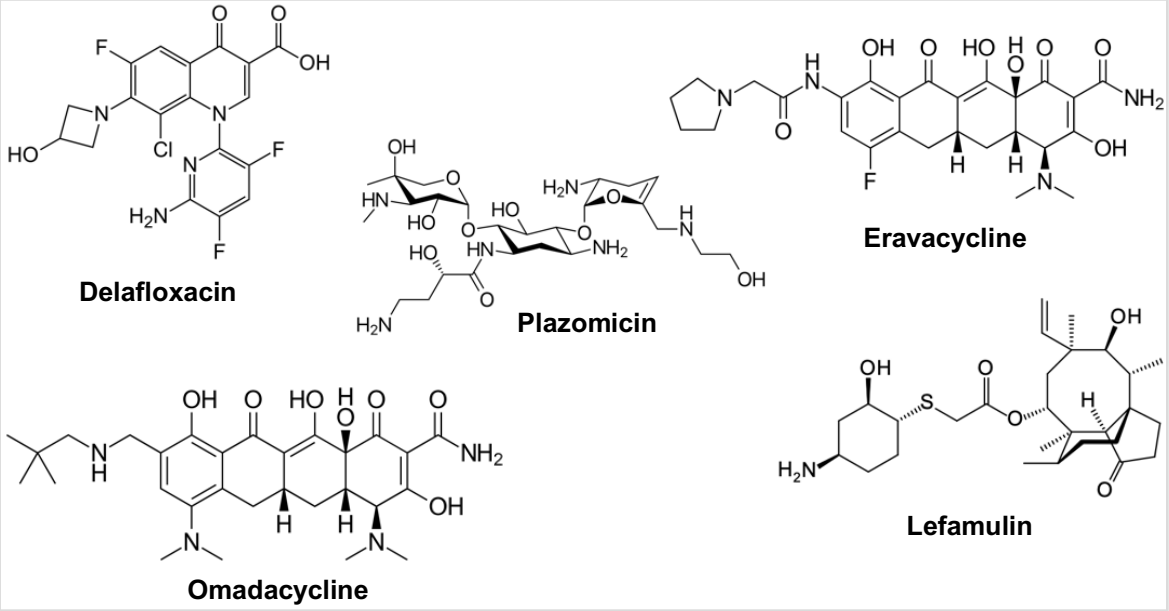

Figure 8. Structures of novel portfolio of antibacterial agents with activity against MDR *S. aureus*.

Eravacycline (Xerava™, Table 2, Figure 8) is a novel fluorocycline antibiotic with activity against both Gram-positive (including MRSA) and Gram-negative resistant pathogens [77,78,85,86]. It is structurally similar to tigecycline but is not affected by the major mechanisms of tetracycline resistance, such as efflux pumps and ribosomal hydrolysis [77,78,85,86]. Moreover, eravacycline has fourfold higher activity compared with tigecycline for Gram-positive organisms [77,78]. In a multicentre II trial conducted between 2011 and 2012, the efficacy and safety of eravacycline was compared to ertapenem in patients with complicated intra-abdominal infections (cIAIs) [77,86]. Adult patients requiring urgent surgical or percutaneous intervention were randomized to receive one of three medications [eravacycline 1.5 mg/kg once daily; eravacycline 1.0 mg/kg twice daily or ertapenem 1.0 g daily]. The primary efficacy endpoint was the clinical response in microbiologically evaluable (ME) patients at the test-of-cure (TOC) visit 10 to 14 days after the last dose of study drug. In the pooled analysis of the trial, 39 (92.9 %) of 42 patients in the eravacycline 1.5 mg/kg group, 100 % (41/41) in the eravacycline 1.0 mg/kg and 24 (92.3 %) of 26 in the ertapenem group had a successful outcome at the TOC visit [77,78,86]. Nevertheless, a relatively low proportion (6/191) of *S. aureus* isolates were identified in baseline cultures from patients and it is not known if any of them were MRSA [77,86]. In addition, a study conducted by

Grossmann *et al*. [78] showed that eravacycline performed, similarly to linezolid, against MRSA in neutropenic mouse lung infection model.

Omadacycline (Nuzyra™, Table 2, Figure 8) is an aminomethylcycline antimicrobial that has demonstrated activity against MRSA [77,87–90]. It was developed for ABSSSI and community-acquired pneumonia (CAP) [78,88,90]. Omadacycline has been compared with linezolid (with or without addition of aztreonam) in a phase II trial in patients with cSSSI that took place between July 2007 and January 2008 [77,88,89]. Patients were evaluated in 4 structured moments: baseline, end of i.v. treatment, end of treatment (EOT) and at TOC visit. Rates of successful clinical response in the intent-to-treat (ITT), modified intent-to-treat (MITT), clinical evaluable (CE) and ME populations were higher in the omadacycline group compared with the linezolid group. When the data were analysed against the newer regulatory criteria of clinical response during the first 72 h of therapy (no increase in lesion surface area from baseline and oral temperature $\leq$ 38ºC), patients in the omadacycline and linezolid groups had similar response rates (96.8 % *vs*. 94.4 %) [77,78,89,91].

Lefamulin (Xenleta™, Table 2, Figure 8) is a novel pleuromutilin antibiotic for CAP developed for oral and intravenous administration [92–94]. Although pleuromutilin antibiotics have been used in veterinary practice for many years, lefamulin is the first to be used for systemic treatment of bacterial infections in humans [77,80,94]. It showed to retain activity against an expanded Gram-positive spectrum including *S. aureus* (*i.e.*, methicillin-resistant, vancomycin-resistant and vancomycin-intermediate strains) [78]. A phase II ABSSSI trial (performed in 20 centres throughout the US) in patients receiving 100 mg of i.v. lefamulin reported a clinical success rate of 90 % at the TOC visit [77]. Additionally, lefamulin showed comparable efficacy to vancomycin for treating ABSSSI.

1.3.3. Antibiotics in clinical development

There are currently thirty-two antibiotics in clinical development (in clinical assays Phases 1-3) targeting WHO priority pathogens, with just over half of the thirty-two targeting at least one of the critical Gram-negative bacteria. An additional fifteen are possibly active or active against “high” and/or “medium” priority pathogens [70]. Table 3 summarizes clinical development of thirty-two antibacterial agents to target WHO priority pathogens list, focusing on agents under investigation for the treatment of MDR *S. aureus* infections. Other antibacterial agents with potent Gram-positive and/or Gram-negative activity are also in the pipeline, but are beyond the scope of this summary as they are not expected to be effective against MDR pathogens from the previously mentioned list.

Table 3. Antibacterial agents in clinical development (modified according to the WHO clinical pipeline report [70]).

Name (synonym)	Phase	Company	Antibiotic class	Spectrum against Organisms	Potential Indication	Ongoing Clinical Trials (ClinicalTrial.gov No.)
Lascufloxacin	NDA	Kyorin	Fluoroquinolone	MRSA, *S. epidermidis*, *E. faecalis*, *S. pyogenes*, *S. agalactiae*, and penicillin-resistant *S. pneumoniae* [95]	CAP; URTI [95]	
Cefiderocol	NDA MAA	Shionogi	Siderophore cephalosporin	*Enterobacteriaceae*, *Acinetobacter*, *Pseudomonas*	cUTI, HAP, VAP, blood-stream infections and sepsis	NCT04215991, NCT03869437
Sulopenem, Sulopenem etzadroxil/ probenecid	3	Iterum	Penem	ESBL- producing cephalosporin-resistant (but not carbapenem-resistant *Enterobacteriaceae*)	uUTI; cUTI; cIAI	
Durlobactam (ETX-2514) + sulbactam	3	Entasis	DBO-BLI/PBP2 binder + β-lactam-BLI/PBP1,3 binder	*Acinetobacter* spp.	HAP, VAP, cUTI, including pyelonephritis	NCT03894046
Taniborbactam (VNRX-5133) + cefepime	3	VenatoRx	Boronate-BLI + cephalosporin	*Enterobacteriaceae* and *P. aeroginosa* producing SBLs and MBLs, including NDM- and VIM-type β- lactamases	cUTI, cIAI	NCT03840148
Emmetazobactam (AAI-101) + cefepime	3	Allecra	β-lactam-BLI + cephalosporin	ESBL-producing cephalosporin-resistant and some KPC-producing CRE	cUTI, cIAI, HAP, VAP	NCT03680352
Zoliflodacin	3	Entasis/GARDP	Topoisomerase inhibitor (spiropyrimidenetrione)	*N. gonorrhoea* and Gram-positive cocci	Uncomplicated gonorrhoea	NCT03959527
Gepotidacin	3	GSK	Topoisomerase inhibitor (triazaacenaphtylene)	MRSA, levofloxacin-resistant and multidrug-resistant *S. aureus* [95]	ABSSSI [95]	NCT04020341, NCT04010539, NCT04187144
Levonadifloxacin Alalevonadifloxacin	3	Wockhardt	Fluoroquinolone	MRSA and staphylococci resistant to levofloxacin and moxifloxacin [95]	ABSSSI; HAP [95]	
Cefilavancin (TD-1792)	3	Theravance/ R Pharm	Glycopeptide-cephalosporin conjugate	*Staphylococci* and *Streptococci*	ABSSSI	
Solithromycin	3	Melinta/Fujifilm Toyama Chemical	Macrolide	MRSA, and macrolide-resistant *M. pneumoniae* [95]	CAP [95]	

Table 3. *(Continued)*

Name (synonym)	Phase	Company	Antibiotic class	Spectrum against Organisms	Potential Indication	Ongoing Clinical Trials (ClinicalTrial.gov No.)
Contezolid Contezolid acefosamil	2/3	MicuRx	Oxazolidinone	MRSA, penicillin-resistant and penicillin-intermediate *S. pneumoniae*, and VRE [95]	ABSSSI [95]	NCT03747497
Afabicin (Debio-1450)	2	Debiopharm	FabI inhibitor	MRSA [95]	ABSSSI [95]	NCT03723551
BOS-228 (LYS-228)	2	Boston Pharmaceuticals	Monobactam	Serine and metallo-β- lactamase expressing CRE	cUTI; cIAI	
Nafithromycin (WCK-4873)	2	Wockhardt	Macrolide	*S. pneumoniae*, *S. aureus*, *H. influenzae*, *M. catarrhalis*, *L. pneumophila*, *M. pneumoniae* and *C. pneumoniae*	CAP	
TNP-2092	2	TenNor	Rifamycin-quinolizinone hybrid	*E. faecium*, *S. aureus*, *C. difficile*, *H. pylori*	ASSSI, catheter-related bloodstream and prosthetic joint infections	NCT03964493, NCT04294862
Benapenem	2	Sichuan Pharmaceutical	Carbapenem	*Enterobacter* spp.	cUTI, CAP	NCT04200261
Zidebactam + cefepime	1	Wockhardt	DBO-BLI/PBP2 binder + cephalosporin	CRPA, CRE, CRAB	cUTI, HAP, VAP	
Nacubactam + meropenem	1	NacuGen Therapeutics	DBO-BLI/PBP2 binder + meropenem	ESBL, OXA-48 and KPC- producing *Enterobacteriaceae*	cUTI, HAP, VAP, cIAI	
ETX0282 + cefpodoxime	1	Entasis	DBO-BLI/PBP2 binder + cephalosporin	ESBL, OXA-48 and KPC, but not MBL-producing *Enterobacteriaceae*	UTI	
VNRX-7145 + ceftibuten	1	VenatoRx	Boronate-BLI + cephalosporin	CRE (KPC and OXA carbapenemases) and ESBLs	Gram-negative bacterial infections	
SPR-741 + β-lactam	1	Spero	Polymyxin (potentiator) + β-lactam	Not specified [95]	Gram-positive bacterial infections [95]	
SPR-206	1	Spero	Polymyxin	Broad Gram-negative	Gram-negative bacterial infections	

Table 3. (*Continued*)

Name (synonym)	Phase	Company	Antibiotic class	Spectrum against Organisms	Potential Indication	Ongoing Clinical Trials (ClinicalTrial.gov No.)
KBP-7072	1	KBP BioSciences	Tetracycline	*S. aureus* and *S. pneumoniae* strains that exhibit higher minocycline MIC and beta-lactam resistance; CRAB [95]	CAP [95]	
TP-271	1	Tetraphase	Tetracycline	MRSA, *S. pneumoniae, S. pyogenes* and CRAB [95]	CAP [95]	NCT03234738
TP-6076	1	Tetraphase	Tetracycline	CRE, CRAB	Gram-negative bacterial infections	NCT03691584
EBL-10031 (apramycin)	1	Juvabis	Aminoglycoside	CRPA, CRAB, CRE	Gram-negative bacterial infections	NCT04105205
AIC-499 + unknown BLI	1	AiCuris	β-lactam + BLI	Gram-negative pathogens, including MDR *Pseudomonas* and *Acinetobacter*	cUTI, cIAI	
TNP-2198	1	TenNor	Rifamycin-nitroimidazole conjugate	Anaerobes; *C. difficile* and *H. pylori*	Gastrointestinal diseases, CDAD, bacterial vaginosis	
TXA-709	1	Taxis	FtsZ inhibitor	*S. aureus* (MRSA)	ABSSSI	
BCM-0184	1	Biocidium	undisclosed	*S. aureus* (MRSA)	Infections caused by MRSA	
ARX-1796 (oral avibactam prodrug)	1	Arixa Phaemaceuticals	DBO-BLI + β-lactam	Not specified	Gram-negative bacterial infections	NCT03931876

Abbreviations: ABSSSI (Acute Bacterial Skin and Skin Structure Infection), CAP (community-acquired pneumonia), CDAD (*Clostridioides difficile*-associated disease), CRAB (carbapenem-resistant *Acinetobacter baumannii*), CRE (carbapenem-resistant *Enterobacteriaceae*), CRPA (carbapenem-resistant *Pseudomonas aeruginosa*), cIAI (complicated intra-abdominal infections), cUTI (complicated urinary tract infection), ESBL (extended-spectrum beta lactamase), HAP (hospital-acquired pneumonia), KPC (*Klebsiella pneumoniae* carbapenemase), MAA (marketing authorization application), NDA (New Drug Application), URTI (upper respiratory tract infection), UTI (urinary tract infection), uUTI (uncomplicated urinary tract infection), VAP, (ventilator-associated pneumonia).

Bacteria abbreviations: *C. difficile* (*Clostridium difficile*), *E. faecalis* (*Enterococcus faecalis*), *H. pylori* (*Helicobacter pylori*), MRSA (methicillin-resistant *Staphylococcus aureus*), *S. agalactiae* (*Streptococcus agalactiae*), *S. aureus* (*Staphylococcus aureus*), *S. epidermis* (*Staphylococcus epidermis*), *S. pneumoniae* (*Streptococcus pneumoniae*), *S. pyogenes* (*Streptococcus pyogenes*).

The bold names denote emerging antibiotics for MDR *S. aureus*.

1.4. Looking for potential antimicrobial agents based on ionic liquids

The field of ionic liquids (ILs) began, almost occasionally, in 1914 with an observation performed by Paul Walden, who reported the synthesis of ethylammonium nitrate [96–98]. By the neutralization of ethylamine with concentrated nitric acid it was possible to obtain this material, with a melting point around 13-14 ºC [99,100]. However, the discovery of this liquid salt did not prompt any significant interest at that time [98]. In 1934, Charles Graenacher suggested a process for the preparation of cellulose solutions by heating cellulose in N-alkylpyridinium salts in the presence of nitrogen-containing bases. After another fallow phase in their history, ionic liquids emerged in 1948, being applied in mixtures of aluminium (III) chloride and 1-ethylpyridinium bromide for the electrodeposition of aluminium [100]. Despite these findings, only in a recent past the interest in ionic liquids emerged with a variety of ILs synthesized and applications being proposed.

By definition, ILs are a class of low temperature (<100 ºC) molten salts, usually comprising a nitrogen or phosphorus-containing organic head group containing as substituent a linear alkyl chain, with a small counter-anion [96,99]. The delocalized charge on bulky aromatic cores, alongside a general lack of symmetry and weakly coordinating anions prevent the formation of an ordered crystalline structure [101]. The increasing attention devoted to ILs is largely justified by their unique physicochemical properties, such as their high solvation power, negligible vapour pressure, high chemical and thermal stability, high ionic conductivity and wide electrochemical window [101–103]. Furthermore, these ionic liquids are accolade as “designer solvents” due to their tuneable properties, which means that they can be designed for a specific application by the appropriate selection of anion, cation, and substituents located on the cation [97,102–104]. Examples of most described cations, anions, and alkyl chain substituents are presented in Figure 9.

The properties of ILs have led to their use as solvent in organic chemistry (*e.g.*, homogeneous catalysis, Heck reaction, or Suzuki reaction), inorganic synthesis, and biocatalysis, in biomass conversion and polymerization, and as active pharmaceutical ingredients (APIs) [97,99,105].

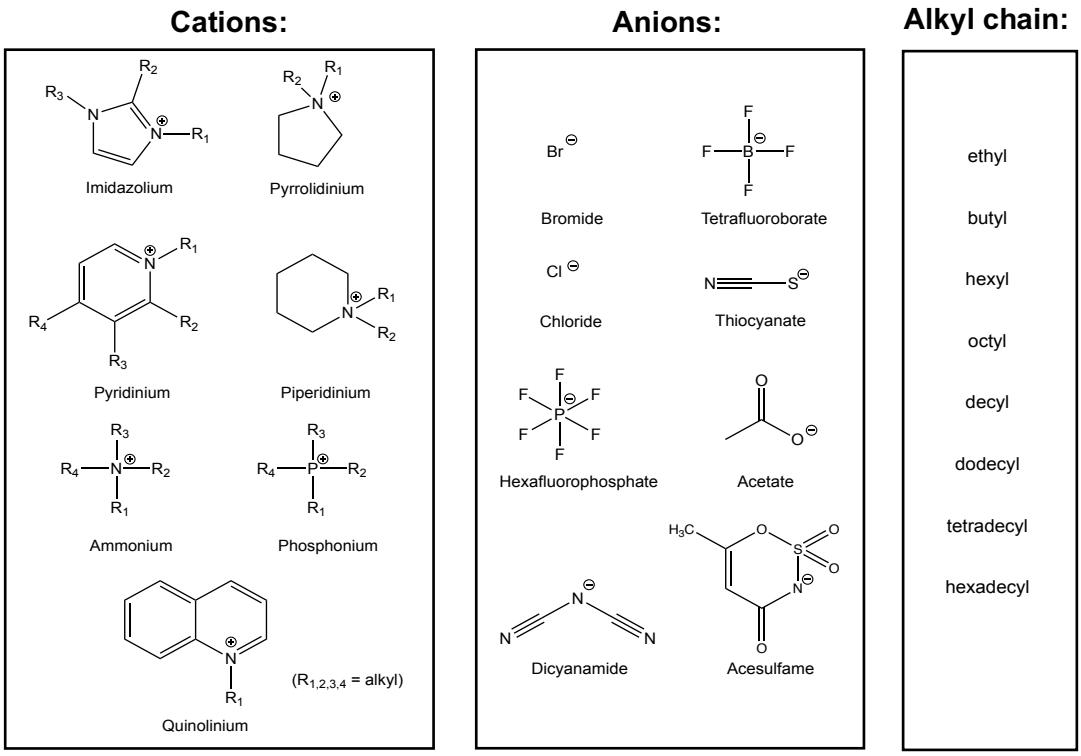

Figure 9. Examples of most described cations, anions and alkyl chain substituents used in the preparation of ILs.

1.4.1. Antimicrobial potential and cytotoxic profile of ionic liquids

The antimicrobial properties of ILs have been documented for more than two decades, indicating a broad-spectrum antimicrobial activity, affecting Gram-positive and Gram-negative bacteria as well as mycobacteria and fungi [106]. A number of recent publications have highlighted the antimicrobial activity of imidazolium, pyridinium, and quaternary ammonium based ionic liquids against pathogenic and nonpathogenic bacteria and fungi [107]. Furthermore, ILs have shown potential even in the case of resistant and biofilm-forming microorganisms [101,107]. Low concentrations of 1-hexadecyl-3-methylimidizolium chloride strongly prevented biofilm formation of multidrug-resistant *Candida tropicalis* [105]; 1-alkyl-3-methylimidazolium halides were effective in controlling *S. aureus* and *Pseudomonas aeruginosa* growth and biofilm formation [108], whereas alkyl-3-methylimidazolium fumarates showed potent activity against rods and fungi, being suggested to be used for medical purposes [109]. 1-alkyl-3-methyimidazolium chlorides and 1-alkylquinolinium bromides demonstrated broad spectrum antibiofilm activity against a variety of clinically important microbes, including MRSA, *P. aeruginosa* and *Escherichia coli* [110]. Hexyl- and octylpyridinium bromides showed potent activity against *E. coli*, *S. aureus*, *Bacillus subtilis*, *P. fluorescens* and *Saccharomyces cerevisiae* [111]. Ammonium ILs with azolate anions were found to be very effective bactericidal and fungicidal agents [105,112];

hydroxylammonium ILs showed high antimicrobial activity against such human pathogens as *S. aureus*, *Listeria monocytogenes*, *Salmonella typhi*, *Vibrio cholerae*, and *Klebsiella pneumoniae* [113], whereas diphosphonium ILs demonstrated potent antimicrobial activity against important ocular pathogens [105,114]. Triphenylamine phosphonium ILs, which are able to self-assemble into nanostructures, revealed potent bactericidal activity for Gram-positive bacteria, particularly against *S. aureus* [115].

Despite the remarkable biological behaviour of certain ILs, the possible detrimental effects associated with their broad application in medicine must be considered [105]. Most of the toxicity studies discussed so far were performed on bacteria, algae, invertebrates or fish systems. Nevertheless only a few studies have analysed the toxicity of ILs on human cell lines [104,116]. In the colon carcinoma HT-29 and Caco-2 cell lines, treatment with 1-octyl- and 1-decyl-3-methylimidazolium drastically reduced the cells' viability [117]. In the mouse mammary carcinoma cells EMT6, treatment with 1-octyl-3-methylimidazolium chloride up-regulates the expression of cytochrome P450 genes, products of which were involved in metabolism and biotransformation of xenobiotic compounds [105,118]. In HeLa cells, three homologues of 1-alkyl-3-methylimidazolium chloride were found to have ability to induce the multixenobiotic/multidrug resistance (MXR/MDR) system [119]. Treatment with 1-methyl-3-octylimidazolium bromide induced apoptosis, overproduction of reactive oxygen species (ROS), inhibition of superoxide dismutase and catalase, reduction of glutathione content, and increase in the cellular malondialdehyde level in the HepG2 cells [120]. In NIH 3T3 murine fibroblast cells, 1-alkylquinolinium bromides caused disruption of cellular membrane integrity [105,121]. Treatment with triethylammonium sulfate, triethylammonium phosphate, 1-methylimidazolium chloride, and 1-butyl-3-methylimidazolium chloride enhanced growth inhibition and cell death in both the T98G and HEK cell lines [122].

Several studies [123–125] have been conducted to evaluate the antimicrobial activity of ILs, as well as *in vitro* cellular cytotoxicity, combining different anions and cations, and changing the alkyl group chain length. These studies indicate that ILs antimicrobial activity and cytotoxicity are primordially determined by the cation nature and are directly correlated with the length of the side alkyl chain and the number of alkyl groups. Commonly, ILs with longer alkyl side chains tend to present a much higher antimicrobial activity ("chain-length effect") until a certain threshold ("cut-off effect"), likely dictated by the interplay between solubility, decreased perturbation, steric effects, and self-aggregation of the IL components in the growth medium [101,104,125–127]. Indeed, MIC/MBC minima are commonly reported across an optimal number of carbon atoms (usually C_{11}-C_{16}) in the chain, with an apparent interspecies variance in the peak antimicrobial action [101]. Furthermore, ILs with longer

alkyl side chains tend to exhibit superior cytotoxicity than the ILs with shorter alkyl side chains [104,126]. Usually, the anion presents a subsidiary role in antimicrobial activity, when compared with the "chain-length effect" and the cation [101,104]. Whilst this is frequently observed, it has also been shown that the anion can contribute to the cytotoxicity profile of ILs – [NTf_2] anion has a pronounced negative effect towards different cell lines, including both MCF7 and HeLa cells [125–128]. Considering the influence of the cation head group to the ILs antimicrobial activity, it was shown that multiple, charged head groups present a significant enhance on activity compared to that of single head groups [101]. The antimicrobial activity outcome observed can be endorsed to their higher solubility in water and the existence of a greater positive charge density per molecule [129]. There has also been an agreement on the fact that ammonium-based ILs present a lower antimicrobial activity than their corresponding phosphonium counterparts, which can be explained by the lower hydrophobic nature (higher polarities) of the former [123,127].

1.4.2. Synthesis of ionic liquids

The synthesis of ILs can generally be divided into two steps: 1) the formation of the desired cation [130–132]., and 2) anion exchange to form the desired IL, as illustrated in Figure 10 [131]. In specific cases, only the first step is required. The formation of the cation may be carried out either by protonation with a free acid or by quaternization of an amine or a phosphine, most commonly using a haloalkane. The anion-exchange reactions of ILs can be divided into two distinct groups, direct treatment of halide salts with Lewis acids, and formation of ILs *via* anion metathesis [97,130]. In this section, special attention will be dedicated to the quaternization reaction that at the formation of quaternary salts, since it is the synthesis reaction followed in this Thesis.

In general, the quaternization reactions are quite simple: the amine or phosphine is mixed with the haloalkane under nitrogen, being then the mixture stirred and heated [132]. The most common starting materials are 1-alkylimidazoles, but others such as pyridine, isoquinoline, 1-methylpyrrolidone and trialkylamines can also be applied [98]. In general, the reaction may be carried out using a diversity of haloalkanes (chloroalkanes, bromoalkanes and iodoalkanes), with the required reaction conditions becoming steadily gentler in the order Cl < Br < I, as expected for nucleophilic substitution reactions [96,131,132]. For example, a reaction of 1-methylimidazole with chloroalkanes is typically complete within 2-3 days at 80 ºC, whereas the equivalent reaction with bromoalkanes is usually complete in 24 h at 50-60 ºC [98]. The reactivity of the haloalkanes also generally decreases with the increase of the alkyl chain length [98]. The reaction temperature and

time are two main conditions highly dependent on the haloalkane used [132]. The reaction is normally carried out without the use of a solvent as the reagents are mutually miscible, while the halide salts are generally immiscible with the starting materials [98]. The halide salts should be kept free of moisture as they are often extremely hygroscopic. This approach has the major advantage of generating the desired ionic liquid with high yield, with a minimal and easily removable impurities.

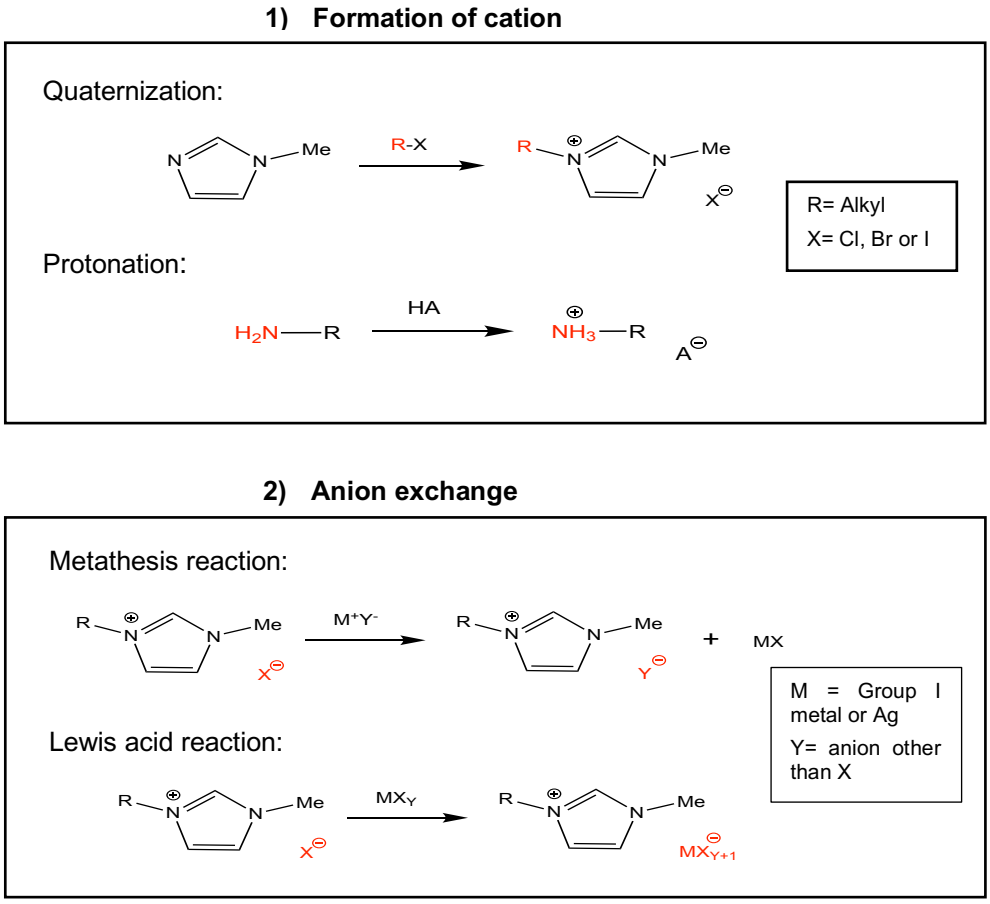

Figure 10. General schematic diagram of the most common steps applied in the synthesis of ILs.

1.5. Thesis objectives

The main objectives of this Thesis are related to the design and synthesis of a concise and chemically related library of alkyl cationic derivatives (ILs) that by means of a structure-activity relationship (SAR) will help to understand how variations in chemical features can impact the activity against bacteria and toxicity in human cells. Structure modifications will be performed on the length of aliphatic carbon chain spacer (six-, eight- and ten- carbon) and on the nature of the cation (triphenylphosphonium, methylimidazolium, isoquinolinium, methylpyridinium, quinolinium, pyridinium and triethylammonium) (Figure 11). Their effects

on planktonic growth control of *S. aureus* (*i.e*., for their antimicrobial activity) and on human cell cytotoxicity will be determined.

In this view, the final goal and contribution of this Thesis would be the rational development of new effective antimicrobial agents, comprised by ionic liquids. The potential of certain ILs to exhibit excellent antimicrobial activity presents an exciting possibility that ILs could be used as a targeted agent for bacterial infections, being a new hope to overcome the bacterial resistance problem. They can constitute scaffolds for drug discovery and development of new antimicrobial agents as they can be tailored and their physical, chemical and biological properties fine-tuned and so replenish the antibiotic pipeline.

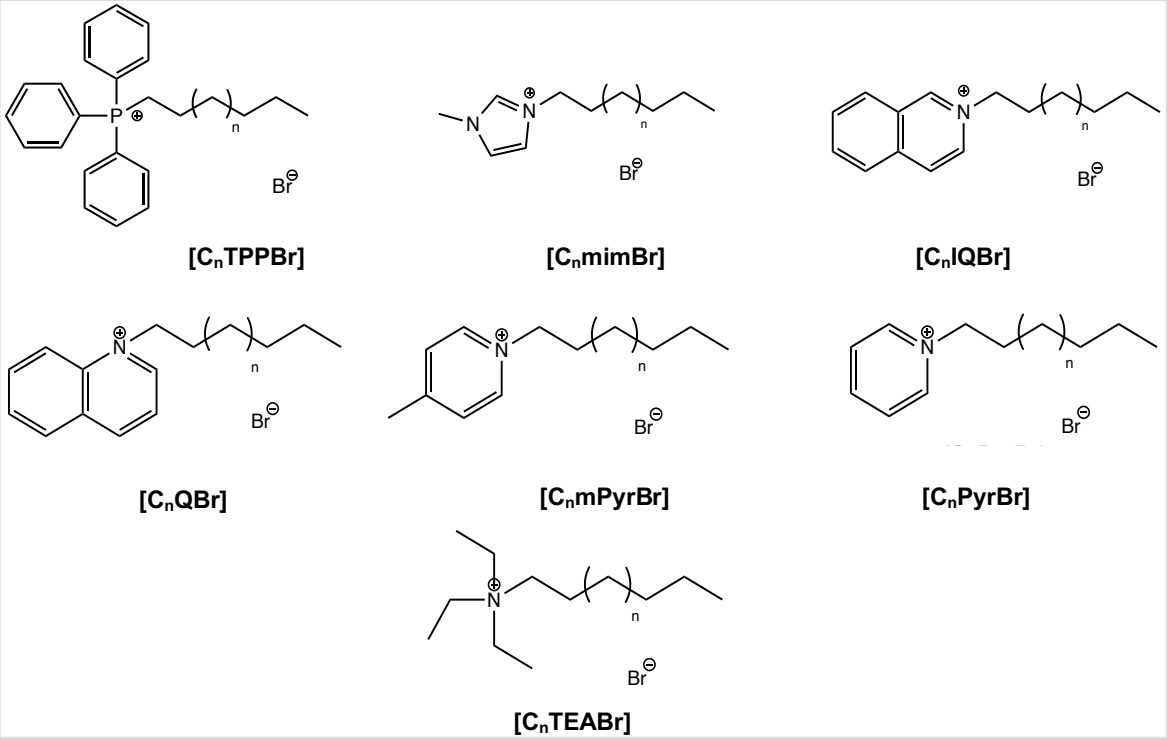

Figure 11. General structure of the compounds developed in this Thesis; *n* = 1, 3, 5.

Chapter 2

EXPERIMENTAL PART

In this Chapter, a description of all the chemical and biological materials used in this study is performed, along with important explanations required for their preparation. The experimental part is subdivided into three sections: Chemical, Microbiological and Human cell Studies. The first section is devoted to the presentation of source, purity of the chemicals and solvents, of the instrumentation (together with details on the working parameters) and information on the synthesis/structural elucidation of the compounds obtained. The second section describes the broth microdilution method used to measure quantitatively the *in vitro* activity of the synthesized compounds against *S. aureus* CECT 976 strain. It addresses preparation of testing conditions (including inoculum preparation and standardization, time and temperature of incubation). The third section describes the *in vitro* assays used to evaluate the cell viability/proliferation of the HK-2 and HepG2 cell lines in response to synthesized compounds.

2.1. Chemical Studies

2.1.1. Reagents and solvents

The reagents used as starting materials were purchased from Sigma-Aldrich and TCI Chemicals: 1-bromohexane (CAS 111-25-1, 99 %), 1-bromooctane (CAS 111-83-1, > 98 %), 1-bromodecane (CAS 112-29-8, 98 %), triphenylphosphine (CAS 603-35-0, > 95 %), 1-methylimidazole (CAS 616-47-7, ≥ 99 %), isoquinoline (CAS 119-65-3, > 95 %), 4-picoline (CAS 108-89-4, 99 %), triethylamine (CAS 121-44-8, 99 %), quinoline (CAS 91-22-5, 98 %) and pyridine (CAS 110-86-1, ≥99%).

Deuterated chloroform ($CDCl_3$) was obtained from Deutero GmbH, whereas dichloromethane, methanol and diethyl ether (all with *pro analysis* grade) were acquired from Merck. All chemicals were used as received without further purification.

2.1.2. Apparatus

Syntheses were performed in a reaction station (Mya 4 system, Radleys).

A laboratory balance (Kern, model ABS 220-4N) with an accuracy of 0.0001 g was used.

Solvents were evaporated under reduced pressure in a Büchi Rotavapor R-210.

Automated flash chromatography was performed with Biotage Isolera Prime system.

The spots from each developed thin-layer chromatography (TLC) plate were visualized under UV light in a Vilber Lourmat system.

NMR data were acquired on a Bruker Avance III 400 NMR spectrometer, located at the Materials Centre of University of Porto (CEMUP), operating at 400.15 MHz for ^{1}H and 100.62 MHz for ^{13}C and DEPT135. Spectra were recorded, at room temperature, in 5 mm outside diameter tubes. $CDCl_3$ was used as solvent and tetramethylsilane (TMS) as internal standard. Chemical shifts were expressed in parts per million (δ scale) and the coupling constants (*J*) were given in Hz. DEPT135 values were included in ^{13}C NMR data (underlined values).

2.1.3. Chromatographic techniques

Analytical TLC was performed using silica gel 60Å F254 pre-coated plates (0.2 mm thickness). Reaction control was monitored using dichloromethane:methanol (9:1) as

eluent. The spots were visualized under UV detection (254 and 366 nm), potassium permanganate ($KMnO_4$) staining or by exposure to iodine (I_2) vapor.

Chromatography glass column[1] was carried out using silica gel 60Å (0.040-0.063 nm) as stationary phase and dichloromethane:methanol (9:1) as elution system. Fractions of approximately 15 mL were collected.

Automatic flash chromatography was performed on the Biotage Isolera Prime, with Biotage SNAP 25 g or 100 g cartridges, using either isocratic elution with dichloromethane:methanol (9:1) or gradient elution from dichloromethane to dichloromethane:methanol (8:2). Detection wavelength 206-366 nm.

2.1.4. Synthesis

2.1.4.1 General synthetic procedure to obtain triphenylphosphonium, methylimidazolium, isoquinolinium, methylpyridinium, quinolinium and pyridinium salts

Triphenylphosphine (1.2 eq.) and the appropriate bromoalkane (0.5 mL; 1 eq.) were added to a 2-5 mL glass vial. The reaction mixture was stirred and heated to 130 ºC for 24 h under argon atmosphere. Thereafter the residue was dissolved in dichloromethane and purified by silica gel flash chromatography: compounds [C_nTPPBr] and [$C_n$mimBr] were purified using dichlorometane:methanol (9:1) as eluting system and compounds [C_nIQBr], [C_nmPyrBr], [C_nQBr] and [C_nPyrBr] using gradient elution from dichloromethane to dichloromethane:methanol (8:2). The fractions containing the intended compound were then collected and the solvent evaporated to dryness. The reaction control was performed by TLC (silica gel, dichlorometane:methanol (9:1)). The synthetic procedure was based on the method reported by Teixeira *et al* [133].

The structural analysis of compounds [C_nTPPBr], [$C_n$mimBr], [C_nIQBr], [C_nmPyrBr], [C_nQBr], [C_nPyrBr] are described below.

[1] In the Thesis initiation phase, the purification of the crude products was performed manually on a glass column.

Triphenylphosphonium–based ILs

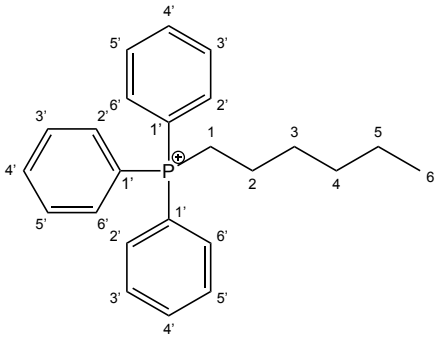

[C_6TPPBr]

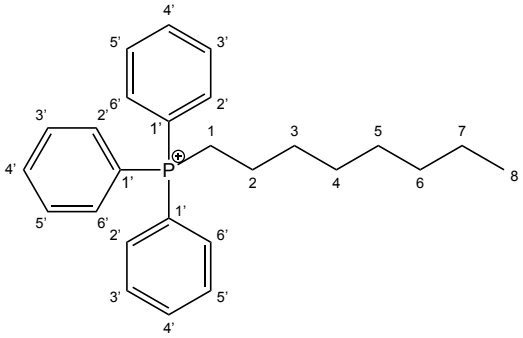

[C_8TPPBr]

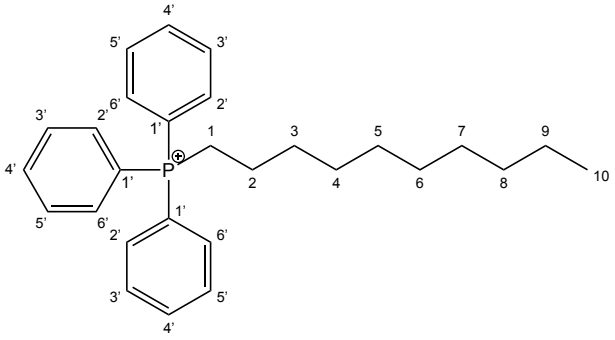

[C_{10}TPPBr]

Figure 12. Structural formulae and numbering of [C_6TPPBr], [C_8TPPBr], [C_{10}TPPBr].

Hexyltriphenylphosphonium bromide **[C_6TPPBr]** (Figure 12). Pale yellow oil. Yield = 95 %.^{1}H NMR (400 MHz, $CDCl_3$): δ = 0.82 (3H, *t*, *J* = 7.1 Hz, H(6)), 1.16 – 1.33 (4H, *m*, H(4), H(5)), 1.54 – 1.72 (4H, *m*, H(2), H(3)), 3.69 – 3.84 (2H, *m*, H(1)), 7.63 – 8.00 (15H, *m*, H(2') – H(6')). ^{13}C NMR (101 MHz, $CDCl_3$): δ = 14.0 (C(6)), 22.2 (C(5)), 22.6 (*d*, J_{CP} = 4.6 Hz, C(3)), 22.8 (*d*, J_{CP} = 49.7 Hz, C(1)), 30.1 (*d*, J_{CP} = 15.5 Hz, C(2)), 31.3 (*d*, J_{CP} = 1.0 Hz, C(4)), 118.4 (*d*, J_{CP} = 85.8 Hz, 3 × C(1')), 130.5 (*d*, J_{CP} = 12.5 Hz, 3 × C(3') and 3 × C(5')), 133.7 (*d*, J_{CP} = 10.0 Hz, 3 × C(2') and 3 × C(6')), 135.0 (*d*, J_{CP} = 3.0 Hz, 3 × C(4')).

Octyltriphenylphosphonium bromide **[C_8TPPBr]** (Figure 12). Pale yellow oil. Yield = 68 %. ^{1}H NMR (400 MHz, $CDCl_3$): δ = 0.83 (3H, *t*, *J* = 6.9 Hz, H(8)), 1.13 – 1.32 (8H, *m*, H(4) – H(7)), 1.56 – 1.70 (4H, *m*, H(2), H(3)), 3.45 – 3.97 (2H, *m*, H(1)), 7.62 – 7.94 (15H, *m*, H(2') – H(6')). ^{13}C NMR (101 MHz, $CDCl_3$): δ = 14.1 (C(8)), 22.5 (C(7)), 22.7 (*d*, J_{CP} = 4.6

Hz, C(3)), 22.8 (*d*, J_{CP} = 49.5 Hz, C(1)), 28.8 (C(6)), 29.2 (*d*, J_{CP} = 1.0 Hz, C(4)), 30.4 (*d*, J_{CP} = 15.5 Hz, C(2)), 31.7 (C(5)), 118.5 (*d*, J_{CP} = 85.8 Hz, 3 × C(1')), 130.5 (*d*, J_{CP} = 12.5 Hz, 3 × C(3') and 3 × C(5')), 133.7 (*d*, J_{CP} = 10.0 Hz, 3 × C(2') and 3 × C(6')), 135.0 (*d*, J_{CP} = 3.0 Hz, 3 × C(4')).

Decyltriphenylphosphonium bromide **[C_{10}TPPBr]** (Figure 12). Pale yellow oil. Yield = 92 %. ^{1}H NMR (400 MHz, $CDCl_3$): δ = 0.85 (3H, *t*, *J* = 7.0 Hz, H(10)), 1.13 – 1.32 (12H, *m*, H(4) – H(9)), 1.55 – 1.69 (4H, *m*, H(2), H(3)), 3.68 – 3.91 (2H, *m*, H(1)), 7.63 – 7.96 (15H, *m*, H(2') – H(6')). ^{13}C NMR (101 MHz, $CDCl_3$): δ = 14.1 (C(10)), 22.5 (C(9)), 22.7 (*d*, J_{CP} = 4.7 Hz, C(3)), 22.8 (*d*, J_{CP} = 49.5 Hz, C(1)), 29.2 (C(7)), 29.2 (C(5), C(6)), 29.5 (C(4)), 30.4 (*d*, J_{CP} = 15.5 Hz, C(2)), 31.8 (C(8)), 118.5 (*d*, J_{CP} = 85.8 Hz, 3 × C(1')), 130.5 (*d*, J_{CP} = 12.5 Hz, 3 × C(3') and 3 × C(5')), 133.7 (*d*, J_{CP} = 9.9 Hz, 3 × C(2') and 3 × C(6')), 135.0 (*d*, J_{CP} = 3.0 Hz, 3 × C(4')).

1-methylimidazolium−based ILs

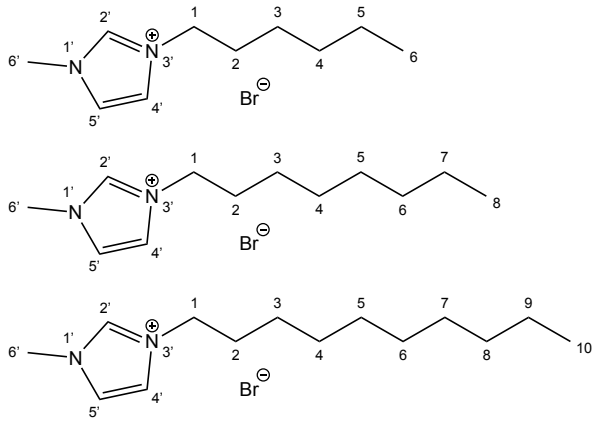

Figure 13. Structural formulae and numbering of [C_6mimBr], [C_8mimBr], [C_{10}mimBr].

3-Hexyl-1-methyl-1H-imidazol-3-ium bromide **[C_6mimBr]** (Figure 13). Pale yellow viscous oil. Yield = 71 %. ^{1}H NMR (400 MHz, $CDCl_3$): δ = 0.87 (3H, *t*, *J* = 7.1 Hz, H(6)), 1.23 – 1.40 (6H, *m*, H(3) – H(5)), 1.85 – 1.98 (2H, *m*, H(2)), 4.13 (3H, *s*, H(6')), 4.33 (2H, *t*, *J* = 7.5 Hz, H(1)), 7.25 (1H, *dd*, J_1 = 1.8 Hz, J_2 = 1.8 Hz, H(4')), 7.32 (1H, *dd*, J_1 = 1.8 Hz, J_2 = 1.8 Hz, H(5')), 10.36 (1H, *bs*, H(2')). ^{13}C NMR (101 MHz, $CDCl_3$): δ = 13.9 (C(6)), 22.4 (C(5)), 25.9 (C(3)), 30.2 (C(2)), 31.1 (C(4)), 36.8 (C(6')), 50.3 (C(1)), 121.5 (C(5')), 123.0 (C(4')), 138.3 (C(2')).

1-Methyl-3-octyl-1H-imidazol-3-ium bromide **[C_8mimBr]** (Figure 13). Pale yellow viscous oil. Yield = 88 %. ^{1}H NMR (400 MHz, $CDCl_3$): δ = 0.84 (3H, *t*, *J* = 6.9 Hz, H(8)), 1.15 – 1.40 (10H, *m*, H(3) – H(7)), 1.84 – 1.94 (2H, *m*, H(2)), 4.11 (3H, *s*, H(6')), 4.33 (2H, *t*, *J* = 7.4 Hz, H(1)), 7.36 (1H, *dd*, J_1 = 1.8 Hz, J_2 = 1.8 Hz, H(4')), 7.50 (1H, *dd*, J_1 = 1.8 Hz, J_2 = 1.8 Hz,

H(5')), 10.40 (1H, *bs*, H(2')). ^{13}C NMR (101 MHz, $CDCl_3$): δ = 14.1 (C(8)), 22.6 (C(7)), 26.3 (C(2)), 28.9 (C(3)), 29.0 (C(5)), 30.3 (C(4)), 31.7 (C(6)), 36.8 (C(6')), 50.2 (C(1)), 121.8 (C(5')), 123.5 (C(4')), 137.7 (C(2')).

3-Decyl-1-methyl-1H-imidazol-3-ium bromide **[C_{10}mimBr]** (Figure 13). Pale yellow viscous oil. Yield = 94 %. ^{1}H NMR (400 MHz, $CDCl_3$): δ = 0.87 (3H, *t*, *J* = 6.9 Hz, H(10)), 1.17 – 1.41 (14H, *m*, H(3) – H(9)), 1.84 – 2.03 (2H, *m*, H(2)), 4.13 (3H, *s*, H(6')), 4.32 (2H, *t*, *J* = 7.4 Hz, H(1)), 7.35 (1H, *dd*, J_1 = 1.8 Hz, J_2 = 1.8 Hz, H(4')), 7.49 (1H, *dd*, J_1 = 1.8 Hz, J_2 = 1.8 Hz, H(5')), 10.42 (1H, *bs*, H(2')). ^{13}C NMR (101 MHz, $CDCl_3$): δ = 14.1 (C(10)), 22.7 (C(9)), 26.3 (C(2)), 29.0 (C(7)), 29.2 (C(6)), 29.4 (C(5)), 29.5 (C(4)), 30.3 (C(8)), 31.8 (C(3)), 36.8 (C(6')), 50.2 (C(1)), 121.7 (C(5')), 123.5 (C(4')), 137.8 (C(2')).

Isoquinolinium−based ILs

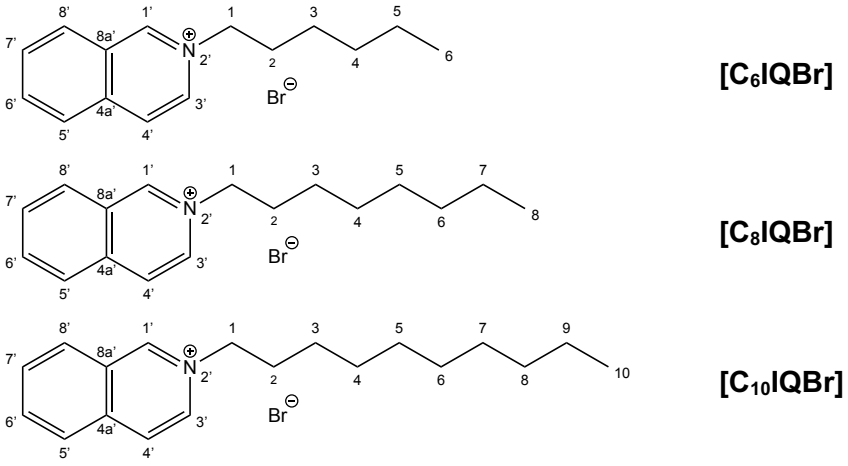

Figure 14. Structural formulae and numbering of [C_6IQBr], [C_8IQBr], [C_{10}IQBr].

2-Hexylisoquinolin-2-ium bromide **[C_6IQBr]** (Figure 14). Brownish solid. Yield = 72 %. ^{1}H NMR (400 MHz, $CDCl_3$): 0.83 (3H, *t*, *J* = 7.1 Hz, H(6)), 1.18 – 1.50 (6H, *m*, H(3) – H(5)), 2.06 – 2.20 (2H, *m*, H(2)), 5.09 (2H, *t*, *J* = 7.4 Hz, H(1)), 7.95 (1H, *ddd*, *J* = 8.2, 6.7, 1.4 Hz, H(7')), 8.08 – 8.20 (2H, *m*, H(5'), H(6')), 8.39 (1H, *d*, *J* = 6.8 Hz, H(4')), 8.79 (2H, *m*, H(3'), H(8')), 11.12 (1H, *dd*, H(1')). ^{13}C NMR (101 MHz, $CDCl_3$): δ = 14.1 (C(6)), 22.3 (C(5)), 25.9 (C(3)), 31.2 (C(2)), 31.9 (C(4)), 61.7 (C(1)), 126.3 (C(8')), 127.1 (C(5')), 127.9 (C(8a')), 131.3 (C(6')), 131.4 (C(7')), 134.4 (C(4')), 137.1 (C(3')), 137.3 (C(4a')), 150.5 (C(1')).

2-Octylisoquinolin-2-ium bromide **[C_8IQBr]** (Figure 14). Brownish solid. Yield = 85 %. ^{1}H NMR (400 MHz, $CDCl_3$): δ = 0.84 (3H, *t*, *J* = 6.9 Hz, H(8)), 1.13 – 1.49 (10H, *m*, H(3) – H(7)), 2.05 – 2.19 (2H, *m*, H(2)), 5.09 (2H, *t*, *J* = 7.4 Hz, H(1)), 7.95 (1H, *ddd*, *J* = 8.2, 6.5, 1.6 Hz, H(7')), 8.07 – 8.20 (2H, *m*, H(5'), H(6')), 8.37 (1H, *d*, *J* = 6.8 Hz, H(4')), 8.77 (2H, *m*, H(3'), H(8')), 11.16 (1H, *dd*, H(1')). ^{13}C NMR (101 MHz, $CDCl_3$): δ = 14.1 (C(8)), 22.6 (C(7)),

26.2 (C(3)), 29.0 (C(5)), 29.1 (C(4)), 31.7 (C(2)), 32.0 (C(6)), 61.7 (C(1)), 126.3 (C(8')), 127.1 (C(5')), 127.9 (C(8a')), 131.4 (C(6')), 131.5 (C(7')), 134.3 (C(4')), 137.1 (C(3')), 137.3 (C(4a')), 150.6 (C(1')).

2-Decylisoquinolin-2-ium bromide **[C_{10}IQBr]** (Figure 14). Brownish solid. Yield = 75 %. ^{1}H NMR (400 MHz, $CDCl_3$): δ = 0.85 (3H, *t*, *J* = 6.9 Hz, H(10)), 1.15 – 1.49 (14H, *m*, H(3) – H(9)), 2.06 – 2.21 (2H, *m*, H(2)), 5.09 (2H, *t*, *J* = 7.4 Hz, H(1)), 7.95 (1H, *ddd*, *J* = 8.2, 6.7, 1.4 Hz, H(7')), 8.08 – 8.20 (2H, *m*, H(5'), H(6')), 8.40 (1H, *d*, *J* = 6.8 Hz, H(4')), 8.74 – 8.84 (2H, *m*, H(3'), H(8')), 11.10 (1H, *dd*, H(1')). ^{13}C NMR (101 MHz, $CDCl_3$): δ = 14.1 (C(10)), 22.7 (C(9)), 26.2 (C(3)), 29.1 (C(7)), 29.2 (C(4)), 29.3 (C(6)), 29.4 (C(5)), 31.8 (C(2)), 31.9 (C(8)), 61.7 (C(1)), 126.2 (C(8')), 127.0 (C(5')), 128.0 (C(8a')), 131.4 (C(6')), 131.5 (C(7')), 134.2 (C(4')), 137.1 (C(3')), 137.3 (C(4a')), 150.8 (C(1')).

4-methylpyridinium−based ILs

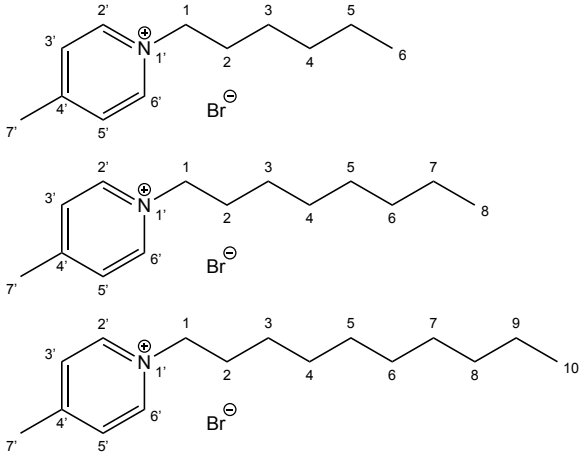

[C_6mPyrBr]

[C_8mPyrBr]

[C_{10}mPyrBr]

Figure 15. Structural formulae and numbering of [C_6mPyrBr], [C_8mPyrBr], [C_{10}mPyrBr].

1-Hexyl-4-methylpyridin-1-ium bromide **[C_6mPyrBr]** (Figure 15). Red oil. Yield = 93 %. ^{1}H NMR (400 MHz, $CDCl_3$): δ = 0.86 (3H, *t*, *J* = 7.1 Hz, H(6)), 1.19 – 1.45 (6H, *m*, H(3) – H(5)), 1.94 – 2.12 (2H, *m*, H(2)), 2.68 (3H, *s*, H(7')), 4.90 (2H, *t*, *J* = 7.4 Hz, H(1)), 7.92 (2H, *d*, *J* = 6.7 Hz, H(3'), H(5')), 9.36 (2H, *d*, *J* = 6.7 Hz, H(2'), H(6')). ^{13}C NMR (101 MHz, $CDCl_3$): δ = 14.0 (C(6)), 22.3 (C(7')), 22.5 (C(5)), 25.8 (C(3)), 31.2 (C(2)), 31.9 (C(4)), 61.4 (C(1)), 129.0 (C(3'), C(5')), 144.4 (C(2'), C(6')), 158.9 (C(4')).

4-Methyl-1-octylpyridin-1-ium bromide **[C_8mPyrBr]** (Figure 15). Red oil. Yield = 78 %. ^{1}H NMR (400 MHz, $CDCl_3$): δ = 0.86 (3H, *t*, *J* = 6.9 Hz, H(8)), 1.15 – 1.44 (10H, *m*, H(3) – H(7)), 1.94 – 2.08 (2H, *m*, H(2)), 2.68 (3H, *s*, H(7')), 4.91 (2H, *t*, *J* = 7.4 Hz, H(1)), 7.91 (2H, *d*, *J* = 6.7 Hz, H(3'), H(5')), 9.34 (2H, *d*, *J* = 6.7 Hz, H(2'), H(6')). ^{13}C NMR (101 MHz, $CDCl_3$):

δ = 14.1 (C(8)), 22.3 (C(7')), 22.6 (C(7)), 26.1 (C(3)), 29.0 (C(5)), 29.0 (C(4)), 31.7 (C(2)), 31.9 (C(6)), 61.4 (C(1)), 128.9 (C(3'), C(5')), 144.4 (C(2'), C(6')), 158.9 (C(4')).

1-Decyl-4-methylpyridin-1-ium bromide **[C_{10}mPyrBr]** (Figure 15). Red oil. Yield = 98 %. ^{1}H NMR (400 MHz, $CDCl_3$): δ = 0.87 (3H, *t*, *J* = 6.9 Hz, H(10)), 1.12 – 1.45 (14H, *m*, H(3) – H(9)), 1.94 – 2.10 (2H, *m*, H(2)), 2.68 (3H, *s*, H(7')), 4.91 (2H, *t*, *J* = 7.4 Hz, H(1)), 7.90 (2H, *d*, *J* = 6.7 Hz, H(3'), H(5')), 9.31 (2H, *d*, *J* = 6.7 Hz, H(2'), H(6')). ^{13}C NMR (101 MHz, $CDCl_3$): δ = 14.1 (C(10)), 22.3 (C(7')), 22.7 (C(9)), 26.1 (C(3)), 29.1 (C(7)), 29.3 (C(6)), 29.4 (C(5)), 29.5 (C(4)), 31.8 (C(2)), 31.9 (C(8)), 61.4 (C(1)), 128.9 (C(3'), C(5')), 144.4 (C(2'), C(6')), 158.9 (C(4')).

Quinolinium−based ILs

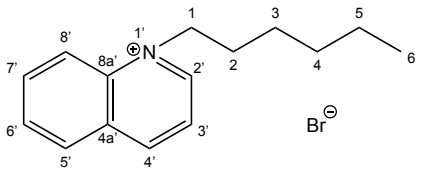

[C_6QBr]

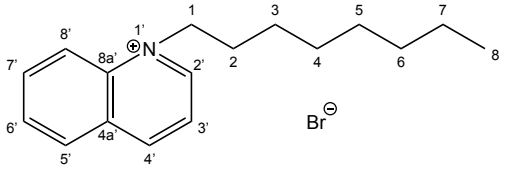

[C_8QBr]

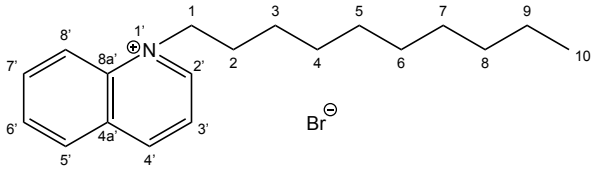

[C_{10}QBr]

Figure 16. Structural formulae and numbering of [C_6QBr], [C_8QBr], [C_{10}QBr].

1-Hexylquinolin-1-ium bromide **[C_6QBr]** (Figure 16). Dark-red solid. Yield = 78 %. ^{1}H NMR (400 MHz, $CDCl_3$): 0.87 (3H, *t*, *J* = 7.1 Hz, H(6)), 1.24 – 1.41 (4H, *m*, H(4), H(5)), 1.45 – 1.61 (2H, *m*, H(3)), 2.05 – 2.19 (2H, *m*, H(2)), 5.42 (2H, *t*, *J* = 7.6 Hz, H(1)), 7.98 (1H, *ddd*, *J* = 8.0, 7.0, 1.0 Hz, H(6')), 8.19 – 8.25 (2H, *m*, H(3'), H(7')), 8.31 – 8.38 (2H, *m*, H(5'), H(8')), 9.06 (1H, *d*, *J* = 8.3 Hz, H(2')), 10.64 (1H, *dd*, *J* = 5.9, 1.4 Hz, H(4')). ^{13}C NMR (101 MHz, $CDCl_3$): δ = 13.9 (C(6)), 22.4 (C(5)), 26.2 (C(3)), 30.4 (C(2)), 31.2 (C(4)), 58.2 (C(1)), 118.4 (C(8')), 122.7 (C(3')), 130.0 (C(4a')), 130.2 (C(6')), 131.2 (C(5')), 136.0 (C(7')), 137.7 (C(8a')), 147.3 (C(2')), 150.6 (C(4')).

1-Octylquinolin-1-ium bromide **[C_8QBr]** (Figure 16). Dark-red solid. Yield = 85 %. ^{1}H NMR (400 MHz, $CDCl_3$): δ = 0.84 (3H, *t*, *J* = 7.1 Hz, H(8)), 1.16 – 1.40 (8H, *m*, H(4) – H(7)), 1.46 – 1.58 (2H, *m*, H(3)), 2.05 – 2.16 (2H, *m*, H(2)), 5.43 (2H, *t*, *J* = 7.6 Hz, H(1)), 7.97 (1H, *ddd*,

J = 8.0, 7.0, 0.9 Hz, H(6')), 8.18 – 8.26 (2H, *m*, H(3'), H(7')), 8.33 – 8.40 (2H, *m*, H(5'), H(8')), 9.10 (1H, *d*, *J* = 8.3 Hz, H(2')), 10.61 (1H, *dd*, *J* = 5.8, 1.4 Hz, H(4')). ^{13}C NMR (101 MHz, $CDCl_3$): δ = 14.0 (C(8)), 22.6 (C(7)), 26.5 (C(3)), 29.0 (C(5)), 29.1 (C(4)), 30.5 (C(2)), 31.7 (C(6)), 58.2 (C(1)), 118.3 (C(8')), 122.8 (C(3')), 130.0 (C(4a')), 130.1 (C(6')), 131.1 (C(5')), 135.9 (C(7')), 137.7 (C(8a')), 146.8 (C(2')), 151.0 (C(4')).

1-Decylquinolin-1-ium bromide **[C_{10}QBr]** (Figure 16). Dark-red solid. Yield = 45 %. ^{1}H NMR (400 MHz, $CDCl_3$): δ = 0.85 (3H, *t*, *J* = 7.1 Hz, H(10)), 1.15 – 1.40 (12H, *m*, H(4) – H(9)), 1.45 – 1.57 (2H, *m*, H(3)), 2.06 – 2.16 (2H, *m*, H(2)), 5.43 (2H, *t*, *J* = 7.6 Hz, H(1)), 7.97 (1H, *ddd*, *J* = 8.0, 7.0, 0.9 Hz, H(6')), 8.18 – 8.25 (2H, *m*, H(3'), H(7')), 8.34 – 8.40 (2H, *m*, H(5'), H(8')), 9.11 (1H, *d*, *J* = 8.4 Hz, H(2')), 10.61 (1H, *dd*, *J* = 5.9, 1.4 Hz, H(4')). ^{13}C NMR (101 MHz, $CDCl_3$): δ = 14.1 (C(10)), 22.6 (C(9)), 26.5 (C(3)), 29.2 (C(7)), 29.2 (C(4)), 29.4 (C(6)), 29.5 (C(5)), 30.5 (C(2)), 31.8 (C(8)), 58.2 (C(1)), 118.3 (C(8')), 122.7 (C(3')), 130.0 (C(4a')), 130.1 (C(6')), 131.2 (C(5')), 135.9 (C(7')), 137.7 (C(8a')), 147.1 (C(2')), 150.8 (C(4')).

Pyridinium−based ILs

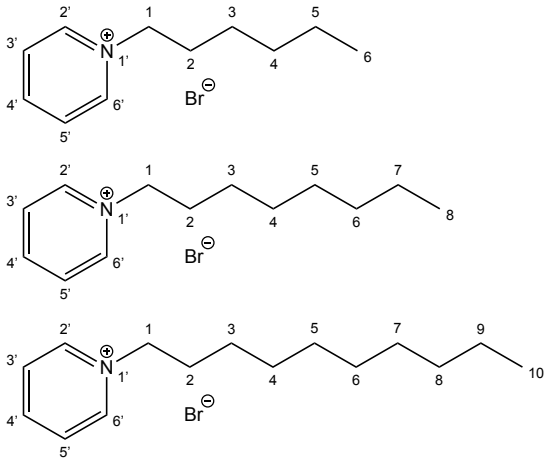

Figure 17. Structural formulae and numbering of [C_6PyrBr], [C_8PyrBr], [C_{10}PyrBr].

1-Hexylpyridin-1-ium bromide **[C_6PyrBr]** (Figure 17). Pale orange viscous oil. Yield = 98 %. ^{1}H NMR (400 MHz, $CDCl_3$): δ = 0.87 (3H, *t*, *J* = 7.1 Hz, H(6)), 1.20 – 1.46 (6H, *m*, H(3) – H(5)), 2.00 – 2.12 (2H, *m*, H(2)), 5.01 (2H, *t*, *J* = 7.5 Hz, H(1)), 8.18 (2H, *dd*, *J* = 7.8, 6.5 Hz, H(3'), H(5')), 8.56 (1H, *tt*, *J* = 7.8, 1.4 Hz, H(4')), 9.56 (2H, *dd*, *J* = 6.5, 1.4 Hz, H(2'), H(6')). ^{13}C NMR (101 MHz, $CDCl_3$): δ = 13.9 (C(6)), 22.4 (C(5)), 25.7 (C(3)), 31.1 (C(2)), 32.0 (C(4)), 62.1 (C(1)), 128.5 (C(3'), C(5')), 145.2 (C(2'), C(4') and C(6')).

1-Octylpyridin-1-ium bromide **[C_8PyrBr]** (Figure 17). Pale orange viscous oil. Yield = 99 %. ^{1}H NMR (400 MHz, $CDCl_3$): δ = 0.85 (3H, *t*, *J* = 7.1 Hz, H(8)), 1.15 – 1.46 (10H, *m*, H(3)

– H(7)), 1.93 – 2.13 (2H, *m*, H(2)), 5.02 (2H, *t*, *J* = 7.5 Hz, H(1)), 8.16 (2H, *dd*, *J* = 7.8, 6.5 Hz, H(3'), H(5')), 8.54 (1H, *tt*, *J* = 7.8, 1.4 Hz, H(4')), 9.52 (2H, *dd*, *J* = 6.5, 1.4 Hz, H(2'), H(6')). ^{13}C NMR (101 MHz, $CDCl_3$): δ = 14.1 (C(8)), 22.6 (C(7)), 26.1 (C(3)), 29.0 (C(5)), 29.0 (C(4)), 31.7 (C(2)), 32.0 (C(6)), 62.2 (C(1)), 128.5 (C(3'), C(5')), 145.1 (C(2'), C(4') and C(6')).

1-Decylpyridin-1-ium bromide **[C_{10}PyrBr]** (Figure 17). Pale orange viscous oil. Yield = 99 %. ^{1}H NMR (400 MHz, $CDCl_3$): δ = 0.86 (3H, *t*, *J* = 7.1 Hz, H(10)), 1.17 – 1.44 (14H, *m*, H(3) – H(9)), 1.96 – 2.09 (2H, *m*, H(2)), 5.01 (2H, *t*, *J* = 7.5 Hz, H(1)), 8.17 (2H, *dd*, *J* = 7.8, 6.7 Hz, H(3'), H(5')), 8.54 (1H, *tt*, *J* = 7.8, 1.4 Hz, H(4')), 9.51 (2H, *dd*, *J* = 6.7, 1.4 Hz, H(2'), H(6')). ^{13}C NMR (101 MHz, $CDCl_3$): δ = 14.1 (C(10)), 22.7 (C(9)), 26.1 (C(3)), 29.1 (C(7)), 29.2 (C(6)), 29.3 (C(5)), 29.4 (C(4)), 31.8 (C(2)), 32.0 (C(8)), 62.2 (C(1)), 128.4 (C(3'), C(5')), 145.1 (C(2'), C(4') and C(6')).

2.1.4.2 General synthetic procedure to obtain triethylammonium salts

Triethylamine (1.2 eq.), 4 mL of acetonitrile (ACN) and the appropriate bromoalkane (0.5 mL; 1 eq.) were added to a 2-5 mL glass vial. The reaction mixture was stirred and heated to 85 ºC for 48 h. Acetonitrile was evaporated and the reaction mixture was poured into water (15 mL) and extracted with diethyl ether (2 × 5 mL). The aqueous phases were combined, and the solvent was evaporated under reduced pressure. The synthetic procedure was based on the method reported by Meng *et al* [134]. The structural analysis of compounds [C_nTEABr] are described below.

Triethylammonium−based ILs

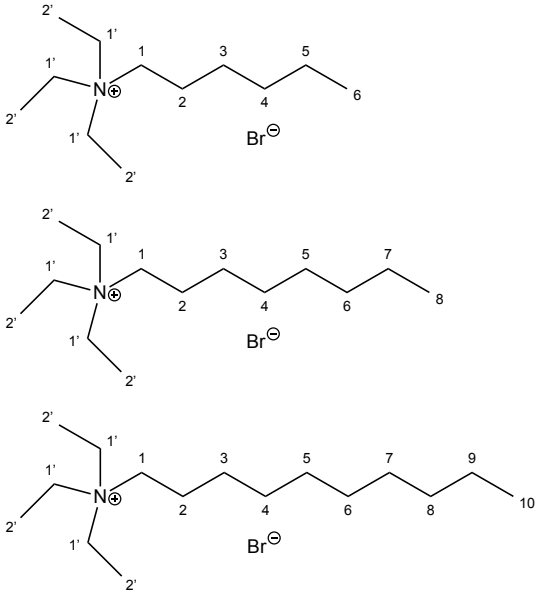

[C_6TEABr]

[C_8TEABr]

[C_{10}TEABr]

Figure 18. Structural formulae and numbering of [C_6TEABr], [C_8TEABr], [C_{10}TEABr].

N,N,N-Triethylhexan-1-aminium bromide **[C_6TEABr]** (Figure 18). White foam. Yield = 77 %. ^{1}H NMR (400 MHz, $CDCl_3$): δ = 0.90 (3H, *t*, *J* = 7.1 Hz, H(6)), 1.26 – 1.49 (6H, *m*, H(3) – H(5)), 1.40 (9H, *t*, *J* = 7.3 Hz, 3 × H(2')), 1.63 – 1.77 (2H, *m*, H(2)), 3.19 –3.39 (2H, *m*, H(1)), 3.53 (6H, *q*, *J* = 7.3 Hz, 3 × H(1')). ^{13}C NMR (101 MHz, $CDCl_3$): δ = 8.2 (3 × C(2')), 14.0 (C(6)), 22.2 (C(5)), 22.4 (C(3)), 26.2 (C(2)), 31.2 (C(4)), 53.7 (3 × C(1')), 57.7 (C(1)).

N,N,N-Triethyloctan-1-aminium bromide **[C_8TEABr]** (Figure 18). White foam. Yield = 84 %. ^{1}H NMR (400 MHz, $CDCl_3$): δ = 0.88 (3H, *t*, *J* = 6.9 Hz, H(8)), 1.17 – 1.49 (10H, *m*, H(3) – H(7)), 1.40 (9H, *t*, *J* = 7.3 Hz, 3 × H(2')), 1.62 – 1.78 (2H, *m*, H(2)), 3.25 – 3.30 (2H, *m*, H(1)), 3.52 (6H, *q*, *J* = 7.3 Hz, 3 × H(1')). ^{13}C NMR (101 MHz, $CDCl_3$): δ = 8.2 (3 × C(2')), 14.0 (C(8)), 22.1 (C(7)), 22.6 (C(2)), 26.5 (C(3)), 29.1 (C(5)), 29.2 (C(4)), 31.8 (C(6)), 53.7 (3 × C(1')), 57.7 (C(1)).

N,N,N-Triethyldecan-1-aminium bromide **[C_{10}TEABr]** (Figure 18). White foam. Yield = 81 %. ^{1}H NMR (400 MHz, $CDCl_3$): δ = 0.88 (3H, *t*, *J* = 6.9 Hz, H(10)), 1.18 – 1.50 (14H, *m*, H(3) – H(9)), 1.40 (9H, *t*, *J* = 7.3 Hz, 3 × H(2')), 1.63 – 1.77 (2H, *m*, H(2)), 3.10 – 3.32 (2H, *m*, H(1)), 3.53 (6H, *m*, *J* = 7.3 Hz, 3 × H(1')). ^{13}C NMR (101 MHz, $CDCl_3$): δ = 8.2 (3 × C(2')), 14.1 (C(10)), 22.1 (C(9)), 22.7 (C(2)), 26.5 (C(3)), 29.2 (C(7)), 29.2 (C(4)), 29.4 (C(5)), 31.8 (C(8)), 53.6 (3 × C(1')), 57.6 (C(1)).

2.1.5. Evaluation of drug-likeness properties

The drug-likeness properties of the synthetized compounds were analysed according to the Lipinski's "rule of five" which predicts the absorption, distribution, metabolism and excretion (ADME), using the Molinspiration Cheminformatics software [htttp://www.molinspiration.com] for parameters determination.

2.2. Microbiological Studies

2.2.1. Experimental setup and design

The protocol described below was delineated for bacterial studies with *S. aureus* CECT 976. This bacterial strain is commonly used as routine quality control, and as reference for antimicrobial testing [135].

In vitro antimicrobial susceptibility testing methods are widely used in clinical practice to assess the potential therapeutic value of antibiotics [136]. When assessing the susceptibility of bacteria to antimicrobial products it is important to promote the uniform application of

terminology to the methods used. According to Clinical and Laboratory Standards Institute (CLSI) and European Committee on Antimicrobial Susceptibility Testing (EUCAST), the dilution methods (agar dilution and broth microdilution) are the most common designated standard reference methods for antimicrobial susceptibility testing [137]. As with any test of antibiotic activity, it is of utmost importance specifications regarding the inoculum size, the medium composition, the incubation time and the inoculum preparation. Therefore, broth microdilution method carried out has been standardized by CLSI for testing bacterium. If rigorously implemented according to the procedures described herein, the uniformity of the result obtained among different laboratories as well as clinical relevance of results are guarantee.

The medium of choice for the susceptibility testing should fulfil the following requirements: (i) the composition of the medium should give sufficient growth for the tested strain; (ii) the medium must not contain material that would interfere with the test itself or react with any antimicrobial agent tested, and (iii) the media used in performing such tests should be specifically formulated [136]. As the CLSI-recommended method, the broth microdilution was performed with Mueller-Hinton broth (MHB) and does not require supplementation. MHB is a general-purpose medium that may be used in the cultivation of a wide variety of nonfastidious microorganisms [138].

For the preparation of the inoculum, a fresh pure culture should be used. Besides that, the standardization of the bacterial cell number used is of critical importance as the interpretation of the results is based on a certain inoculum. Both inoculum size and growth phase may lead to false results regarding antibacterial susceptibility.

A standardized bacterial suspension may be prepared by the growth method using either fresh or overnight cultures, or by direct suspension of organisms to the turbidity of the 0.5 McFarland standard [138]. In this Thesis, the growth method using overnight cultures was preferred for *S. aureus*. The density of the bacterial suspension was assessed spectrophotometrically at OD_{600nm} and adjust turbidity to equivalent 0.5 McFarland units/1-2 $\times$ 10^8 CFU/mL. CLSI [139] recommended a final inoculum size for susceptibility testing of aerobic bacteria in broth around of 5 $\times$ 10^5 CFU/mL. Incubation is typically in air at 35 $\pm$ 2 ºC, overnight (16h-20 h), and increased CO_2 is not required.

Experimental controls are necessary for test validation of the potential antibiotics or other compounds with antibacterial activity. For broth microdilution, a column containing only medium was included as a control, to ensure that the microplates maintain the sterility during the assay running. To ensure that the bacterium in study is in perfect condition and

grown normally a growth control was included by comparison with medium only. As some of the synthetized compounds were not soluble in water, the solvent DMSO was used for their preparation, and so was tested for their antimicrobial activity (as negative control).

2.2.2. Microorganism and culture conditions

The Gram-positive bacterium *S. aureus* CECT 976, obtained from the Spanish Type Culture Collection, was selected for this study. The bacterium was stored at −80 ºC, in a mixture of MHB (Oxoid, England) and 30 % (v/v) glycerol, and prior to use, transferred onto Plate Count Agar (PCA, Merck) at 37 ºC for 24 h. Bacterial suspensions were obtained from overnight culture (16-18 h) in 100 mL flasks containing 50 mL of MHB, at 37 ºC under agitation (150 rpm; Orbital IKA KS, 130 basic, Germany).

2.2.3. Preparation of the solutions of alkyl cationic derivatives

The compounds tested included the previously synthetized twenty-one alkyl cationic derivatives (aforementioned conditions). The collection includes C6, C8 and C10 alkyl cationic derivatives.

Each compound was tested at different concentrations in the range of 0.0625 to 64 µg/mL prepared in sterile distillate water or DMSO (99 % v/v). The concentrations tested (0.0625, 0.125, 0.25, 0.5, 1, 2, 4, 8, 16, 32, 64 µg/mL) were chosen based in the range of the expected MIC determined by preliminary results of broth microdilution assays. Stock solutions/serial dilutions of all the compounds were kept in the dark and stored at 4 ºC prior to use.

2.2.4. Determination of the minimum inhibitory concentration (MIC)

The MIC of each compound was determined by the broth microdilution method according to the CLSI guidelines [140]. After overnight growth at 37 ºC in MHB an inoculum was taken, and bacterial culture was adjusted to the O.D = 0.132 $\pm$ 0.02 (λ = 600 nm). MIC values were determined in sterile 96-well polystyrene microtiter plates (VWR). In each well, a volume of 20 µL of each compound (10% v/v) at different concentrations was added to 180 µL of bacterial suspension (90% v/v). Cell suspensions only with DMSO and cell suspensions without alkyl cationic derivatives were used as negative controls. After 24 h incubation at 37 ºC and 150 rpm, the bacterial growth was analysed by absorbance (λ = 600 nm) measurement in a microtiter plate reader (SpectraMax M2e, Molecular Devices, Inc). The MIC value was recorded as the lowest concentration of a compound that inhibits the growth

of a microorganism (*i.e.*, corresponds to the concentration in which the final OD was equal or bellow to the initial OD.) [135]. All tests were performed with six replicates and a minimum of two independent repeats.

2.2.5. Determination of the minimum bactericidal concentration (MBC)

In order to determine the MBC, 10 µL of each concentration tested for MIC assessment was plated out on PCA and incubated at 37 ºC for 24 h. The MBC of each compound was recorded as the lowest concentration which totally inhibited the bacterial growth on solid medium [141]. All tests were performed in triplicate with a minimum of two independent repeats.

2.3. Human cell Studies

2.3.1. Experimental setup and design

In parallel with the assessment of microbiological activity, the evaluation of the cytotoxic profile of alkyl cationic derivatives is of great relevance in the process of developing new therapeutic agents, as their detrimental effects may severely compromise their clinical application [142].

The gold standard toxicological approach for evaluating chemical toxicity involves complex and time-consuming *in vivo* studies. However, due to concerns about animal welfare, time and cost constraints, establishing workable *in vitro* culture systems has become a priority for the toxicological community [143]. Indeed, if the experiment characteristics are well defined, *in vitro* systems for toxicological evaluation can be predictive of susceptibility observed in *in vivo* models. The cellular tests currently used for the toxicity evaluation, measure the concentration of a chemical substance which damages components, structures, or biochemical pathways within the cells. This range of injury is further specified by the length of exposure to the chemical, allowing the test to be predictive for risks associated with toxic effects *in vivo* [144].

The first variables to consider are the cell model and the tissue origin of the cell model being used. Accumulating data indicates the important role of the kidney in the metabolism, transport and clearance of many xenobiotics and prescription drugs [145,146]. As the kidney is one of the targets for drug-induced toxicity, the human proximal tubule epithelial cell line HK-2 was chosen for the preliminary cytotoxicity studies. Besides the kidney, the liver is known to be one of the main targets for drug toxicity in humans [142,143]. Hence,

the immortalized human hepatocarcinoma cell line HepG2 was also chosen for the cytotoxicity studies. These cells preserve morphological and functional differentiation of *in vivo* hepatocytes and a wide variety of enzymes involved in the metabolism and detoxification of xenobiotics. Therefore, it was considered an appropriate model to attain the goals of the Thesis [142,147].

An important factor influencing the growth of cells in culture is the choice of tissue culture medium. Indeed, the composition of cell culture medium may vary extensively, and depending on the experimental conditions may affect the results from biochemical, toxicological and pharmacological studies [148]. Information for selecting the appropriate medium for a given cell type is usually available in published literature and may also be obtained from certified cell banks. In this Thesis, HK-2 cells were maintained in RPMI-1640 medium (Sigma-Aldrich, Catalog No. R6504), that includes glutathione and high concentrations of vitamins as well as biotin, vitamin B12, and 4-aminobenzoic acid (PABA) [148]. HepG2 cells were maintained on a relatively simple medium such as Dulbecco's modified Eagle's medium (DMEM, Sigma-Aldrich, Catalog No. D7777). As per vendor indications, powdered medium is formulated without proteins or growth promoting agents. Therefore, it requires supplementation with 10 % v/v of Fetal Bovine Serum (FBS), 1 % antibiotic and sodium bicarbonate (3.7 g/L) for use with 5 % CO_2.

Other important factors to consider regarding the design of the study are the doubling rate of the cell line, and the initial cell seeding density. The first one refers to the time it takes cells to double in number, while the second one is the number of cells at time zero placed on the growth material per unit area. Each cell line has a specific doubling rate, and this information has to be considered when evaluating the number of cells that will be used as the seeding density [149]. Adjusting the initial cell seeding density is important in standardization of culture conditions and in performing accurate quantitative experiments. Cells plated at too low density may be inhibited/delayed in entry into growth stage and may not be detectable by some of the most common toxicity assays. On the other side, cells plated at too high density may reach confluence too fast, leading to cell loss and/or cessation of proliferation; and consequently, be out of the measuring range of these same assays [150]. In all experiments, HK-2 cells were seeded in a 96-well plate at an initial concentration of 5,000 cells/well, while HepG2 cells were seeded at density of 25,000 cells/well.

The choice of the method for the measurement of cell viability depends on the particular cellular process of interest, as different cytotoxicity effects can be detected with various end points experiments (Figure 19). Accordingly, simultaneous use of two or more dissimilar

assays can indicate more or less sensitive cellular compartments to the chemical compound under investigation [151]. In this study, three different cell viability assays were performed. Cell metabolic competence was measured by reduction of 3-(4,5-dimethylthiazol-2-yl)-2,5-diphenyltetrazolium bromide (MTT), lysosomal activity by neutral red (NR) uptake assay and the protein inhibition assay by affinity of electrostatic binding of protein with Sulforhodamine B dye (SRB).

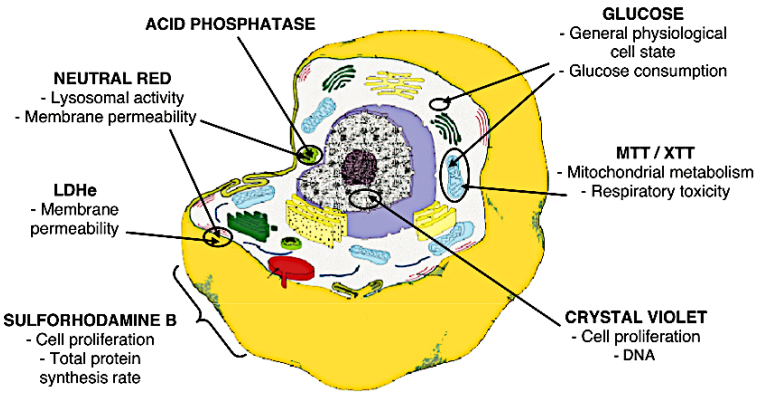

Figure 19. Cell viability assays and associated targets in cell (Adapted from [152]).

Experimental controls are required for test validation of the toxic compound. In all experiments, a solvent control (cells treated with 0.1 % DMSO, v/v) was included to mimic the maximum concentration of DMSO present in the treatments. In preliminary assays, a negative control (complete cell culture medium without treatments) was also included. No significant differences (p > 0.05) were observed between solvent and negative controls (data not shown).

2.3.2. Reagents and solvents

All reagents used in this study were of analytical grade or of the highest grade available. Human proximal tubule epithelial cell line HK-2 and human hepatocarcinoma cell line HepG2 were purchased from American Type Culture Collection (ATCC, Manassas, VA, USA). DMEM with 4.5 g/L glucose, RPMI-1640 medium, NR solution, MTT and dichloro-dihydrofluorescein diacetate (DCFH-DA) probe were obtained from Sigma-Aldrich (St. Louis, MO, USA). FBS, 0.25 % trypsin, antibiotic (penicillin 10,000 U/mL + streptomycin 10,000 µg/mL), phosphate-buffered saline solution (PBS) and Hank's balanced salt solution without calcium and magnesium (HBSS) were purchased from Gibco Laboratories (Lenexa, KS, USA). Dimethylsulfoxide (DMSO) and acetic acid were obtained from Merck (Darmstadt, Germany). Water was Milli-Q filtered (conductivity < 0.1 µS cm^{-1}).

2.3.3. Cell line and culture conditions

HK-2 cells (ATCC® CRL-2190™) were cultured in 75-cm^2 flasks using RPMI-1640 medium, supplemented with 10 % FBS (v/v), sodium bicarbonate (2 g/L) and 1 % penicillin/streptomycin (v/v) at 37 ºC in a humidified 5 % CO_2 – 95 % air atmosphere. Cultures were passaged by trypsinization (0.25 % trypsin) when cells reached 70-80 % confluence and were subcultured over a maximum of 10 passages. For all experiments, cells were plated onto 96-well plates at a density of 5,000 cells/well (150 µL of suspension to each well) and placed in the incubator at 37 ºC, for 24 h, prior to the compound treatments.

HepG2 cells (ATCC® HB-8065™) were routinely maintained in 75-cm^2 flasks and cultured as monolayer in DMEM with 4.5 g/L glucose, supplemented with 10 % FBS (v/v), sodium bicarbonate (3.7 g/L) and 1 % penicillin/streptomycin (v/v). Cells were maintained at 37ºC, in a humidified 5 % CO_2 – 95 % air atmosphere. Cultures were passaged by trypsinization (0.25 % trypsin) when cells reached 70-80 % confluence and were subcultured over a maximum of 10 passages. For all experiments, cells were plated onto 96-well plates at a density of 25,000 cells/well (150 µL of suspension to each well) and placed in the incubator at 37 ºC, for 24 h, prior to the compound treatments.

2.3.4. Incubation of the solutions of alkyl cationic derivatives

On the day of the experiment, the medium was removed and the cells were exposed to a set of concentrations of each alkyl cationic derivative (2, 4, 8, 16, 32, 64, 90, 128 µg/mL) for a fixed time interval (24 h). The range of concentrations were selected on the basis of the concentrations tested from previous study (See *Section 2.2.3.)* for the evaluation of the antimicrobial activity.

Stock solutions (128 mg/mL) were prepared in DMSO and stored at −20ºC, whereas test dilutions were freshly prepared in complete cell culture medium on the day of the experiment (ensuring that DMSO did not exceed 0.1 % of the exposure media in the cell viability assays).

2.3.5. Cell viability evaluation

After 24 h exposure to each of the cell lines, colorimetric assays for the quantification of the metabolic competence, lysosomal integrity and activity, and total protein synthesis rate of cells were evaluated in response to alkyl cationic derivatives treatment.

2.3.5.1 3-(4,5-dimethylthiazol-2-yl)-2,5-diphenyltetrazolium bromide reduction assay

In the MTT reduction assay, the water-soluble MTT tetrazolium salt is reduced inside viable cells with active metabolism to an insoluble purple formazan product [153]. The reduction of the tetrazolium salt is explicitly carried out by oxidoreductase enzymes in the mitochondria, as well as by endosome and lysosome compartments [154]. As the quantity of MTT reduction is directly proportional to the number of viable cells in the culture, it enables the estimation of cell viability by measuring the optical density (OD) of the purple formazan product produced by the cells [142,155]. Therefore, if cell viability is affected by the presence of the test compound, less dye would be reduced and the optical density measured would in turn be lower (Figure 20).

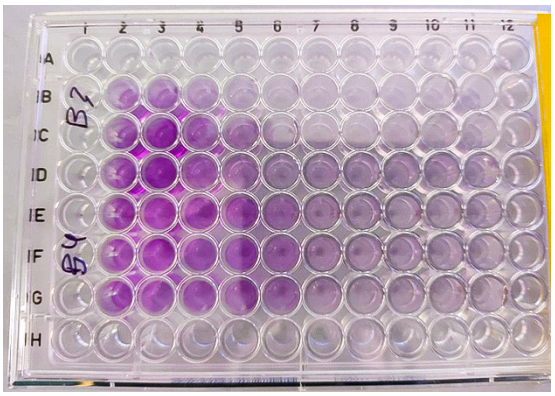

Figure 20. A profile of microtiter plate after an MTT assay. High intensity of the purple colour indicates greater cell viability, while the decrease in the intensity of the purple colour means the reduced number of cells (cytotoxicity of the given test compound).

The MTT reduction assay was performed as previously described by Chavarria *et al*. [156]. After the incubation periods with test compounds, the cell culture medium was removed and 150 µL of 0.5 mg/mL MTT (prepared in fresh culture medium) were added to the attached cells. The plates were incubated for 2 h at 37 ºC in a humidified, 5 % CO_2 – 95 % air atmosphere. Then, the MTT solution was aspirated and the formed intracellular formazan crystals were dissolved in 150 µL of DMSO. The plates were shaken for 20 min and, as MTT is photosensitive, all steps of the procedure were executed under light protection. The absorbance was recorded at 550 nm, using a multi-well plate reader BioTek Synergy HT (BioTek Instruments, Inc). Data were normalized to solvent control (100 %) and results were graphically presented as percentage of MTT reduction relative to control *versus* concentration (µg/mL).

2.3.5.2 Neutral red uptake assay

The NR uptake assay relies upon the uptake of the weakly cationic dye NR, which preferentially concentrates in the lysosomes and endosomes of viable cells, but not in dead or dying cells, by non-ionic passive diffusion [157] (Figure 21). Consequently, after washing, viable cells can release the incorporated dye in under acidified extracted conditions. The amount of released dye can be quantified spectroscopically by the OD at 540 nm [158]. The estimation of dye extracted from the cells after their exposure to alkyl cationic derivatives is indirectly proportional to the drug-induced toxicity.

Figure 21. The last three filled lines of the microtiter plate show the appearance of the microtiter plate after adding NR solution.

The NR uptake assay was performed as previously described by Fernandes *et al*. [159]. At the end of the incubation periods with the test compounds, the cell culture medium was removed and 150 µL of 50 µg/mL NR solution (prepared in fresh culture medium) were added to the attached cells. The plates were incubated at 37 ºC in a humidified, 5 % CO_2 – 95 % air atmosphere for 2 h. Then, the NR solution was aspirated and 100 µL of a bleaching solution containing 50 % ethanol, 49 % distilled water and 1 % acetic acid was added to extract the NR dye meanwhile captured within the cells. The plates were then shaken for 20 min, at room temperature and protected from light. The absorbance was measured at 540 nm, using a multi-well plate reader BioTek Synergy HT (BioTek Instruments, Inc) and results were compared to solvent control whose average of values was set to 100 %.

2.3.5.3 Sulforhodamine B assay

The SRB assay is based on the ability of the dye SRB to bind electrostatically to protein basic amino acid residues of fixed cells, on a pH-dependent manner. Under slightly acidic conditions, SRB binds to the basic amino acid residues present in proteins, and under basic conditions, SRB can be extracted from these residues [160]. As the binding of SRB is

stoichiometric, the amount of dye extracted from stained cells after washing is directly proportional to the cell biomass and OD can be measured at 540 nm [161]. SRB assay is one of the most widely used methods for *in vitro* cytotoxicity studies, although it does not distinguish between viable and dead cells and is independent of cell metabolic activity [162].

SRB assay was performed as previously described by Fernandes *et al*. [163]. After the 24 h incubation periods with the test compounds, the cell culture medium was removed, and cells were fixed by adding 100 µL of a methanolic solution of acetic acid (1 %). The plates were incubated at −20ºC for at least 24 h. Thereafter, the plates were gently washed under flowing deionized water and allowed to dry for approximately 1 h before staining with 100 µL of 0.05 % SRB solution. After 1 h the plates were washed with 1 % acetic acid in water to remove excess stain. The plates were again allowed to dry for approximately 1 h. A volume of 150 µL of Tris buffer (10 mM, pH = 10.5) was added and the plates were placed on a shaker until dye was dissolved. The absorbance was measured at 540 nm, using a multi-well plate reader BioTek Synergy HT (BioTek Instruments, Inc) and results were compared to solvent control whose average of values was set to 100 %.

2.3.6. Intracellular ROS and RNS production

The intracellular reactive oxygen (ROS) and nitrogen (RNS) species production was monitored by means of the DCFH-DA assay as previously described by Fernandes *et al*. [163]. In this assay, the diacetate form of the DCFH-DA probe is used since it can freely permeate cell membranes. Once inside the cells, DCFH-DA is hydrolyzed by esterases to the impermeable non-fluorescent reduced dichlorodihydrofluorescein (DCFH) which is rapidly oxidized by the intracellular ROS and RNS to green fluorescent 2',7'-dichlorofluorescein (DCF) [164,165].

For this determination, HK-2 and HepG2 cells were seeded at a density of 5,000 cells/well and 25,000 cells/well, respectively, and pre-incubated with 20 µM DCFH-DA at 37 ºC, in the dark, for 90 min. As DCFH-DA is a non-water-soluble powder, it was initially prepared as a 20 mM stock solution in DMSO and made up to the final concentration in fresh culture medium immediately before each experiment. After removing the culture medium, the cells were incubated with the testing compounds at 37 ºC in a humidified, 5 % CO_2 – 95 % air atmosphere. Fluorescence was measured on a fluorescence microplate reader (BioTek Instruments, Vermont, USA) set to 485 excitation and 528 emission at time 24 h after incubation. Results were normalized to solvent control (100 %) and calculated as fluorescence fold increase over control conditions.

2.3.7. Statistical analysis

Data are expressed as mean ± standard deviation (SD) of three independent experiments, each performed in triplicate, and are presented relative to solvent control (100 %). A parametric analysis of variance (ANOVA) was performed when data distribution was normal. Statistical significance was reached when $p < 0.05$. All statistical analyses were performed in GraphPad Prism version 6.0 software. Details of the statistical analyses are provided in the text and legend of the figures. The solvent and negative control values (raw data) were compared and differences were considered insignificant (data not shown).

Chapter 3

RESULTS AND DISCUSSION

In this section, all the results obtained within this Thesis are described, analysed and discussed. The data analysis will be supported by evidences coming from bibliography. The organization of this chapter is done with the same logic sequence performed in the Experimental Part comprised by Chemical, Microbiological and Human cell Studies.

3.1. Chemical Studies

3.1.1. Synthesis of alkyl cationic derivatives

Alkyl cationic derivatives [C_nTPPBr], [$C_n$mimBr], [C_nIQBr], [C_nmPyrBr], [C_nQBr], [C_nPyrBr], [C_nTEABr] were synthesized *via* a quaternization reaction using commercially available amines or phosphines and suitable bromoalkanes as starting materials (Figure 22). To obtain a concise library of ILs the structural modifications were focused on the structural modification of the cationic moiety (triphenylphosphine, 1-methylimidazole, isoquinoline, 4-picoline, triethylamine, quinoline and pyridine) and on the length of alkyl chain (6- (n=1), 8- (n=3) or 10-carbon atoms (n=5)). The reagents and reaction conditions used for the synthesis of the library of alkyl cationic derivatives are shown in Figure 23.

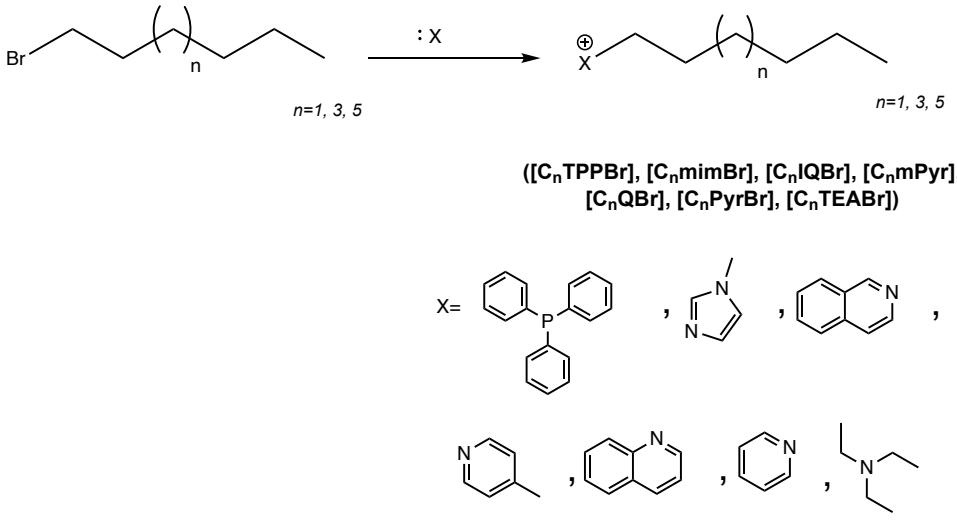

Figure 22. Quaternization reaction followed for the synthesis of the library of alkyl cationic derivatives.

In the case of derivatives [C_nTPPBr], [$C_n$mimBr], [C_nIQBr], [C_nmPyrBr], [C_nQBr], [C_nPyrBr], the reaction was carried out at 130 ºC for approximately 24 h in a hermetically sealed vessel without solvent. The progress of the reaction was monitored by TLC, which was used both for the reaction analysis and to choose the appropriate eluent system(s) for the further purification step. A range of mobile phases was studied (*e.g.*, CH_2Cl_2, EtOAc or EtOAc:MeOH (9:1)). The best resolution was achieved by eluting the TLC plate with the dichloromethane:methanol (9:1) system. After completion of the reaction, the mixture was purified by column chromatography with silica gel as stationary phase and the previous mentioned elution system. The eluent was designed to remove the impurities present in the

crude products. The solvents were then evaporated to dryness and the purified compounds were analysed by NMR for structural identification (see Figure 24).

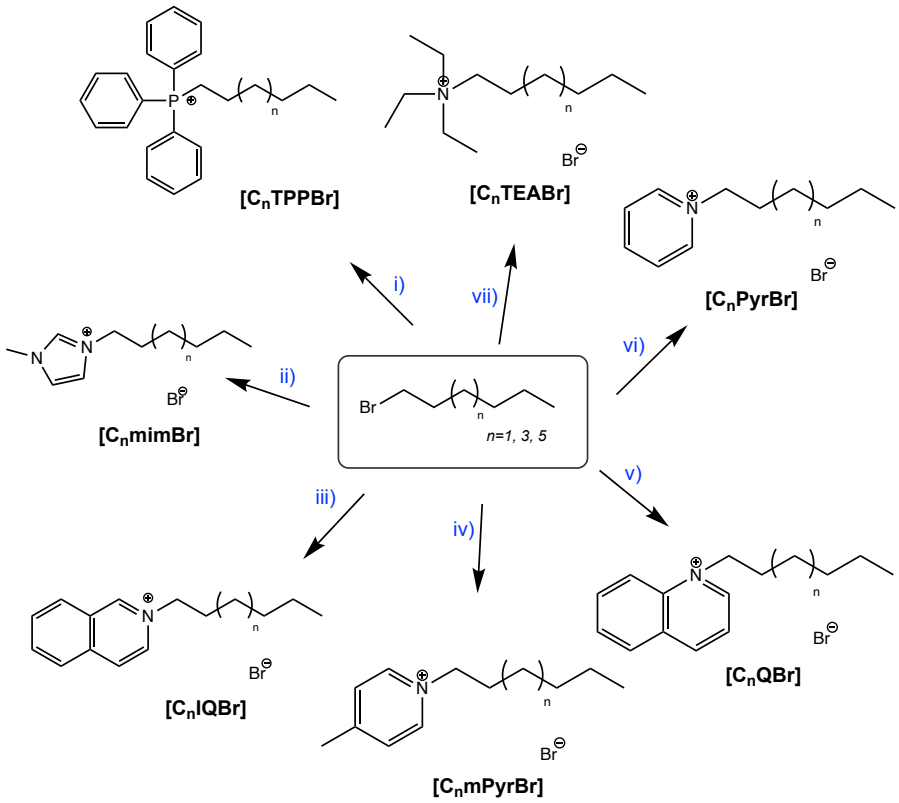

Figure 23. Reagents and reaction conditions used for the synthesis of the library of alkyl cationic derivatives: i) PPh_3, 130 ºC, 24-48 h; ii) $C_4H_6N_2$, 130 ºC, 24 h; iii) C_9H_7N, 130 ºC, 21 h; iv) C_6H_7N, 130 ºC, 24 h; v) C_9H_7N, 130 ºC, 21 h; vi) C_5H_5N, 130 ºC, 24 h; vii) $N(CH_2CH_3)_3$, ACN, reflux, 85 ºC, 48 h.

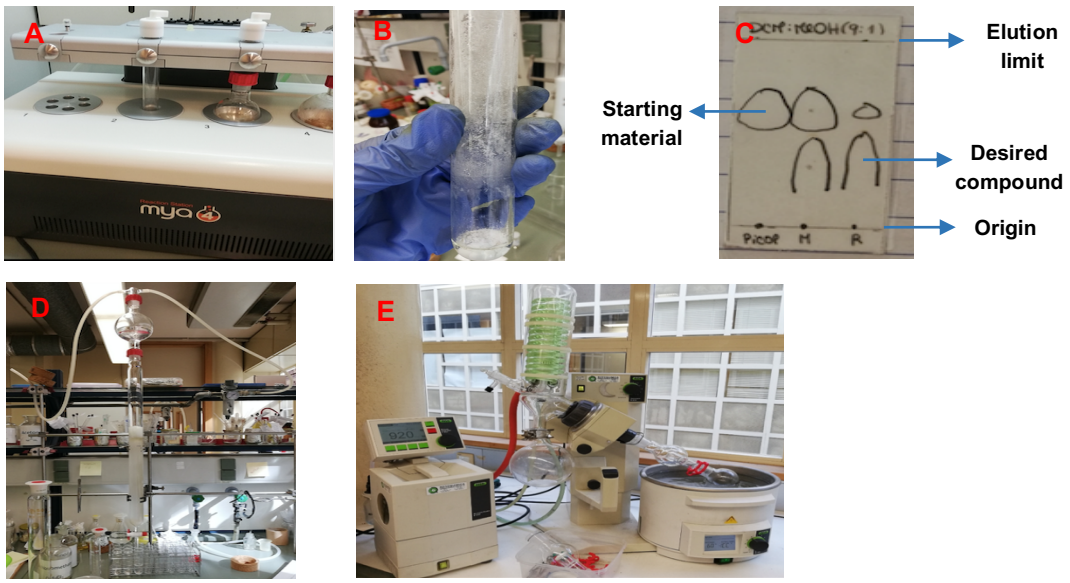

Figure 24. Pictures of the experiment process. **(A)** Mya4 reaction station. Temperature reaction was set to 130 ºC for around 24 h; **(B)** Crude product ([C_nTPPBr]) outlook; **(C)** TLC plate of crude product ([C_nmPyrBr]) using dichloromethane:methanol (9:1) as mobile phase; **(D)** [C_nTPPBr] column chromatography by elution with the mixture of dichloromethane:methanol (9:1); **(E)** Solvent removal using a rotary evaporator.

The preparation of [C_nTEABr] was carried out under conditions dissimilar to those described above for the purification of [C_nTPPBr], [$C_n$mimBr], [C_nIQBr], [C_nmPyrBr], [C_nQBr], [C_nPyrBr] derivatives, due to the difference of the physicochemical properties of the triethylamine structure. Preliminary attempts to prepare the [C_nTEABr] were performed by reacting the suitable bromoalkane (1 eq.) with excess amounts of triethylamine (10 eq.). The subsequent precipitation of resulting reactional mixture with dichloromethane/*n*-hexane resulted in trace amounts of the starting material and a mixture of compounds that were not successfully separated. Another approach of purification was performed by precipitation with two different solvent mixtures (dichloromethane/diethyl ether or dichloromethane/ethyl acetate) and subsequent purification by silica gel chromatography (eluent: dichloromethane:methanol (9:1)). However, an elusive isolation of the desired product was achieved. Considering the unsatisfactory previous results, it was decided to change the methodology. Therefore, it was decided to synthetize [C_nTEABr] following the methodology described in literature by Meng *et al* [134], where the corresponding bromoalkane (1 eq.) was heated with triethylamine (1.2 eq.) in acetonitrile at 85 ºC for two days. Upon solvent concentration, the crude product was isolated by liquid-liquid extraction.

Employing the methodologies previously described, a library of twenty-one alkyl cationic derivatives was successfully obtained with moderate-to-high yields (Table 4).

Table 4. Yield of the twenty-one synthetized alkyl cationic derivatives.

Compound	Yield
[C_6TPPBr]	95 %
[C_8TPPBr]	68 %
[C_{10}TPPBr]	92 %
[C_6mimBr]	71 %
[C_8mimBr]	88 %
[C_{10}mimBr]	94 %
[C_6IQBr]	78 %
[C_8IQBr]	85 %
[C_{10}IQBr]	45 %
[C_6mPyrBr]	93 %
[C_8mPyrBr]	78 %
[C_{10}mPyrBr]	98 %
[C_6QBr]	78 %
[C_8QBr]	85 %
[C_{10}QBr]	45 %
[C_6PyrBr]	98 %
[C_8PyrBr]	99 %
[C_{10}PyrBr]	99 %
[C_6TEABr]	77 %
[C_8TEABr]	84 %
[C_{10}TEABr]	81 %

3.1.2. Structural elucidation of alkyl cationic derivatives

The synthesized compounds were characterised by NMR spectroscopy (^{1}H, ^{13}C and DEPT135), thereby confirming their chemical identity (See *Section 2.1.4.* and *Appendix I*).

^{1}H NMR and ^{13}C NMR data of compounds are summarized in Tables 5 and 6, respectively. The assignment of the aliphatic and aromatic signals was based on their chemical shifts, multiplicity and coupling constants. Assignments were also made from DEPT (underlined values) on ^{13}C NMR data.

Table 5. ^{1}H NMR data of compounds [C_nTPPBr], [$C_n$mimBr], [C_nIQBr], [C_nmPyrBr], [C_nQBr], [C_nPyrBr] and [C_nTEABr].

Compound		H(1)	H(2)	H(3)	H(4)	H(5)	H(6)	H(7)	H(8)	H(9)	H(10)	H(1')	H(2')	H(3')	H(4')	H(5')	H(6')	H(7')	H(8')
[C_6TPPBr]	(δ/ppm)	3.69-3.84	1.54-1.72	1.54-1.72	1.16-1.33	1.16-1.33	0.82	-	-	-	-	-	7.63-8.00	7.63-8.00	7.63-8.00	7.63-8.00	7.63-8.00	-	-
	Mult	*m*	*m*	*m*	*m*	*m*	*t*	-	-	-	-	-	*m*	*m*	*m*	*m*	*m*	-	-
	(J/Hz)	-	-	-	-	-	7.1	-	-	-	-	-	-	-	-	-	-	-	-
[C_8TPPBr]	(δ/ppm)	3.45-3.97	1.56-1.70	1.56-1.70	1.13-1.32	1.13-1.32	1.13-1.32	1.13-1.32	0.83	-	-	-	7.62-7.94	7.62-7.94	7.62-7.94	7.62-7.94	7.62-7.94	-	-
	Mult	*m*	*m*	*m*	*m*	*m*	*m*	*m*	*t*	-	-	-	*m*	*m*	*m*	*m*	*m*	-	-
	(J/Hz)	-	-	-	-	-	-	-	6.9	-	-	-	-	-	-	-	-	-	-
[C_{10}TPPBr]	(δ/ppm)	3.68-3.91	1.55-1.69	1.55-1.69	1.13-1.32	1.13-1.32	1.13-1.32	1.13-1.32	1.13-1.32	1.13-1.32	0.85	-	7.63-7.96	7.63-7.96	7.63-7.96	7.63-7.96	7.63-7.96	-	-
	Mult	*m*	*m*	*m*	*m*	*m*	*m*	*m*	*m*	*m*	*t*	-	*m*	*m*	*m*	*m*	*m*	-	-
	(J/Hz)	-	-	-	-	-	-	-	-	-	7.0	-	-	-	-	-	-	-	-
[C_6mimBr]	(δ/ppm)	4.33	1.85-1.98	1.23-1.40	1.23-1.40	1.23-1.40	0.87	-	-	-	-	-	10.36	-	7.25	7.32	4.13	-	-
	Mult	*t*	*m*	*m*	*m*	*m*	*t*	-	-	-	-	-	*bs*	-	*dd*	*dd*	*s*	-	-
	(J/Hz)	7.5	-	-	-	-	7.1	-	-	-	-	-	-	-	1.8, 1.8	1.8, 1.8	-	-	-
[C_8mimBr]	(δ/ppm)	4.33	1.84-1.94	1.15-1.40	1.15-1.40	1.15-1.40	1.15-1.40	1.15-1.40	0.84	-	-	-	10.40	-	7.36	7.50	4.11	-	-
	Mult	*t*	*m*	*m*	*m*	*m*	*m*	*m*	*t*	-	-	-	*bs*	-	*dd*	*dd*	*s*	-	-
	(J/Hz)	7.4	-	-	-	-	-	-	6.9	-	-	-	-	-	1.8, 1.8	1.8, 1.8	-	-	-
[C_{10}mimBr]	(δ/ppm)	4.32	1.84-2.03	1.17-1.41	1.17-1.41	1.17-1.41	1.17-1.41	1.17-1.41	1.17-1.41	1.17-1.41	0.87	-	10.42	-	7.35	7.49	4.13	-	-
	Mult	*t*	*m*	*m*	*m*	*m*	*m*	*m*	*m*	*m*	*t*	-	*bs*	-	*dd*	*dd*	*s*	-	-
	(J/Hz)	7.4	-	-	-	-	-	-	-	-	6.9	-	-	-	1.8, 1.8	1.8, 1.8	-	-	-
[C_6IQBr]	(δ/ppm)	5.09	2.06-2.20	1.18-1.50	1.18-1.50	1.18-1.50	0.83	-	-	-	-	11.12	-	8.79	8.39	8.08-8.20	8.08-8.20	7.95	8.79
	Mult	*t*	*m*	*m*	*m*	*m*	*t*	-	-	-	-	*dd*	-	*m*	*d*	*m*	*m*	*ddd*	*m*
	(J/Hz)	7.4	-	-	-	-	7.1	-	-	-	-	-	-	-	6.8	-	-	8.2, 6.7, 1.4	-

Table 5. (*Continued*)

Compound		H(1)	H(2)	H(3)	H(4)	H(5)	H(6)	H(7)	H(8)	H(9)	H(10)	H(1')	H(2')	H(3')	H(4')	H(5')	H(6')	H(7')	H(8')
[C_8IQBr]	(δ/ppm)	5.09	2.05-2.19	1.13-1.49	1.13-1.49	1.13-1.49	1.13-1.49	1.13-1.49	0.84	-	-	11.16	-	8.77	8.37	8.07-8.20	8.07-8.20	7.95	8.77
	Mult	*t*	*m*	*m*	*m*	*m*	*m*	*m*	*t*	-	-	*dd*	-	*m*	*d*	*m*	*m*	*ddd*	*m*
	(J/Hz)	7.4	-	-	-	-	-	-	6.9	-	-	-	-	-	6.8	-	-	8.2, 6.5, 1.6	-
[C_{10}IQBr]	(δ/ppm)	5.09	2.06-2.21	1.15-1.49	1.15-1.49	1.15-1.49	1.15-1.49	1.15-1.49	1.15-1.49	1.15-1.49	0.85	11.10	-	8.74-8.84	8.40	8.08-8.20	8.08-8.20	7.95	8.74-8.84
	Mult	*t*	*m*	*m*	*m*	*m*	*m*	*m*	*m*	*m*	*t*	*dd*	-	*m*	*d*	*m*	*m*	*ddd*	*m*
	(J/Hz)	7.4	-	-	-	-	-	-	-	-	6.9	-	-	-	6.8	-	-	8.2, 6.7, 1.4	-
[C_6mPyrBr]	(δ/ppm)	4.90	1.94-2.12	1.19-1.45	1.19-1.45	1.19-1.45	0.86	-	-	-	-	-	9.36	7.92	-	7.92	9.36	2.68	-
	Mult	*t*	*m*	*m*	*m*	*m*	*t*	-	-	-	-	-	*d*	*d*	-	*d*	*d*	*s*	-
	(J/Hz)	7.4	-	-	-	-	7.1	-	-	-	-	-	6.7	6.7	-	6.7	6.7	-	-
[C_8mPyrBr]	(δ/ppm)	4.91	1.94-2.08	1.15-1.44	1.15-1.44	1.15-1.44	1.15-1.44	1.15-1.44	0.86	-	-	-	9.34	7.91	-	7.91	9.34	2.68	-
	Mult	*t*	*m*	*m*	*m*	*m*	*m*	*m*	*t*	-	-	-	*d*	*d*	-	*d*	*d*	*s*	-
	(J/Hz)	7.4	-	-	-	-	-	-	6.9	-	-	-	6.7	6.7	-	6.7	6.7	-	-
[C_{10}mPyrBr]	(δ/ppm)	4.91	1.94-2.10	1.12-1.45	1.12-1.45	1.12-1.45	1.12-1.45	1.12-1.45	1.12-1.45	1.12-1.45	0.87	-	9.31	7.90	-	7.90	9.31	2.68	-
	Mult	*t*	*m*	*m*	*m*	*m*	*m*	*m*	*m*	*m*	*t*	-	*d*	*d*	-	*d*	*d*	*s*	-
	(J/Hz)	7.4	-	-	-	-	-	-	-	-	6.9	-	6.7	6.7	-	6.7	6.7	-	-
[C_6QBr]	(δ/ppm)	5.42	2.05-2.19	1.45-1.61	1.24-1.41	1.24-1.41	0.87	-	-	-	-	-	9.06	8.19-8.25	10.64	8.31-8.38	7.98	8.19-8.25	8.31-8.38
	Mult	*t*	*m*	*m*	*m*	*m*	*t*	-	-	-	-	-	*d*	*m*	*dd*	*m*	*ddd*	*m*	*m*
	(J/Hz)	7.6	-	-	-	-	7.1	-	-	-	-	-	8.3	-	5.9, 1.4	-	8.0, 7.0, 1.0	-	-
[C_8QBr]	(δ/ppm)	5.43	2.05-2.16	1.46-1.58	1.16-1.40	1.16-1.40	1.16-1.40	1.16-1.40	0.84	-	-	-	9.10	8.18-8.26	10.61	8.33-8.40	7.97	8.18-8.26	8.33-8.40
	Mult	*t*	*m*	*m*	*m*	*m*	*m*	*m*	*t*	-	-	-	*d*	*m*	*dd*	*m*	*ddd*	*m*	*m*
	(J/Hz)	7.6	-	-	-	-	-	-	7.1	-	-	-	8.3	-	5.8, 1.4	-	8.0, 7.0, 0.9	-	-

Table 5. (*Continued*)

Compound		H(1)	H(2)	H(3)	H(4)	H(5)	H(6)	H(7)	H(8)	H(9)	H(10)	H(1')	H(2')	H(3')	H(4')	H(5')	H(6')	H(7')	H(8')
[C_{10}QBr]	(δ/ppm)	5.43	2.06-2.16	1.45-1.57	1.15-1.40	1.15-1.40	1.15-1.40	1.15-1.40	1.15-1.40	1.15-1.40	0.85	-	9.11	8.18-8.25	10.61	8.34-8.40	7.97	8.18-8.25	8.34-8.40
	Mult	*t*	*m*	*m*	*m*	*m*	*m*	*m*	*m*	*m*	*t*	-	*d*	*m*	*dd*	*m*	*ddd*	*m*	*m*
	(J/Hz)	7.6	-	-	-	-	-	-	-	-	7.1	-	8.4	-	5.9, 1.4	-	8.0, 7.0, 0.9	-	-
[C_6PyrBr]	(δ/ppm)	5.01	2.00-2.12	1.20-1.46	1.20-1.46	1.20-1.46	0.87	-	-	-	-	-	9.56	8.18	8.56	8.18	9.56	-	-
	Mult	*t*	*m*	*m*	*m*	*m*	*t*	-	-	-	-	-	*dd*	*dd*	*tt*	*dd*	*dd*	-	-
	(J/Hz)	7.5	-	-	-	-	7.1	-	-	-	-	-	6.5, 1.4	7.8, 6.5	7.8, 1.4	7.8, 6.5	6.5, 1.4	-	-
[C_8PyrBr]	(δ/ppm)	5.02	1.93-2.13	1.15-1.46	1.15-1.46	1.15-1.46	1.15-1.46	1.15-1.46	0.85	-	-	-	9.52	8.16	8.54	8.16	9.52	-	-
	Mult	*t*	*m*	*m*	*m*	*m*	*m*	*m*	*t*	-	-	-	*dd*	*dd*	*tt*	*dd*	*dd*	-	-
	(J/Hz)	7.5	-	-	-	-	-	-	7.1	-	-	-	6.5, 1.4	7.8, 6.5	7.8, 1.4	7.8, 6.5	5.3, 1.4	-	-
[C_{10}PyrBr]	(δ/ppm)	5.01	1.96-2.09	1.17-1.44	1.17-1.44	1.17-1.44	1.17-1.44	1.17-1.44	1.17-1.44	1.17-1.44	0.86	-	9.51	8.17	8.54	8.17	9.51	-	-
	Mult	*t*	*m*	*m*	*m*	*m*	*m*	*m*	*m*	*m*	*t*	-	*dd*	*dd*	*tt*	*dd*	*dd*	-	-
	(J/Hz)	7.5	-	-	-	-	-	-	-	-	7.1	-	6.7, 1.4	7.8, 6.7	7.8, 1.4	7.8, 6.7	6.7, 1.4	-	-
[C_6TEABr]	(δ/ppm)	3.19-3.39	1.63-1.77	1.26-1.49	1.26-1.49	1.26-1.49	0.90	-	-	-	-	3.53	1.40	-	-	-	-	-	-
	Mult	*m*	*m*	*m*	*m*	*m*	*t*	-	-	-	-	*q*	*t*	-	-	-	-	-	-
	(J/Hz)	-	-	-	-	-	7.1	-	-	-	-	7.3	7.3	-	-	-	-	-	-
[C_8TEABr]	(δ/ppm)	3.25-3.30	1.62-1.78	1.17-1.49	1.17-1.49	1.17-1.49	1.17-1.49	1.17-1.49	0.88	-	-	3.52	1.40	-	-	-	-	-	-
	Mult	*m*	*m*	*m*	*m*	*m*	*m*	*m*	*t*	-	-	*q*	*t*	-	-	-	-	-	-
	(J/Hz)	-	-	-	-	-	-	-	6.9	-	-	7.3	7.3	-	-	-	-	-	-
[C_{10}TEABr]	(δ/ppm)	3.10-3.32	1.63-1.77	1.18-1.50	1.18-1.50	1.18-1.50	1.18-1.50	1.18-1.50	1.18-1.50	1.18-1.50	0.88	3.53	1.40	-	-	-	-	-	-
	Mult	*m*	*m*	*m*	*m*	*m*	*m*	*m*	*m*	*m*	*t*	*m*	*t*	-	-	-	-	-	-
	(J/Hz)	-	-	-	-	-	-	-	-	-	6.9	7.3	7.3	-	-	-	-	-	-

Table 6. ^{13}C NMR spectra of [C_nTPPBr], [$C_n$mimBr], [C_nIQBr], [C_nmPyrBr], [C_nQBr], [C_nPyrBr] and [C_nTEABr].

Compound		C(1)	C(2)	C(3)	C(4)	C(5)	C(6)	C(7)	C(8)	C(9)	C(10)	C(1')	C(2')	C(3')	C(4')	C(4a')	C(5')	C(6')	C(7')	C(8')	C(8a')
[C_6TPPBr]	(δ/ppm)	22.8	30.1	22.6	31.3	22.5	14.0	-	-	-	-	118.4	133.7	130.5	135.0	-	130.5	133.7	-	-	-
	(J/Hz)	49.7	15.5	4.6	1.0	-	-	-	-	-	-	85.8	10.0	12.5	3.0	-	12.5	10.0	-	-	-
[C_8TPPBr]	(δ/ppm)	22.8	30.4	22.7	29.2	31.7	28.8	22.5	14.1	-	-	118.5	133.7	130.5	135.0	-	130.5	133.7	-	-	-
	(J/Hz)	49.5	15.5	4.6	1.0	-	-	-	-	-	-	85.8	10.0	12.5	3.0	-	12.5	10.0	-	-	-
[C_{10}TPPBr]	(δ/ppm)	22.8	30.4	22.7	29.5	29.2	29.2	29.2	31.8	22.5	14.1	118.5	133.7	130.5	135.0	-	130.5	133.7	-	-	-
	(J/Hz)	49.5	15.5	4.7	-	-	-	-	-	-	-	85.8	9.9	12.5	3.0	-	12.5	9.9	-	-	-
[C_6mimBr]	(δ/ppm)	50.3	30.2	25.9	31.1	22.4	13.9	-	-	-	-	-	138.3	-	123.0	-	121.5	36.8	-	-	-
	(J/Hz)	-	-	-	-	-	-	-	-	-	-	-	-	-	-	-	-	-	-	-	-
[C_8mimBr]	(δ/ppm)	50.2	26.3	28.9	30.3	29.0	31.7	22.6	14.1	-	-	-	137.7	-	123.5	-	121.8	36.8	-	-	-
	(J/Hz)	-	-	-	-	-	-	-	-	-	-	-	-	-	-	-	-	-	-	-	-
[C_{10}mimBr]	(δ/ppm)	50.2	26.3	31.8	29.5	29.4	29.2	29.0	30.3	22.7	14.1	-	137.8	-	123.5	-	121.7	36.8	-	-	-
	(J/Hz)	-	-	-	-	-	-	-	-	-	-	-	-	-	-	-	-	-	-	-	-
[C_6IQBr]	(δ/ppm)	61.7	31.2	25.9	31.9	22.3	14.1	-	-	-	-	150.5	-	137.1	134.4	137.3	127.1	131.3	131.4	126.3	127.9
	(J/Hz)	-	-	-	-	-	-	-	-	-	-	-	-	-	-	-	-	-	-	-	-
[C_8IQBr]	(δ/ppm)	61.7	31.7	26.2	29.1	29.0	32.0	22.6	14.1	-	-	150.6	-	137.1	134.3	137.3	127.1	131.4	131.5	126.3	127.9
	(J/Hz)	-	-	-	-	-	-	-	-	-	-	-	-	-	-	-	-	-	-	-	-
[C_{10}IQBr]	(δ/ppm)	61.7	31.8	26.2	29.2	29.4	29.3	29.1	31.9	22.7	14.1	150.8	-	137.1	134.2	137.3	127.0	131.4	131.5	126.2	128.0
	(J/Hz)	-	-	-	-	-	-	-	-	-	-	-	-	-	-	-	-	-	-	-	-
[C_6mPyrBr]	(δ/ppm)	61.4	31.2	25.8	31.9	22.5	14.0	-	-	-	-	-	144.4	129.0	158.9	-	129.0	144.4	22.3	-	-
	(J/Hz)	-	-	-	-	-	-	-	-	-	-	-	-	-	-	-	-	-	-	-	-
[C_8mPyrBr]	(δ/ppm)	61.4	31.7	26.1	29.0	29.0	31.9	22.6	14.1	-	-	-	144.4	128.9	158.9	-	128.9	144.4	22.3	-	-
	(J/Hz)	-	-	-	-	-	-	-	-	-	-	-	-	-	-	-	-	-	-	-	-
[C_{10}mPyrBr]	(δ/ppm)	61.4	31.8	26.1	29.5	29.4	29.3	29.1	31.9	22.7	14.1	-	144.4	128.9	158.9	-	128.9	144.4	22.3	-	-
	(J/Hz)	-	-	-	-	-	-	-	-	-	-	-	-	-	-	-	-	-	-	-	-
[C_6QBr]	(δ/ppm)	58.2	30.4	26.2	31.2	22.4	13.9	-	-	-	-	-	147.3	122.7	150.6	130.0	131.2	130.2	136.0	118.4	137.7
	(J/Hz)	-	-	-	-	-	-	-	-	-	-	-	-	-	-	-	-	-	-	-	-
[C_8QBr]	(δ/ppm)	58.2	30.5	26.5	29.1	29.0	31.7	22.6	14.0	-	-	-	146.8	122.8	151.0	130.0	131.1	130.1	135.9	118.3	137.7
	(J/Hz)	-	-	-	-	-	-	-	-	-	-	-	-	-	-	-	-	-	-	-	-
[C_{10}QBr]	(δ/ppm)	58.2	30.5	26.5	29.2	29.5	29.4	29.2	31.8	22.6	14.1	-	147.1	122.7	150.8	130.0	131.2	130.1	135.9	118.3	137.7
	(J/Hz)	-	-	-	-	-	-	-	-	-	-	-	-	-	-	-	-	-	-	-	-
[C_6PyrBr]	(δ/ppm)	62.1	31.1	25.7	32.0	22.4	13.9	-	-	-	-	-	145.2	128.5	145.2	-	128.5	145.2	-	-	-
	(J/Hz)	-	-	-	-	-	-	-	-	-	-	-	-	-	-	-	-	-	-	-	-

Table 6. (*Continued*)

Compound		C(1)	C(2)	C(3)	C(4)	C(5)	C(6)	C(7)	C(8)	C(9)	C(10)	C(1')	C(2')	C(3')	C(4')	C(4a')	C(5')	C(6')	C(7')	C(8')	C(8a')
[C_8PyrBr]	(δ/ppm)	62.2	31.7	26.1	29.0	29.0	32.0	22.6	14.1	-	-	-	145.1	128.5	145.1	-	128.5	145.1	-	-	-
	(J/Hz)	-	-	-	-	-	-	-	-	-	-	-	-	-	-	-	-	-	-	-	-
[C_{10}PyrBr]	(δ/ppm)	62.2	31.8	26.1	29.4	29.3	29.2	29.1	32.0	22.7	14.1	-	145.1	128.4	145.1	-	128.4	145.1	-	-	-
	(J/Hz)	-	-	-	-	-	-	-	-	-	-	-	-	-	-	-	-	-	-	-	-
[C_6TEABr]	(δ/ppm)	57.7	26.2	22.4	31.2	22.2	14.0	-	-	-	-	53.7	8.2	-	-	-	-	-	-	-	-
	(J/Hz)	-	-	-	-	-	-	-	-	-	-	-	-	-	-	-	-	-	-	-	-
[C_8TEABr]	(δ/ppm)	57.7	22.6	26.5	29.2	29.1	31.8	22.1	14.0	-	-	53.7	8.2	-	-	-	-	-	-	-	-
	(J/Hz)	-	-	-	-	-	-	-	-	-	-	-	-	-	-	-	-	-	-	-	-
[C_{10}TEABr]	(δ/ppm)	57.6	22.7	26.5	29.2	29.4	-	29.2	31.8	22.1	14.1	53.6	8.2	-	-	-	-	-	-	-	-
	(J/Hz)	-	-	-	-	-	-	-	-	-	-	-	-	-	-	-	-	-	-	-	-

Structural characterization of the alkyl cationic derivatives

The ^{1}H NMR and ^{13}C NMR data confirmed that the synthesis of the alkyl cationic derivatives was successfully achieved, confirming the presence of the bromoalkane fragment and of the amine/phosphine cation head. For simplicity the analysis will be performed in two parts: analysis of the alkyl side chain and of the cationic head.

Analysis of the data related to the alkyl side chain

The attachment of the aliphatic side chains onto the cationic head groups, forming the alkyl cationic salts, was confirmed by the location of the signals of protons at position one (H(1)). The protons in the H(1) position appear in the middle region of the spectra (3 to 5 ppm) due to a deprotecting effect caused by the presence of the cation attached to them. The other protons of the aliphatic chain are observed in the spectra from 0.82 to 2.21 ppm. The aliphatic protons H(1) of [TPP] compounds are shifted to lower chemical shifts than those of [mim], [IQ], [mPyr], [Q], [Pyr], [TEA] due to lower electronegativity of P and greater delocalization of the cation in the three aromatic rings of the [TPP]. From the ^{13}C-NMR chemical shift range (δ = 13.9 - 62.2 ppm), it is possible to assign the highest values to the carbon nearest the cation and the lowest values to the last carbon in the chain (Table 6). Except for the compounds with [TPP] in which C(1) appears at 22.8 ppm, it is in agreement with what is described in the literature for similar compounds [166]. In these compounds the typical carbon phosphorus coupling constants (J_{C-P}) are also observed [166].

Analysis of the data related to the cation head

In compounds [C_nTPPBr], the detection of the 15 aromatic protons above 7.5 ppm in ^{1}H NMR spectra confirmed that the halogen nucleophilic substitution with triphenylphosphine occurred. The number of aromatic carbons was also clearly assigned by the analysis of ^{13}C NMR spectra. These compounds with a phosphorus atom present a specific ^{13}C NMR spectra, because a unique splitting pattern of the carbon peaks, with very typical coupling constants (J_{C-P}) along the aromatic ring, was clearly observed. The ^{13}C NMR spectra shows four set of signals: one at 118.4-118.5 ppm, attributable to C(1') position (J_{C-P} = 85.8 Hz), one at 133.7 ppm, attributable to C(2') and C(6') positions (J_{C-P} = 10.0 Hz), one at 130.5 ppm, attributable to C(3') and C(5') positions (J_{C-P} = 12.5 Hz), and one at 135.0 ppm, J_{C-P} = 3.0 Hz, due to C(4').

In compounds [$C_n$mimBr], the peaks were also readily identified in the ^{1}H and ^{13}C NMR spectra. The protons of the imidazole ring were easily assigned by their chemical shifts

(H(2') 10.36-10.42 ppm as *bs*, H(4') 7.25-7.36 as *dd* and H(5') 7.32-7.50 as *dd*) was observed. The methyl group (H(6')) attached to the imidazole ring appears as a singlet at 4.11-4.13 ppm. The ^{13}C-NMR spectra showed three downfield signals (δ = 121.5-121.8, 123.0-123.5 and 137.7-138.3 ppm) for the CH substituents on the imidazole ring and one upfield peak (δ = 36.8 ppm) which is assigned to the methyl group on the ring.

In compounds [C_nIQBr] and [C_nQBr], the peaks were also readily identified in the ^{1}H and ^{13}C NMR spectra. The H(4')s of quinoline (δ = 10.61-10.64 ppm as *dd*) and H(1')s of isoquinoline (δ = 11.10-11.16 ppm as *dd*) have the highest chemical shifts, whereas the H(6')s of quinoline (δ = 7.97-7.98 ppm as *ddd*) and H(7')s of isoquinoline (δ = 7.95 ppm as *ddd*) have the lowest chemical shifts. The multiplicities of H(2'), H(4') and H(6') of quinoline, and H(4') and H(7') of isoquinoline provide further confirmation for the assignment of these protons on the rings. The data that were outlined from the ^{13}C and DEPT135 analysis allowed the recognition of the nature of the carbons. By subtracting DEPT135 signals from the original ^{13}C NMR spectra, two signals remain that can be assigned to two quaternary carbons ((C(4a') and C(8a')). The rest of the carbons were assigned by their chemical shift (Table 6). In compounds [C_nIQBr], the C(1') appear at 150.5-150.8 ppm, the C(3') at 137.1 ppm, the C(4') at 134.2-134.4 ppm, the C(5') at 127.0-127.1 ppm, the C(6') at 131.3-131.4 ppm, the C(7') at 131.4-131.5 ppm and the C(8') at 126.2-126.3 ppm. In compounds [C_nQBr], the C(2') appear at 146.8-147.3 ppm, the C(3') at 122.7-122.8 ppm, the C(4') at 150.6-151.0 ppm, the C(5') at 131.1-131.2 ppm, the C(6') at 130.1-130.2 ppm, the C(7') at 135.9-136.0 ppm and the C(8') at 118.3-118.4 ppm.

From the analysis of the peaks of the compounds [C_nPyrBr] in ^{1}H and ^{13}C NMR spectra, it was possible to confirm the synthesis of the pyridinium salts. From the ^{1}H-NMR chemical shift range, the H(2')s and H(6')s (δ = 9.51-9.56 ppm) of pyridine are the most deshielded ones due to vicinity of electronegative nitrogen. The proton signals belonging to the H(2')s, H(6')s and H(3')s, H(5')s appear as doublet of doublets at 8.16-9.56 ppm and H(4')s (δ = 8.54-8.56 ppm) appear as triplet of triplets (Table 5). The compounds [C_nmPyrBr] were also successfully synthesized, since the methyl group attached to C(4') position in methylpyridines is presented and appear as a singlet in the spectra (δ = 2.68 ppm). The proton signals belonging to the H(2')s, H(6')s and H(3')s, H(5')s appear as doublet at 7.90-9.36 ppm (Table 5). All the ^{13}C-NMR data confirmed that the desired compounds were obtained (Table 6). The C(2'), C(4') and C(6') of [C_nPyrBr] appear at 145.1-145.2 ppm and C(3'), C(5') at 128.4-128.5 ppm, whereas for [C_nmPyrBr] the C(2') and C(6') appear at 144.4 ppm, the C(3') and C(5') at 128.9-129.0 ppm, the C(4') at 158.9 ppm and the methyl group on the ring (C7') at 22.3 ppm.

For compounds [C_nTEABr], the methylene group protons of the triethylamine counterpart give quartet signals at 3.53 ppm with J = 7.3 Hz, whereas the methyl group protons show the expected triplet at 1.40 ppm with J = 7.3 Hz. ^{13}C NMR signals showed signals at expected chemical shifts [166] for the structures (δ = 53.6-53.7 ppm for C(1'), and δ = 8.2 ppm for C(2')).

3.1.3. Evaluation of drug-like properties

Currently, many potential drugs fail to reach the clinic because of the absorption, distribution, metabolism and excretion (ADME) complications. ADME processes play a crucial role in defining the therapeutic efficacy of a drug candidate. The concept of drug-likeness appears as an auspicious model of a compound that helps to optimize their ADME in the human body [167]. With the aim of estimating the drug-likeness of the compounds, the compliance of the synthetized molecules to the Lipinski's "rule of five" was determined. According to this rule, poor absorption or permeation is more likely when molecular weight is greater than 500, the log$P$ (logarithmic ratio of the octanol−water partitioning coefficient) is greater than 5, and there are more than 5 hydrogen bond donors and 10 hydrogen bond acceptors [167,168]. Molecules violating more than one of these parameters may have problems with bioavailability (*e.g.*, poor oral absorption or membrane permeability) and a high probability of failure to display drug-likeness [167,168]. The theoretical evaluation of some drug-like properties of the compounds under study was performed using Molinspiration Cheminformatics software. The results are depicted on Table 7.

Table 7. Lipinski's "rule of five" parameters for the synthetized alkyl cationic derivatives.

Compound	Molecular weight (Daltons)	*c* Log*P*	Hydrogen bond donors	Hydrogen bond acceptors	Lipinski's violation
Rule	≤ 500	≤ 5	≤ 5	≤ 10	≤ 1
[C_6TPPBr]	347.46	5.86	0	0	1
[C_8TPPBr]	375.52	6.87	0	0	1
[C_{10}TPPBr]	403.57	7.88	0	0	1
[C_6mimBr]	167.28	-1.03	0	2	0
[C_8mimBr]	195.33	-0.02	0	2	0
[C_{10}mimBr]	223.38	0.99	0	2	0
[C_6IQBr]	214.33	0.08	0	1	0
[C_8IQBr]	242.39	1.09	0	1	0
[C_{10}IQBr]	270.44	2.10	0	1	0
[C_6mPyrBr]	178.30	-1.62	0	1	0
[C_8mPyrBr]	206.35	-0.61	0	1	0
[C_{10}mPyrBr]	234.41	0.40	0	1	0
[C_6QBr]	214.33	0.27	0	1	0
[C_8QBr]	242.39	1.28	0	1	0
[C_{10}QBr]	270.44	2.29	0	1	0
[C_6PyrBr]	164.27	-2.02	0	1	0
[C_8PyrBr]	192.33	-1.01	0	1	0
[C_{10}PyrBr]	220.38	-0.00	0	1	0
[C_6TEABr]	186.36	-0.06	0	1	0
[C_8TEABr]	214.42	0.95	0	1	0
[C_{10}TEABr]	242.47	1.96	0	1	0

As expected, the elongation of the alkyl substituent allowed to enhance the lipophilicity, as shown by the increase in *c* log*P* values. In general compounds synthetized in this Thesis comply with these rules. The molecular weight of the [mim], [IQ], [mPyr], [Q], [Pyr] and [TEA] derivatives range from 164.27 to 270.44 Da, *c* log*P* range from -2.02 to 2.29, hydrogen bond acceptors range from 0 to 2 and H-bond donors are all 0. Therefore, theoretically, these compounds have good passive oral absorption and drug-likeness. Only [TPP] derivatives have its partition coefficients beyond the limits established by the Lipinski's "rule of five", possessing an adequate number of proton acceptor and proton donor groups to ensure efficient interaction with the hydrogen bounding groups of the receptors [168]. However, it must be considered that the program used to predict the drug-like properties does not embrace ionic compounds, such as the case of the TPP salts. Thereby, all calculations were performed assuming the neutral molecule, resulting in higher partition coefficients than expected. So, it is possible that this parameter can also be found within the desired values.

3.2. Microbiological Studies

3.2.1. Evaluation of antibacterial activity

The *in vitro* antibacterial activity against *S. aureus* CECT 976 of the twenty-one new synthesized compounds was evaluated. The concentrations of compounds tested ranged from 0.0625 to 64 μg/mL. Therefore, for concentrations higher than 64 μg/mL, MIC and MBC were not tested. The respective results of inhibitory and bactericidal concentrations are presented in Table 8.

The effects of the alkyl side chain length and the type of cation core (triphenylphosphonium, pyridinium, picolinium, quinolinium, methylimidazolium, isoquinolinium and triethylammonium) on antibacterial activity were inspected and a structure activity relationship (SAR) analysis was performed.

Table 8. Minimum inhibitory (MIC) and minimum bactericidal (MBC) concentration values of alkyl cationic derivatives against *S. aureus* CECT 976.

Compound	*S. aureus* CECT 976	
	MIC (μg/mL)	MBC (μg/mL)
[C_6TPPBr]	8	>64
[C_8TPPBr]	2	16
[C_{10}TPPBr]	1	8
[C_6mimBr]	>64	>64
[C_8mimBr]	>64	>64
[C_{10}mimBr]	–[a]	–[a]
[C_6IQBr]	>64	>64
[C_8IQBr]	64	>64
[C_{10}IQBr]	16	64
[C_6mPyrBr]	>64	>64
[C_8mPyrBr]	>64	>64
[C_{10}mPyrBr]	32	>64
[C_6QBr]	>64	>64
[C_8QBr]	16	>64
[C_{10}QBr]	16	32
[C_6PyrBr]	>64	>64
[C_8PyrBr]	>64	>64
[C_{10}PyrBr]	32	>64
[C_6TEABr]	>64	>64
[C_8TEABr]	>64	>64
[C_{10}TEABr]	64	>64

[a] MIC and MBC not available.

From the data it was concluded that the length of the alkyl chain attached to the cation determines the antibacterial activity against bacterium *S. aureus* CECT 976 of the ionic

liquids. The obtained results were in accordance with the literature [169]. The results presented in Table 8 demonstrated that an increase of the chain length results, in general, in a decrease of the MIC and MBC values, meaning that elongation of the alkyl substituent increases antimicrobial activity of the compounds. Among the C_6-homologous, [C_6TPPBr] is the unique compound that showed detectable MIC (but not MBC) for concentrations lower than 64 μg/mL; poor activity was observed for all the other C_6-derivatives (MIC, MBC > 64 μg/mL). In other words, compound [C_6TPPBr] can be looked as the most potent compound in C_6-homologous series. The C_{10}-homologous exhibited the highest antibacterial activity against *S. aureus* CECT 976 across all series of compounds tested (MIC < 64 μg/mL). Summing up, the following trend of activity was observed: $C_6 < C_8 < C_{10}$.

The results reported in the present Thesis are in good agreement with previous observations that denote the dependency on substituent alkyl chain length for antimicrobial potency, indicating a common mechanism for antimicrobial activity of these ILs. Other studies have indicated that the antimicrobial activity of ILs is *via* membrane disruption (*i.e.*, with a target site predominantly at the cytoplasmic (inner) membrane in bacteria) because of their structural similarity to detergents, pesticides and antibiotics that attack lipid structure [170]. Another suggested mode of action is related to acetylcholinesterase inhibition, as illustrated by the inhibition of enzyme by imidazolium and pyridinium ILs (with EC_{50} levels as low as 13 μM) [107,111].

The existence of a correlation between efficiency and the chain length is consistent with data reported in literature, even though the chain length values, of the compounds synthesized in this Thesis are bellow (C_{10}) the maximum threshold established in the literature (16 carbons). As example, maximum antimicrobial efficiency was described for alkylmethylimidazolium, alkylmethylpyridinium, alkylisoquinolinium and alkylquinolinium salts with 12 or 14 carbon atoms in the alkyl chain [171], for alkylpyridinium salts with 14 carbons atoms in the alkyl chain [172], and for alkylmethylpyridinium salts with 14 or 16 carbon atoms [173].

Although the effect of the alkyl chain length on the efficiency as antibacterial agent is relevant, it is also found that the nature of the cationic head group has a significant effect on ILs biological activity. From the data shown in Table 8, it is clear that triphenylphosphonium cation exhibited the most promising activity against *S. aureus* CECT 976, as suggested by the MIC and MBC values obtained for the different cationic cores carrying same-length alkyl side chain. The higher antibacterial activity of the latter could be attributed to its ability to supress bacterial bioenergetics by collapsing membrane potential through activation of protonophorous uncoupling [174]. Triethylammonium cation elicited

the lowest antibacterial activity, with the remaining ionic liquids (containing quinolinium, isoquinolinium, pyridinium, or methylpyridinium cations) lay in between these extremes. The low antibacterial activity of the triethylammonium cation could be reasonably explained by the lack of aromaticity. The decrease in the antibacterial activity towards *S. aureus* CECT 976 is represented by the following trend: [TPP] > [Q] > [IQ] > [mPyr] ≈ [Pyr] > [TEA].

Considering that lipophilicity is an important property for data interpretation the theoretical partition coefficients (*c* Log*P*) were used for the present discussion (Table 7). From the microbiological perspective, comparing [C_6TPPBr], [C_8TPPBr] with [C_{10}TPPBr], which have similar chemical structures, [C_{10}TPPBr] revealed higher hydrocarbon side chain (which is correlated with a higher molecular weight) and lipophilicity (Table 7), and thus better antimicrobial properties than [C_6TPPBr] and [C_8TPPBr]. Comparable effects were found for the other alkyl cationic derivatives in study. Based on the results, it is possible to correlate the lipophilicity with the higher antibacterial activity, suggesting that interaction with the surface of the microbial cells plays a major role [128]. This assumption was validated by the observation made by several authors that Gram-negative bacteria (*e.g.*, *E. coli*) are equal or slightly more resistant towards ILs than Gram-positive ones (*e.g.*, *S. aureus*) [128,168,175]. Differences in susceptibility towards the action of the surface-active ILs can be justified on the basis of the differences in the external structures of these two bacteria strains [175]. While the Gram-positive bacterium has a thick, multi-layered cell wall consisting almost entirely of peptidoglycan surrounding the cytoplasmic membrane, the Gram-negative cell wall contains two layers external to the cytoplasmic membrane – a thin layer of peptidoglycan and an outer membrane with a hydrophilic coating of lipopolysaccharides (LPS) [128,168,175]. The outer membrane of Gram-negative bacteria poses a significant barrier to the penetration of ionic surface-active compounds that would normally disrupt the inner membrane or the peptidoglycan cell wall whereas the bacterial cell wall of Gram-positive bacteria may adsorb these compounds and carry them to the inner membrane [171,176].

3.3. Human cell Studies

3.3.1. Evaluation of cytotoxicity profile

Following assessment of antimicrobial activity against *S. aureus* bacterium, the further step was to appraise the *in vitro* safety profile of the alkyl cationic derivatives, as this is a major requirement to pursue their therapeutic application [142]. Hence, the most bioactive ones (MIC ≤ 32 μg/mL) were selected and a preliminary cytotoxic study in human epithelial

kidney (HK-2) and human hepatocellular carcinoma (HepG2) cells was performed. For that, both cell lines were exposed to [C_6TPPBr], [C_8TPPBr], [C_{10}TPPBr], [C_{10}IQBr], [C_{10}mPyrBr] and [C_{10}QBr] at concentrations from 2 to 128 µg/mL for 24 hours. Cellular cytotoxicity was evaluated by MTT reduction, NR uptake and SRB assays. The results are presented in Figures 25 and 26 and expressed as mean (% of control) ± SD of three independent experiments (*n* = 3).

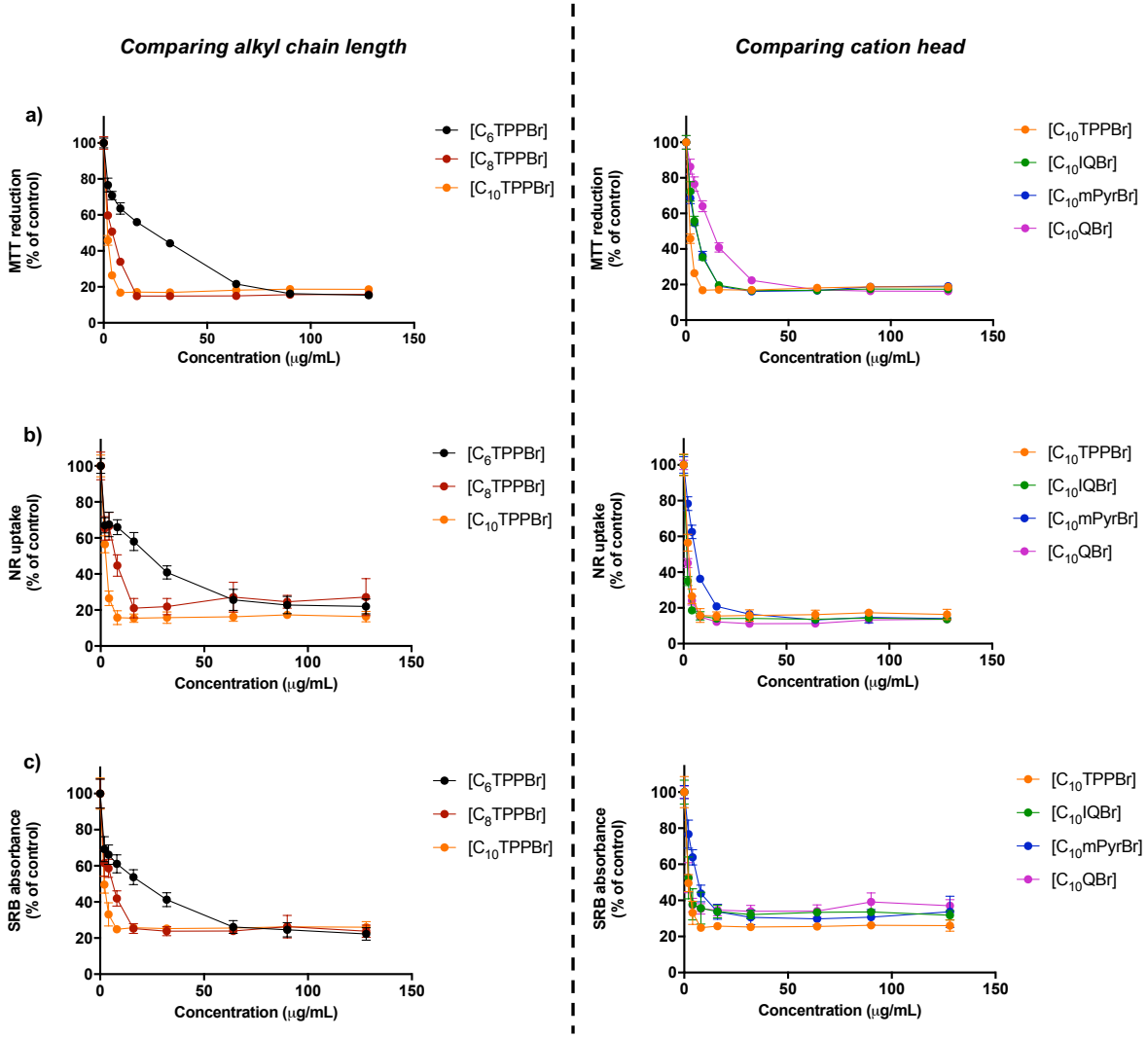

Figure 25. Cellular viability of HK-2 cells after incubation with [C_6TPPBr], [C_8TPPBr], [C_{10}TPPBr] ([TPP] derivatives with variations in alkyl chain length) and [C_{10}IQBr], [C_{10}mPyrBr], [C_{10}QBr] (10-carbon linker compounds with differences in the cation head) to 2-128 µg/mL for 24 h. Cellular viability was measured by determining changes in **(a)** cellular metabolic activity using the MTT assay, **(b)** lysosomal activity using the NR uptake assay, and **(c)** cell density using the SRB assay. Untreated cells were used as control (100 %). All values expressed as mean ± SD (*n* = 3).

After 24 hours of exposure, it was observed a significant (****$p < 0.0001$) decrease in MTT reduction (Figure 25a), NR uptake (Figure 25b), and SRB absorbance (Figure 25c) of *in vitro* HK-2 cells when treated with all compounds at the tested concentrations. All studied

compounds showed cytotoxic effects in metabolic activity, lysosomal activity, and cell density. Despite the differences in the obtained potencies (potency shift), the cytotoxicity profile of the compounds was reasonably the same for the three viability tests. Discrepancies between different viability tests are fairly commonly noted in the literature [177]. For compounds harbouring the triphenylphosphonium [TPP] moiety (Figure 25a-c (left side)), the observed cytotoxicity increase with the increasing of the chain length of the alkyl substituent, once the extent of leftwards shift was higher for [C_{10}TPPBr], then for [C_8TPPBr] and [C_6TPPBr], consistent with what has been observed in other studies [178,179]. On the other way, the influence of the cation head of the ILs in the cytotoxic profile was lesser than that observed with the variation of length of alkyl chain. In what concerns the effect of the variation of cation head (Figure 25a-c (right side)), the data suggests that quinolinium salts [Q] are the least toxic ones, followed closely by methylpyridinium salts [mPyr]. Triphenylphosphonium salts [TPP] are considerably more toxic than their counterparts.

The data pointed out that the cytotoxicity outline observed could be ascribed to be a combination of effects mostly associated with the length of the alkyl chain and the presence of a TPP cation. Lipophilic TPP cations have been described to freely pass through cellular phospholipid bilayers, with the extent of the process being dependent upon their hydrophobicity [178,180]. Thus, it is somehow expected that compounds with lengthier alkyl chains linked to a TPP cation likely disrupt the membrane integrity, especially in mitochondria where such compounds accumulate, and subsequently induce cytotoxic events [180].

Apart from HK-2 cell model, the cytotoxicity of the compounds under study was evaluated in HepG2 cells in order to estimate the cytotoxic effects of these compounds in another cell line that also play a crucial role in metabolism and excretion [181]. The results (Figure 26) are in accordance with the data obtained for HK-2 cells, with exception of methylpyridinium salts [mPyr], which in HepG2 cells are less susceptible to induce cell death, as evidenced by the extent of rightwards shift observed in MTT reduction (Figure 26a), NR uptake (Figure 26b) and SRB (Figure 26c) assays. Indeed, a subset of HepG2 cells appears to have survived the cytotoxic effect, particularly the effect of low doses of [mPyr] (Figure 26a-c (right side); blue data).

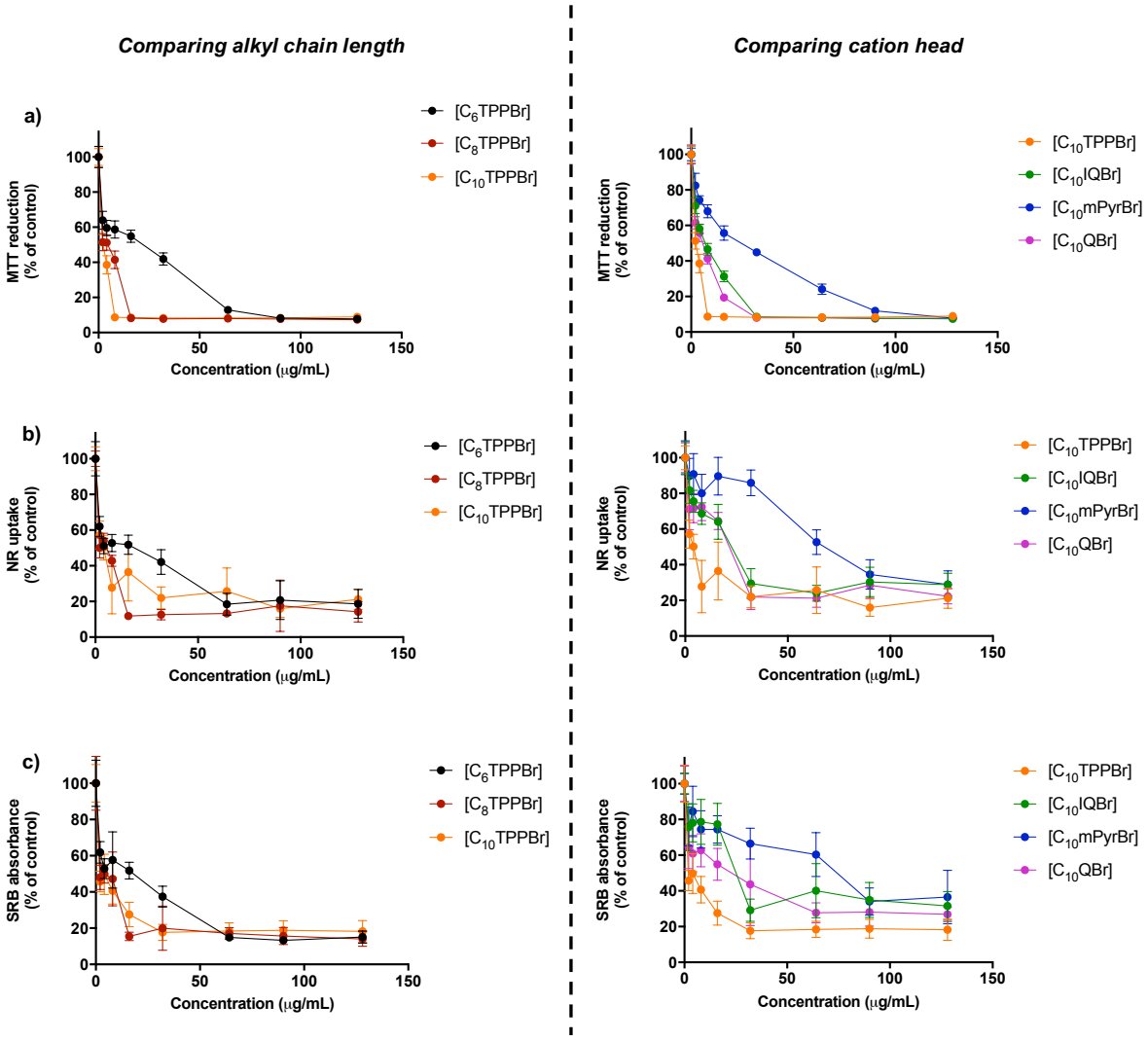

Figure 26. Cellular viability of HepG2 cells after incubation with [C_6TPPBr], [C_8TPPBr], [C_{10}TPPBr] ([TPP] derivatives with variations in alkyl chain length) and [C_{10}IQBr], [C_{10}mPyrBr], [C_{10}QBr] (10-carbon linker compounds with differences in the cation head) to 2-128 μg/mL for 24 hours. Cellular viability was measured by determining changes in **(a)** cellular metabolic activity using the MTT assay, **(b)** lysosomal activity using the NR uptake assay, and **(c)** cell density using the SRB assay. Untreated cells were used as control (100%). All values expressed as mean ± SD (*n* = 3).

3.3.2. Evaluation of intracellular oxidative stress

In the second part of this study, the ability of compounds to exert cytotoxicity by altering intracellular oxidative conditions was investigated. The generation of RS by compounds might be associated with the cytotoxicity levels, by exceeding the cellular defence capacity and directly acting on cell components, including biomolecules, ultimately leading to cell death [182]. Therefore, DCFH-DA assay was performed, as a straightforward and reliable means to assess cellular oxidative stress [183]. The study was performed in the same type of cells (HK-2 and HepG2). The effect of structural modification of the compounds (*i.e.*, alkyl chain length and cation head) in the generation of RS upon 24 hours treatment was also

assessed. The results obtained are shown in Figure 27 and expressed as DCF fluorescence (% vs control) ± SD of three independent experiments (*n* = 3).

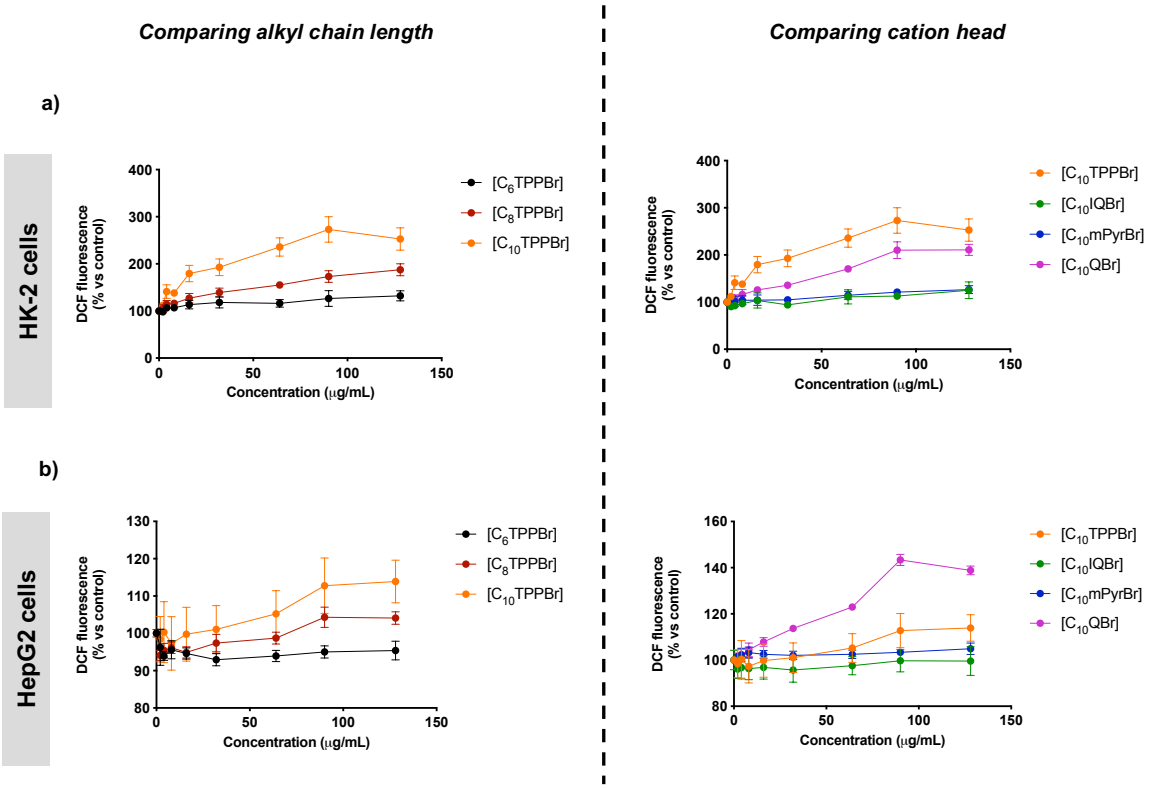

Figure 27. Evaluation of intracellular oxidative stress levels in HK-2 cells **(a)** and HepG2 cells **(b)** evaluated by the DCF fluorescence assay, after treatment with [C_6TPPBr], [C_8TPPBr], [C_{10}TPPBr], ([TPP] derivatives with variations in alkyl chain length) and [C_{10}IQBr], [C_{10}mPyrBr], [C_{10}QBr] (10-carbon linker compounds with differences in the cation head) to 2-128 μg/mL for 24 hours. Results are expressed as DCF fluorescence (% vs control) ± SD (*n* = 3).

An overproduction of RS was detected after incubation of HK-2 cells with TPP derivatives at the range of concentrations tested (2-128 μg/mL). This pro-oxidant effect was much more pronounced for [C_{10}TPPBr] with a maximum of 273.26 ± 27.01 % (vs. 187.58 ± 12.70 % for [C_8TPPBr], and 132.16 ± 10.73 % for [C_6TPPBr]) when compared to nontreated cells (Figure 27a (left side)). The significant increment of oxidative stress observed for TPP derivatives, particularly harbouring a 10-carbon linker, can trigger apoptotic pathways, which may be related with the observed cytotoxic effects in these cells (Figure 25). On the contrary, by treating HepG2 cells with compounds [C_6TPPBr] and [C_8TPPBr] a slight but significant decrease in DCF fluorescence was detected, with exception of [C_8TPPBr] for concentrations above 90 μg/mL (Figure 27b (left side)). No visible effects in RS levels were observed until 90 μg/mL when compound [C_{10}TPPBr] was used. Altogether, the data obtained so far point out that TPP derivatives, in general, can behave as pro-oxidants, even though the effects on RS production were dependent on the cell line.

Regarding the effect of the variation of the cation head of the ILs (Figure 27a-b (right side)), triphenylphosphonium [TPP] and quinolinium [Q] cations caused a superior alteration on cell's oxidative status. Indeed, for [C_{10}TPPBr] and [C_{10}QBr] the presence of cytotoxic effects was paralleled by the highest increase in intracellular RS levels (in HK-2 and HepG2 cells, respectively) of all studied compounds. Interestingly, among the C_{10}-homologous, isoquinolinium [IQ] cation seems not to induce RS formation, with exception of the highest concentration of exposure in HK-2 cells (125.25 $\pm$ 17.77 %, ****p < 0.0001). In the present case, oxidative stress does not seem to contribute to the cytotoxic effects elicited by the [C_{10}IQBr]. Additionally, methylpyridinium [mPyr] cation does not stimulate intracellular RS formation until 64 µg/mL (in HK-2 cells) and 90 µg/mL (in HepG2 cells).

3.4. Selection of the lead compound

The key to the successful selection of a new antimicrobial drug is to have a chemical entity that demonstrate low MICs against the targeted bacteria but also low cytotoxicity towards human cell lines unless exposed at substantially higher concentrations [184,185]. An optimal structure of alkyl cationic derivatives is thus associated with a fine balance between antimicrobial properties and cell cytotoxicity [185]. In Figure 28, the cytotoxicity profile of HK-2 and HepG2 cell lines *vs*. the MIC and MBC values of compounds [C_6TPPBr], [C_8TPPBr], [C_{10}TPPBr], [C_{10}IQBr], [C_{10}mPyrBr] and [C_{10}QBr] is shown. Compounds that did not show bactericidal activity (MBC) in the range of concentrations tested are omitted from Figure 28 (right side). These findings may be modulated to achieve high antimicrobial efficacy and low cell cytotoxicity with the long-range perspective of finding candidates suitable for developing an antimicrobial agent.

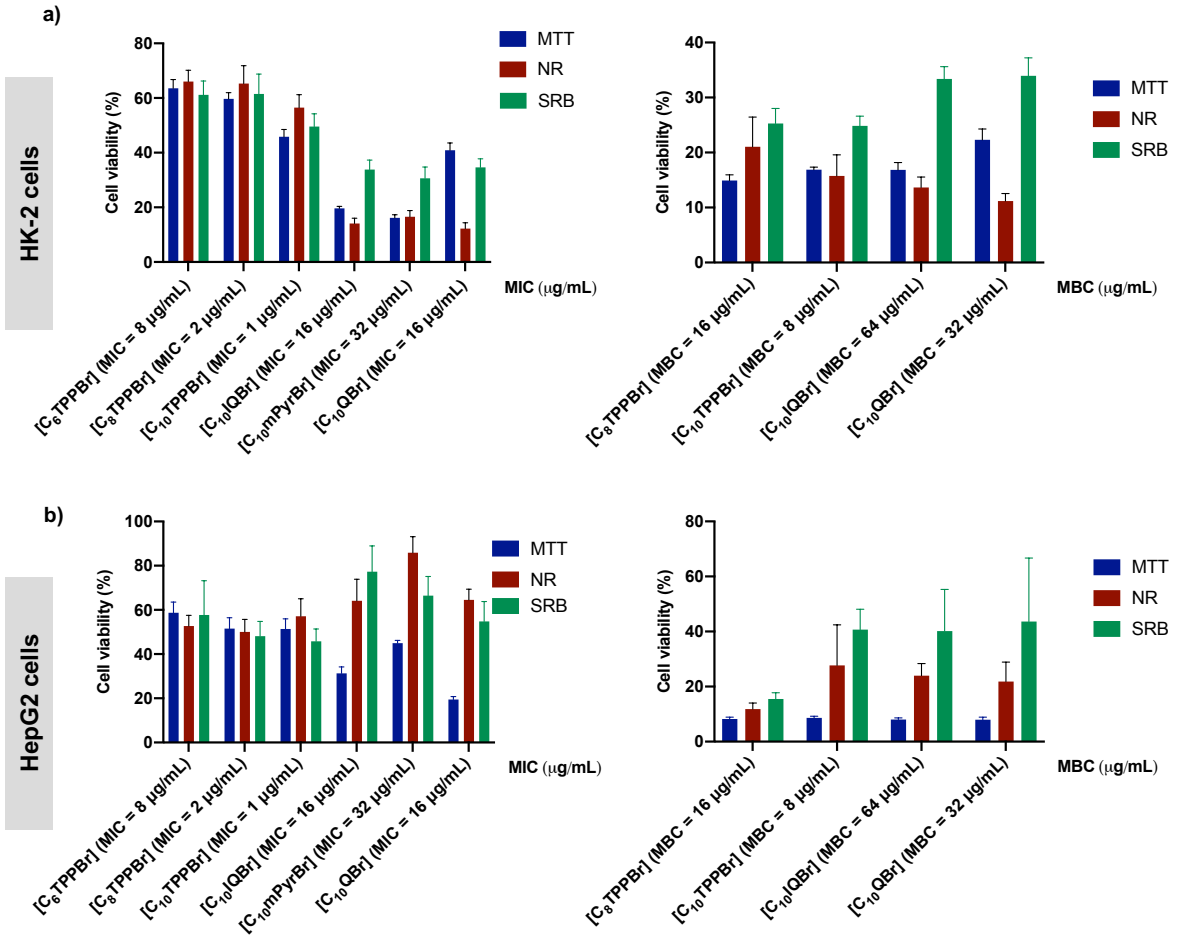

Figure 28. Cytotoxicity profile of HK-2 **(a)** and HepG2 **(b)** cell lines *vs.* the MIC and MBC values of compounds [C_6TPPBr], [C_8TPPBr], [C_{10}TPPBr], [C_{10}IQBr], [C_{10}mPyrBr] and [C_{10}QBr] against *S. aureus*. Results are expressed as the percentage of viable cells compared to the control (100%, data not shown). The data are presented as the mean ± SD of three independent experiments.

At MIC/MBC concentrations, a quite different response pattern across the six compounds was seen among cell types (Figure 28). In general, HepG2 cells were more sensitive to TPP derivatives-induced toxicity than HK-2; the former cells (malignant cells) have markedly higher mitochondrial transmembrane potential than HK-2 (normal cells), which likely leads their selective accumulation within cancer cell mitochondria, thereby enhancing cytotoxicity [186,187]. Contrariwise, HepG2 cells were least sensitive to the other cations tested (IQ, mPyr and Q). It was demonstrated that the cytotoxicity of these derivatives nonmonotonically changes between cell types. These studies reinforce the hypothesis that *in vitro* cytotoxicity is frequently cell-type specific and that cytotoxicity in one cell type does not necessarily predict cytotoxicity in another [188].

From Figure 28a, one observes that for TPP cation there is simultaneously higher antimicrobial activity (MIC ≤ 8 μg/mL) and lower cytotoxicity than other cations. Thus, it

was identified as the optimal cation for this specific set of compounds. However, the influence of the alkyl chain in the proper cytotoxicity/antimicrobial efficacy ratio is not yet fully understood, once no obvious pattern was observed apart from the fact that longer alkyl side chain compounds had better results in inhibiting bacterial growth for *S. aureus* bacterium and apparently present an enhance in cytotoxicity towards HK-2 cells. Another interesting observation arises from a similar cell viability percent for [C_{10}IQBr], [C_{10}mPyrBr] and [C_{10}QBr] to HK-2 cells. Despite their similarity, and also low cell viability at MIC/MBC concentrations, they have different indices cytotoxicity/antimicrobial activity, with compound [C_{10}mPyrBr] showing the worst equilibrium between these two phenomena.

Concerning HepG2 cells (Figure 28b), at MIC/MBC concentrations, IQ, mPyr and Q cations exhibit lower cytotoxicity than TPP, but is follow a trend that is difficult to discern given the experimental uncertainties (*e.g.*, MTT assay). Despite their apparently less pronounced cytotoxicity, they show low antimicrobial activities (MIC ≥ 16 μg/mL, MBC ≥ 32 μg/mL). On the other hand, TPP derivatives [C_6TPPBr] and [C_8TPPBr] do not show promising indices cytotoxicity/antimicrobial activity due their cytotoxicity. It was demonstrated that the cytotoxicity of TPP derivatives nonmonotonically changes between cell types. The differential behaviour of TPP cation compared to IQ, mPyr and Q cations imply contribution by a specific, molecular-structure dependent mechanism that impacts cytotoxicity and antimicrobial efficacy.

Among the tested compounds, [C_{10}TPPBr] (Figure 29) is proposed as a potential candidate for further optimization, due to their excellent antimicrobial activity, even though at this level present a noticeable *in vitro* toxic effect on human cell lines, thereby setting limits to its possible *in vivo* use.

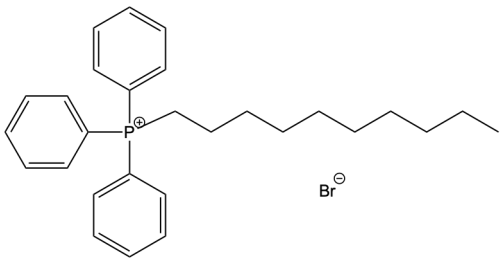

Figure 29. Structure of the lead compound for further optimization [C_{10}TPPBr].

Chapter 4

CONCLUDING REMARKS AND FUTURE PERSPECTIVES

In this Chapter, the main conclusions obtained with this Thesis are highlighted and summarized. Some main difficulties and challenges that arised during this Thesis are described. Perspectives and suggestions for further research are also identified and provided.

4.1. Concluding remarks

In the quest for innovative antimicrobial agents that keep pace with the rising challenge of bacterial resistance, the benefits to activity, bioavailability and multifunctionality possible through ionic liquids chemistry present a promising novel platform for future strategies. Besides, the described antimicrobial potential of certain ILs offers a distinct advantage to their application as novel antimicrobial agents.

In this Thesis a series of alkyl cationic derivatives comprised by seven different families of ionic liquids (TPP, mim, IQ, mPyr, Q, Pyr, TEA) with different alkyl chain lengths (C_6, C_8 and C_{10}) were synthetized to explore the relationships between molecular features and antimicrobial efficacies and human cell cytotoxicity. Twenty-one compounds were obtained in moderate-to-high yields *via* a simple, safe, solvent-free quaternization reaction. The structural elucidation by NMR (^{1}H, ^{13}C, and DEPT) technique confirm the compounds' structure and led to the obtainment of a valuable database for accurate identification.

The data of antibacterial activity, by MIC and MBC determination, allow to validate that antimicrobial efficiency of ILs can be modulated by both altering alkyl chain length and modifying the nature of the cation head. Additionally, it was shown that ILs structure flexibility is relevant to the design of novel antimicrobial agents targeted at specific infections. Alkyl triphenylphosphonium derivatives ([C_nTPPBr]) proved to be effective antimicrobial agents for *S. aureus* bacterium in planktonic state. Bacterial susceptibility to these TPP derivatives was much superior to that observed for the other cationic derivatives tested ([$C_n$mimBr], [C_nIQBr], [C_nmPyrBr], [C_nQBr], [C_nPyrBr] and [C_nTEABr]), proving that the presence of the TPP moiety contributed significantly for the antimicrobial activity of these compounds. It was also concluded that there was a clear correlation between antimicrobial activity (*i.e.*, for decreasing MIC values) and the length of the alkyl chain in the compounds. In fact, bacterial growth inhibition in the planktonic state and bactericidal activity were maximized for alkyl chains with ten-carbon atoms (C_{10}) in *S. aureus*, particularly for [C_{10}TPPBr].

Regarding the potential application in clinic of alkyl cationic derivatives, cytotoxicity is also an important issue that must be considered. Therefore, the cytotoxicity of six selected alkyl cationic derivatives, which have shown better performance on the *in vitro* antimicrobial susceptibility testing, were studied ([C_6TPPBr], [C_8TPPBr], [C_{10}TPPBr], [C_{10}mPyrBr], [C_{10}QBr], and [C_{10}IQBr]) against HK-2 and HepG2 cell lines. The data showed that the compounds decreased significantly the cell viability in both cell lines. Also there were

differences in the cytotoxicity of the compounds comparing both cell types. Considering that, at their MICs/MBCs, TPP derivatives showed lower cytotoxicity than other cationic derivatives (IQ, mPyr and Q) to HK-2 cells, even though in HepG2 cells this behaviour is inversed. The influence of the alkyl chain length is not yet clear understood, as no clear pattern was observed. The data obtained by the evaluation of intracellular reactive oxidative stress levels suggested that TPP derivatives can behave as pro-oxidants, although the effects on RS production were dependent on the cell line. Additionally, TPP and Q cations presented the highest increase in intracellular oxidative stress (in HK-2 and HepG2 cells, respectively) of all studied cationic heads.

Overall, the potential candidate for further optimization within the series of alkyl cationic derivatives studied was found to be [C_{10}TPPBr] based on its cytotoxicity/antimicrobial efficacy ratio. Although the results of this Thesis with [C_{10}TPPBr] were encouraging regarding the excellent antimicrobial efficacy of this compound, the apparently conflicting pro- and antioxidants effects, apart from the noticeable *in vitro* cytotoxicity, require further structural optimization before being considered a drug candidate.

4.2. Future perspectives

Throughout the development of this work, it was noticed that additional data coming from complementary tests could enrich the results obtained in this Thesis. However, due to time and pandemic constraints some tests were not possible to perform. For instance, it would be important to expand the screening against other bacterial species to explore the selectivity of the studied compounds. Moreover, the studies should also be continued by evaluating their performance towards resistant bacterial strains, namely clinical isolates.

There is still much to be learned about the impact of ILs on bacteria and their response to it. Thus, it would be interesting to evaluate the mechanisms of antibacterial action and toxicity to obtain relevant information for the optimization of the lead compound. Also, it is known that bacteria in biofilms are inherently more tolerant to antimicrobial agents when compared directly to planktonic cells of the same strain. With this in mind, it would be of great importance the assessment of the effects of the most promising alkyl cationic derivatives in the prevention and control of biofilms formed by *S. aureus*. Finally, it would be interesting to conduct the same studies with the cationic derivatives bearing long lengths of the alkyl chain (from C_{11} to C_{16}), since several studies have reported that these compounds exhibit an optimum efficiency as antimicrobial agents between an optimal number of carbon atoms (usually C_{11}-C_{16}). The data can be relevant to perform the lead optimization and develop a drug candidate.

REFERENCES

[1] M. Boylan, *International Public Health and Ethics*. Dordrecht, Netherlands: Springer, 2008, p. 297.

[2] Á. San Millán, "Dodging Magic Bullets: the Evolution of Bacterial Antibiotic Resistance," *Mètode Science Studies Journal*, no. 10, pp. 207–211, 2019. doi:10.7203/metode.10.14838

[3] M. Ferri, E. Ranucci, P. Romagnoli and V. Giaccone, "Antimicrobial Resistance: a Global Emerging Threat to Public Health Systems," *Critical Reviews in Food Science and Nutrition*, vol. 57, no. 13, pp. 2857–2876, 2017. doi:10.1080/10408398.2015.1077192

[4] B. Ribeiro da Cunha, L. P. Fonseca and C. R. C. Calado, "Antibiotic Discovery: Where Have We Come From, Where Do We Go?," *Antibiotics*, vol. 8, no. 2, pp. 1–21, 2019. doi:10.3390/antibiotics8020045

[5] S. Sanchez and A. L. Demain, *Antibiotics: Current Innovations and Future Trends*. USA: Caister Academic Press, 2015, p. 430. doi:10.21775/9781908230546

[6] L. Rajeev, "Antibiotic Discovery," *Mater Methods*, vol. 8, no. 2671, 2018. doi:10.13070/mm.en.8.2671

[7] N. Kresge, R. D. Simoni and R. L. Hill, "Selman Waksman: the Father of Antibiotics, *Journal of Biological Chemistry*, vol. 279, no. 48, pp. 101–102, 2004.

[8] T. T. Thomsen, "Peptide Antibiotics for ESKAPE Pathogens: Past, Present and Future Perspectives of Antimicrobial Peptides for the Treatment of Serious Gram-Negative and Gram-Positive Infections," (Doctoral dissertation, Department of Biology, Faculty of Science, University of Copenhagen, 2016).

[9] OpenLearn Science Course, "Understanding Antibiotic Resistance," Free learning from The Open University, 2018.

[10] J. W. Sanders, G. S. Fuhrer, M. D. Johnson and M. S. Riddle, "The Epidemiological Transition: the Current Status of Infectious Diseases in the Developed World *Versus* the Developing World," *Science Progress*, vol. 91, no. 1, pp. 1–38, 2008. doi:10.3184/003685008X284628

[11] K. I. Mohr, "History of Antibiotics Research," in *How to Overcome the Antibiotic Crisis,* Springer, Cham, 2016, pp. 237–272. doi:10.1007/82_2016_499

[12] B. Parsonage *et al*., "Control of Antimicrobial Resistance Requires an Ethical Approach," *Frontiers in Microbiology*, vol. 8, no. 2124, pp. 1–14, 2017. doi:10.3389/fmicb.2017.02124

[13] F. Prestinaci, P. Pezzotti and A. Pantosti, "Antimicrobial Resistance: a Global Multifaceted Phenomenon," *Pathogens and Global Health*, vol. 109, no. 7, pp. 309–318, 2015. doi:10.1179/2047773215Y.0000000030

[14] W. A. McGuinness, N. Malachowa and F. R. DeLeo, "Vancomycin Resistance in *Staphylococcus aureus*," *Yale Journal of Biology and Medicine*, vol. 90, no. 2, pp. 269–281, 2017.

[15] K. Bush, "Past and Present Perspectives on β-lactamases," *Antimicrobial Agents and Chemotherapy*, vol. 62, no. 10, pp. 1–20, 2018. doi:10.1128/AAC.01076-18

[16] A. H. A. M. van Hoek *et al*., "Acquired Antibiotic Resistance Genes: an Overview," *Frontiers in Microbiology*, vol. 2, no. 203, pp. 1–27, 2011. doi:10.3389/fmicb.2011.00203

[17] R. A. Smith, N. M. M'ikanatha and A. F. Read, "Antibiotic Resistance: a Primer and Call to Action," *Health Communication*, vol. 30, no. 3, pp. 309–314, 2015. doi:10.1080/10410236.2014.943634

[18] R. Nassiri, "Global Spread of Antibiotic Resistance Renders Current Antibiotics Infective," *Pharmacol Drug Action Study Journal*, vol. 2019, no. 1, pp. 01–02, 2019.

[19] H. Harbottle, S. Thakur, S. Zhao and D. G. White, "Genetics of Antimicrobial Resistance," *Animal Biotechnology*, vol. 17, no. 2, pp. 111–124, 2006. doi:10.1080/10495390600957092

[20] C. L. Ventola, "The Antibiotic Resistance Crisis - Part 1: Causes and Threats," *Pharmacy and Therapeutics*, vol. 40, no. 4, pp. 277−283, 2015.

[21] I. A. Rather, K. Byung-Chun, V. K. Bajpai and Y. H. Park, "Self-medication and Antibiotic Resistance: Crisis, Current Challenges, and Prevention," *Saudi Journal of Biological Sciences*, vol. 24, no. 4, pp. 808−812, 2017. doi:10.1016/j.sjbs.2017.01.004

[22] O. Genilloud, "Natural Products Discovery and Potential for New Antibiotics," *Current Opinion in Microbiology*, vol. 51, pp. 81−87, 2019. doi:10.1016/j.mib.2019.10.012

[23] J. Dietvorst, L. Vilaplana, N. Uria, M. P. Marco and X. Muñoz-Berbel, "Current and Near-Future Technologies for Antibiotic Susceptibility Testing and Resistant Bacteria Detection," *TrAC Trends in Analytical Chemistry*, vol. 127, no. 115891, pp. 1−13, 2020. doi:10.1016/j.trac.2020.115891

[24] B. Aslam *et al*., "Antibiotic Resistance: a Rundown of a Global Crisis," *Infection and Drug Resistance*, vol. 11, pp. 1645−1658, 2018. doi:10.2147/IDR.S173867

[25] J. M. Munita and C. A. Arias, "Mechanism of Antibiotic Resistance," *Microbiology Spectrum*, vol. 4, no. 2, pp. 1−37, 2016. doi:10.1128/microbiolspec.VMBF-0016-2015

[26] D. Mazel, "Integrons: Agents of Bacterial Evolution," *Nature Reviews Microbiology*, vol. 4, no. 8, pp. 608−620, 2006. doi:10.1038/nrmicro1462

[27] S. B. Levy and B. Marshall, "Antibacterial Resistance Worldwide: Causes, Challenges and Responses," *Nature Medicine*, vol. 10, no. 12, pp. 122−129, 2004. doi:10.1038/nm1145

[28] Online Course, "Bacterial Genomes: Antimicrobial Resistance in Bacterial Pathogens," FutureLearn platform, 2020.

[29] N. Woodford and M. J. Ellington, "The Emergence of Antibiotic Resistance by Mutation," *Clinical Microbiology and Infection*, vol. 13, no. 1, pp. 5−18, 2007. doi:10.1111/j.1469-0691.2006.01492.x

[30] M. J. Struelens, "The Epidemiology of Antimicrobial Resistance in Hospital Acquired Infections: Problems and Possible Solutions," *Bmj*, vol. 317, no. 7159, pp. 652−654, 1998. doi:10.1136/bmj.317.7159.652

[31] M. E. A. de Kraker, A. J. Stewardson and S. Harbarth, "Will 10 million People Die a Year due to Antimicrobial Resistance by 2050?," *PLoS medicine*, vol. 13, no. 11, pp. 1−6, 2016. doi:10.1371/journal.pmed.1002184

[32] J. O'Neill, "Antimicrobial resistance: Tackling a crisis for the health and wealth of nations. Review on Antimicrobial Resistance," *Review on Antimicrobial Resistance, London, United Kingdom*, pp. 1−20, 2014.

[33] G. V. Asokan, T. Ramadhan, E. Ahmed and H. Sanad, "WHO Global Priority Pathogens List: a Bibliometric Analysis of Medline-PubMed for Knowledge Mobilization to Infection Prevention and Control Practices in Bahrain," *Oman Medical Journal*, vol. 34, no. 3, pp. 184−193, 2019. doi:10.5001/omj.2019.37

[34] O. L. Davies and S. Bennett, "WHO Publishes List of Bacteria for Which New Antibiotics are Urgently Needed," *WHO Department of Communications*, 2017.

[35] D. Koulenti *et al*., "Lefamulin. Comment on: Novel antibiotics for multidrug-resistant gram-positive microorganisms," *Microorganisms*, vol. 7, no. 10, pp. 1−4, 2019. doi:10.3390/microorganisms7080270

[36] T. Funaki *et al*., "SCC*mec* Typing of PVL-Positive Community-Acquired *Staphylococcus aureus* (CA-MRSA) at a Japanese Hospital," *Heliyon*, vol. 5, no. 3, pp. 1−11, 2019. doi:10.1016/j.heliyon.2019.e01415

[37] P. D. Stapleton and P. W. Taylor, "Methicillin Resistance in *Staphylococcus aureus*: Mechanisms and Modulation," *Science Progress*, vol. 85, no. 1, pp. 57−72, 2002. doi:10.3184/003685002783238870

[38] R. J. Fair and Y. Tor, "Antibiotics and Bacterial Resistance in the 21st Century," *Perspectives in Medicinal Chemistry*, vol. 6, pp. 25−64, 2014. doi:10.4137/PMc.s14459

[39] H. F. Chambers and F. R. DeLeo, "Waves of Resistance: *Staphylococcus aureus* in the Antibiotic Era," *Nature Reviews Microbiology*, vol. 7, no. 9, pp. 629−641, 2009. doi:10.1038/nrmicro2200

[40] Y. Y. Yong, G. A. Dykes and W. S. Choo, "Biofilm Formation by Staphylococci in Health-related Environments and Recent Reports on their Control using Natural Compounds," *Critical Reviews in Microbiology*, vol. 45, no. 2, pp. 201−222, 2019. doi:10.1080/1040841X.2019.1573802

[41] M. M. H. Abdelbary, P. Basset, D. S. Blanc and E. J. Feil, "The Evolution and Dynamics of Methicillin-resistant *Staphylococcus aureus*," in *Genetics and Evolution of Infectious Diseases*, Elsevier, 2nd Ed., pp. 553−572, 2017.

[42] E. Chukwunonso *et al*., "Methicillin-resistant *Staphylococcus aureus*: a Mini Review," *International Journal of Medical Research & Health Sciences*, vol. 7, no. 1, pp. 122−127, 2018.

[43] M. Otto, "MRSA virulence and spread," *Cellular Microbiology*, vol. 14, no. 10, pp. 1513−1521, 2012. doi:10.1111/j.1462-5822.2012.01832.x

[44] V. Rungelrath and F. R. Deleo., "*Staphylococcus aureus*, Antibiotic Resistance, and the Interaction with Human Neutrophils," *Antioxidants and Redox Signaling*, pp. 1−56, 2020. doi:10.1089/ars.2020.8127

[45] C. Arjyal, J. KC and S. Neupane, "Prevalence of Methicillin-Resistant *Staphylococcus aureus* in Shrines," *International Journal of Microbiology*, vol. 2020, no. 7981648, pp. 1−10, 2020. doi:10.1155/2020/7981648

[46] H. Huang *et al*., "Comparisons of Community-associated Methicillin-resistant *Staphylococcus aureus* (MRSA) and Hospital-associated MSRA Infections in Sacramento, California," *Journal of Clinical Microbiology*, vol. 44, no. 7, pp. 2423−2427, 2006. doi:10.1128/JCM.00254-06

[47] S. Lakhundi and K. Zhang, "Methicillin-resistant *Staphylococcus aureus*: Molecular Characterization, Evolution, and Epidemiology," *Clinical Microbiology Reviews*, vol. 31, no. 4, pp. 1−103, 2018. doi:10.1128/CMR.00020-18

[48] U. Abubakar and S. A. S. Sulaiman, "Prevalence, Trend and Antimicrobial Susceptibility of Methicillin Resistant *Staphylococcus aureus* in Nigeria: a Systematic Review," *Journal of Infection and Public Health*, vol. 11, no. 6, pp. 763−770, 2018. doi:10.1016/j.jiph.2018.05.013

[49] A. Pantosti and M. Venditti, "What is MRSA?," *European Respiratory Journal*, vol. 34, no. 5, pp. 1190−1196, 2009. doi:10.1183/09031936.00007709

[50] N. A. Turner *et al*., "Methicillin-resistant *Staphylococcus aureus*: an Overview of Basic and Clinical Research," *Nature Reviews Microbiology*, vol. 17, no. 4, pp. 203−218, 2019. doi:10.1038/ s41579-018-0147-4

[51] A. Dorado-García *et al*., "Risk Factors for Persistence of Livestock-associated MRSA and Environmental Exposure in Veal Calf Farmers and their Family Members: an Observational Longitudinal Study," *BMJ Open*, vol. 3, no. 9, pp. 1−10, 2013. doi:10.1136/ bmjopen-2013-003272

[52] S. H. Back *et al*., "Livestock-associated Methicillin-resistant *Staphylococcus aureus* in Korea: Antimicrobial Resistance and Molecular Characteristics of LA-MRSA Strains Isolated From Pigs, Pig Farmers, and Farm Environment," *Journal of Veterinary Science*, vol. 21, no. 1, pp. 1−14, 2019. doi:10.4142/jvs.2020.21.e2

[53] K. T. Bæk *et al*., "β-Lactam Resistance in Methicillin-resistant *Staphylococcus aureus* USA300 is Increased by Inactivation of the ClpXP Protease," *Antimicrobial Agents and Chemotherapy*, vol. 58, no. 8, pp. 4593−4603, 2014. doi:10.1128/AAC.02802-14

[54] M. Ebadi and H. Ashrafi, "Typing of methicillin-resistant *Staphylococcus aureus* isolate from healthcare workers in Larestan," *Journal of Microbiology and Infectious Diseases*, vol. 8, no. 1, pp. 1−7, 2018. doi:10.5799/jmid.393890

[55] S. M. Abdelaziz, K. M. Aboshanab, M. Yassien and N. A. Hassouna, "Antimicrobial Resistance Patterns of MDR *Staphylococcus aureus* Clinical Isolates Involved in the Lower Respiratory Tract Infections in Egypt," *Archives of Pharmaceutical Sciences Ain Shams University*, vol. 3, no. 2, pp. 294−304, 2019. doi:10.21608/APS.2019.17391.1014

[56] B. Li and T. J. Webster, "Bacteria Antibiotic Resistance: New Challenges and Opportunities for Implant-associated Orthopedic Infections," *Journal of Orthopaedic Research®*, vol. 36, no. 1, pp. 22−32, 2018. doi:10.1002/jor.23656

[57] Q. Hu, H. Peng and X. Rao, "Molecular Events for Promotion of Vancomycin Resistance in Vancomycin Intermediate *Staphylococcus aureus*," *Frontiers in Microbiology*, vol. 7, no. 1601, pp. 1−18, 2016. doi:10.3389/fmicb.2016.01601

[58] M. Miragaia, "Factors Contributing to the Evolution of *mecA*-mediated β-lactam Resistance in Staphylococci: Update and New Insights From Whole Genome Sequencing (WGS)," *Frontiers in Microbiology*, vol. 9, no. 2723, pp. 1−16, 2018. doi:10.3389/fmicb.2018.02723

[59] H. Saber, A. S. Jasni, T. Z. M. T. Jamaluddin and R. Ibrahim, "A Review of Staphylococcal Cassette Chromosome *mec* (SCC*mec*) Types in Coagulase-negative Staphylococci (CoNS) Species," *The Malaysian Journal of Medical Sciences*, vol. 24, no. 5, pp. 7−18, 2017. doi:10.1128/AAC.02731-13

[60] B. Ballhausen, A. Kriegeskorte, N. Schleimer, G. Peters and K. Becker, "The *mecA* Homolog *mecC* Confers Resistance Against β-lactams in *Staphylococcus aureus* Irrespective of the Genetic Strain Background," *Antimicrobial Agents and Chemotherapy*, vol. 58, no. 7, pp. 3791−3798, 2014.

[61] B. Tarai, P. Das and D. Kumar, "Recurrent Challenges for Clinicians: Emergence of Methicillin-resistant *Staphylococcus aureus*, Vancomycin Resistance, and Current Treatment Options," *Journal of Laboratory Physicians*, vol. 5, no. 2, pp. 71−78, 2013. doi:10.4103/0974-2727.119843

[62] S. G. Gardner, D. D. Marshall, R. S. Daum, R. Powers and G. A. Somerville, "Metabolic Mitigation of *Staphylococcus aureus* Vancomycin Intermediate-Level Susceptibility," *Antimicrobial Agents and Chemotherapy*, vol. 62, no. 1, pp. 1−13, 2018. doi:10.1128/AAC.01608-17.

[63] B. Périchon and P. Courvalin, "Minireview-VanA-Type Vancomycin-Resistant *Staphylococcus aureus*," *Antimicrobial Agents and Chemotherapy*, vol. 53, no. 11, pp. 4580−4587, 2009. doi:10.1128/AAC.00346-09

[64] H. Peng *et al*., "WalK (S221P), a Naturally Occurring Mutation, Confers Vancomycin Resistance in VISA Strain XN108," *Journal of Antimicrobial Chemotherapy*, vol. 72, no. 4, pp. 1006−1013, 2017. doi:10.1093/jac/dkw518

[65] K. Ishii *et al*., "Phenotypic and Genomic Comparisons of Highly Vancomycin-Resistant *Staphylococcus aureus* Strains Developed From Multiple Clinical MRSA Strains by *In Vitro* Mutagenesis," *Scientific reports*, vol. 5, no. 17092, pp. 1−10, 2015. doi:10.1038/srep17092

[66] F. Grein, T. Schneider and H. G. Sahl, "Docking on Lipid II—a Widespread Mechanism for Potent Bactericidal Activities of Antibiotic Peptides," *Journal of Molecular Biology*, vol. 431, no. 18, pp. 3520−3530, 2019. doi:10.1016/j.jmb.2019.05.014

[67] J. L. Mainardi, R. Villet, T. D. Bugg, C. Mayer and M. Arthur, "Evolution of Peptidoglycan Biosynthesis Under the Selective Pressure of Antibiotics in Gram-Positive Bacteria," *FEMS Microbiology Reviews*, vol. 32, no. 2, pp. 386−408, 2008. doi:10.1111/j.1574-6976.2007.00097.x

[68] J. J. Malin and E. de Leeuw, "Therapeutic Compounds Targeting Lipid II for Antibacterial Purposes," *Infection and Drug Resistance*, vol. 12, pp. 2613−2625, 2019. doi:10.2147/IDR.S215070

[69] M. J. Kwun, G. Novotna, A. R. Hesketh, L. Hill and H. J. Hong, "*In Vivo* Studies Suggest That Induction of VanS-Dependent Vancomycin Resistance Requires Binding of the Drug to D-Ala-D-Ala Termini in the Peptidoglycan Cell Wall," *Antimicrobial Agents and Chemotherapy*, vol. 57, no. 9, pp. 4470−4480, 2013. doi:10.1128/AAC.00523-13

[70] World Health Organization, "2019 antibacterial agents in clinical development: an analysis of the antibacterial clinical development pipeline," 2019.

[71] M. S. Niederman, *Pneumonia, An Issue of Clinics in Chest Medicine*. Elsevier Health Sciences, vol. 39, no. 4, pp. 862−864, 2018.

[72] S. Andrei, G. Droc and G. Stefan, "FDA Approved Antibacterial Drugs: 2018-2019," *Discoveries*, vol. 7, no. 4, pp. 1−11, 2019. doi:10.15190/d.2019.15

[73] L. D. Saravolatz and G. E. Stein, "Delafloxacin: a New Anti–Methicillin-Resistant *Staphylococcus aureus* Fluoroquinolone," *Clinical Infectious Diseases*, vol. 68, no. 6, pp. 1058−1062, 2019. doi:10.1093/cid/ciy600

[74] M. S. Rahman and Y. S. Koh, "Delafloxacin, a New Miracle in Antibiotics Armamentarium for Bacterial Infections," *Journal of Bacteriology and Virology*, vol. 49, no. 1, pp. 39−43, 2019. doi:10.4167/JBV.2019.49.1.39

[75] R. Tirupathi, S. Areti, S. A. Salim, V. Palabindala and N. Jonnalagadda, "Acute Bacterial Skin and Soft Tissue Infections: New Drugs in ID Armamentarium," *Journal of Community Hospital Internal Medicine Perspectives*, vol. 9, no. 4, pp. 310−313, 2019. doi:10.1080/20009666.2019.1651482

[76] G. L. Voulgaris, M. L. Voulgari and M. E. Falagas, "Developments on Antibiotics for Multidrug Resistant Bacterial Gram-Negative Infections," *Expert Review of Anti-infective Therapy*, vol. 17, no. 6, pp. 387−401, 2019. doi:10.1080/14787210.2019.1610392

[77] A. M. Bal *et al*., "Future Trends in the Treatment of Methicillin-Resistant *Staphylococcus aureus* (MRSA) Infection: an In-Depth Review of Newer Antibiotics Active Against an Enduring Pathogen," *Journal of Global Antimicrobial Resistance*, vol. 10, pp. 295−303, 2017. doi:10.1016/j.jgar.2017.05.019

[78] M. Bassetti, A. Russo, A. Carnelutti and M. Wilcox, "Emerging Drugs for Treating Methicillin-Resistant *Staphylococcus aureus*," *Expert Opinion on Emerging Drugs*, vol. 24, no. 3, pp. 191−204, 2019. doi:10.1080/14728214.2019.1677607

[79] W. O'Riordan *et al*., "A Randomized Phase 2 Study Comparing Two Doses of Delafloxacin With Tigecycline in Adults With Complicated Skin and Skin-Structure Infections," *International Journal of Infectious Diseases*, vol. 30, pp. 67−73, 2015. doi:10.1016/j.ijid.2014.10.009

[80] A. Liapikou, C. Cilloniz, A. Palomeque and T. Torres, "Emerging Antibiotics for Community-Acquired Pneumonia," *Expert Opinion on Emerging Drugs*, vol. 24, no. 4, pp. 221−231, 2019. doi:10.1080/14728214.2019.1685494

[81] M. Castanheira *et al*., "*In Vitro* Activity of Plazomicin Against Gram-Negative and Gram-Positive Isolates Collected From U.S Hospitals and Comparative Activities of Aminoglycosides Against Carbapenem-Resistant *Enterobacteriaceae* and Isolates Carrying Carbapenemase Genes," *Antimicrobial Agents and Chemotherapy*, vol. 62, no. 8, pp. 1−8, 2018. doi:10.1128/AAC.00313-18

[82] M. Bassetti, A. Carnelutti, N. Castaldo and M. Peghin, "Important New Therapies for Methicillin-Resistant *Staphylococcus aureus*," *Expert Opinion on Pharmacotherapy*, vol. 20, no. 18, pp. 2317−2334, 2019. doi:10.1080/14656566.2019.1675637

[83] M. Bassetti and E. Righi, "Development of Novel Antibacterial Drugs to Combat Multiple Resistant Organisms," *Langenbeck's Archives of Surgery*, vol. 400, no. 2, pp. 153−165, 2015. doi:10.1007/s00423-015-1280-4

[84] M. S. Butler and D. L. Paterson, "Antibiotics in the Clinical Pipeline in October 2019," *The Journal of Antibiotics*, vol. 73, no. 6. pp. 329−364, 2019. doi:10.1038/s41429-020-0291-8

[85] T. H. Grossman, T. M. Murphy, A. M. Slee, D. Lofland and J. A. Sutcliffe, "Eravacycline (TP-434) is Efficacious in Animal Models of Infection," *Antimicrobial Agents and Chemotherapy*, vol. 59, no. 5, pp. 2567−2571, 2015. doi:10.1128/AAC.04354-14

[86] J. S. Solomkin *et al*., "Phase 2, Randomized, Double-Blind Study of the Efficacy and Safety of Two Dose Regimens of Eravacycline Versus Ertapenem for Adult Community-Acquired Complicated Intra-Abdominal Infections," *Antimicrobial Agents and Chemotherapy*, vol. 58, no. 4, pp. 1847−1854, 2014. doi:10.1128/AAC.01614-13

[87] F. M. Abrahamian, "Omadacycline for Acute Bacterial Skin and Skin Structure Infections," *Clinical Infectious Diseases*, vol. 69, no. Supplement 1, pp. 23−32, 2019. doi:10.1093/cid/ciz396

[88] M. A. Pfaller, P. R. Rhomberg, M. D. Huband and R. K. Flamm, "Activities of Omadacycline and Comparator Agents Against *Staphylococcus aureus* Isolates From a Surveillance Program Conducted in North America and Europe," *Antimicrobial Agents and Chemotherapy*, vol. 61, no. 3, pp. 1−5, 2017. doi:10.1128/AAC.02411-16

[89] G. J. Noel, M. P. Draper, H. Hait, S. K. Tanaka and R. D. Arbeit, "A Randomized, Evaluator-Blind, Phase 2 Study Comparing the Safety and Efficacy of Omadacycline to Those of Linezolid for Treatment of Complicated Skin and Skin Structure Infections," *Antimicrobial Agents and Chemotherapy*, vol. 56, no. 11, pp. 5650−5654, 2012. doi:10.1128/AAC.00948-12

[90] J. A. Karlowsky, J. Steenbergen and G. G. Zhanel, "Microbiology and Preclinical Review of Omadacycline," *Clinical Infectious Diseases*, vol. 69, no. Supplement 1, pp. 6−15, 2019. doi:10.1093/cid/ciz395

[91] L. M. Avery and D. P. Nicolau, "Investigational Drugs for the Treatment of Infections Caused by Multidrug-Resistant Gram-Negative Bacteria," *Expert Opinion on Investigational Drugs*, vol. 27, no. 4, pp. 325−338, 2018. doi:10.1080/13543784.2018.1460354

[92] S. Paukner, S. P. Gelone, S. J. R. Arends, R. K. Flamm and H. S. Sader, "Antibacterial Activity of Lefamulin Against Pathogens Most Commonly Causing Community-Acquired Bacterial Pneumonia: SENTRY Antimicrobial Surveillance Program (2015–2016)," *Antimicrobial Agents and Chemotherapy*, vol. 63, no. 4. pp. 1−6, 2019. doi:10.1128/AAC.02161-18.

[93] W. W. Wicha, W. T. Prince, C. Lell, W. Heilmayer and S. P. Gelone, "Pharmacokinetics and tolerability of lefamulin following intravenous and oral dosing," *Journal of Antimicrobial Chemotherapy*, vol. 74, no. Supplement 3, pp. 19−26, 2019. doi:10.1093/jac/dkz087

[94] M. P. Veve and J. L. Wagner, "Lefamulin: Review of a Promising Novel Pleuromutilin Antibiotic," *The Journal of Human Pharmacology and Drug Therapy*, vol. 38, no. 9, pp. 935−946, 2018. doi:10.1002/phar.2166

[95] D. Koulenti *et al*., "Emerging Treatment Options for Infections by Multidrug-Resistant Gram-Positive Microorganisms," *Microorganisms*, vol. 8, no. 2, pp. 1−40, 2020. doi:10.3390/microorganisms8020191

[96] J. M. Lévêque, J. Estager, M. Draye and G. Cravotto, "Synthesis of Ionic Liquids Using Non Conventional Activation Methods: an Overview," *Monatshefte für Chemie-Chemical Monthly*, vol. 138, no. 11, pp. 1103−1113, 2007. doi:10.1007/s00706-007-0742-y

[97] R. Ratti, "Ionic Liquids: Synthesis and Applications in Catalysis," *Advances In Chemistry*, vol. 2014, no. 729842, pp. 1−16, 2014. doi:10.1155/2014/729842

[98] F. Endres, A. Abbott and D. R. MacFarlane, *Electrodeposition from Ionic Liquids*, 2nd Edition. John Wiley & Sons, 2017, p. 486.

[99] A. Van Den Bossche, "Halogen-free synthesis of 1, 3- dialkylimidazolium ionic liquids," (Master dissertation, Faculty of Science, KU Leuven, 2015).

[100] N. V. Plechkova and K. R. Seddon, "Applications of Ionic Liquids in the Chemical Industry," *Chemical Society Reviews*, vol. 37, no. 1, pp. 123−150, 2008. doi:10.1039/B006677J

[101] J. N. Pendleton and B. F. Gilmore, "The Antimicrobial Potential of Ionic Liquids: A Source of Chemical Diversity for Infection and Biofilm Control," *International Journal of Antimicrobial Agents*, vol. 46, no. 2, pp. 131−139, 2015. doi:10.1016/j.ijantimicag.2015.02.016

[102] J. Wang *et al*., "Recent development of ionic liquid membranes," *Green Energy & Environment*, vol. 1, no. 1, pp. 43−61, 2016. doi:10.1016/j.gee.2016.05.002

[103] I. M. Marucho, L. C. Branco and L. P. N. Rebelo, "Ionic liquids in Pharmaceutical Applications," *Annual Review of Chemical and Biomolecular Engineering*, vol. 5, pp. 527−546, 2014. doi:10.1146/annurev-chembioeng-060713-040024

[104] I. P. E. Macário, T. L. M. Veloso, J. L. Pereira, S. P. M. Ventura and J. A. P. Coutinho, "Potential Threats of Ionic Liquids to the Environment and Ecosphere," in *Encyclopedia of Ionic Liquids*. Springer Singapore, 2020, pp. 1−17. doi:10.1007/978-981-10-6739-6_66-1

[105] K. S. Egorova, E. G. Gordeev and V. P. Ananikov, "Biological Activity of Ionic Liquids and Their Application in Pharmaceutics and Medicine," *Chemical Reviews*, vol. 117, no. 10, pp. 7132−7189, 2017. doi:10.1021/acs.chemrev.6b00562

[106] I. M. Garcia *et al*., "Ionic Liquid as Antibacterial Agent for an Experimental Orthodontic Adhesive," *Dental Materials*, vol. 35, no. 8, pp. 1155–1165, 2019. doi:10.1016/j.dental.2019.05.010

[107] B. F. Gilmore, "Antimicrobial Ionic Liquids," in *Ionic Liquids: Applications and Perspectives*. Alexander Kokorin, IntechOpen, 2011, pp. 587–604, 2011.

[108] Y. V. Nancharaiah, G. K. K. Reddy, P. Lalithamanasa and V. P. Venugopalan, "The Ionic Liquid 1-alkyl-3-methylimidazolium Demonstrates Comparable Antimicrobial and Antibiofilm Behavior to a Cationic Surfactant," *Biofouling*, vol. 28, no. 10, pp. 1141–1149, 2012. doi:10.1080/08927014.2012.736966

[109] B. He, G. Ou, C. Zhou, M. Wang and S. Chen, "Antimicrobial Ionic Liquids with Fumarate Anion," *Journal of Chemistry*, vol. 2013, no. 473153, pp. 1–7, 2013. doi:10.1155/2013/473153

[110] A. Busetti *et al*., "Antimicrobial and Antibiofilm Activities of 1-Alkylquinolinium Bromide Ionic Liquids," *Green Chemistry*, vol. 12, no. 3, pp. 420–425, 2010. doi:10.1039/B919872E

[111] K. M. Docherty and C. F. Kulpa Jr, "Toxicity and Antimicrobial Activity of Imidazolium and Pyridinium Ionic Liquids," *Green Chemistry*, vol. 7, no. 4, pp. 185–189, 2005. doi:10.1039/B419172B

[112] F. Walkiewicz *et al*., "Multifunctional Long-Alkyl-Chain Quaternary Ammonium Azolate Based Ionic Liquids," *New Journal of Chemistry*, vol. 34, no. 10, pp. 2281–2289, 2010. doi:10.1039/C0NJ00228C

[113] M. I. Hossain *et al*., "Synthesis and Anti-Microbial Activity of Hydroxylammonium Ionic Liquids," *Chemosphere*, vol. 84, no. 1, pp. 101–104, 2011. doi:10.1016/j.chemosphere.2011.02.048

[114] G. A. O'Toole *et al*., "Diphosphonium Ionic Liquids as Broad Spectrum Antimicrobial Agents," *Cornea*, vol. 31, no. 7, pp. 810–816, 2012. doi:10.1097/ICO.0b013e31823f0a86

[115] F. Brunel *et al*., "Antibacterial Activities of Fluorescent Nano Assembled Triphenylamine Phosphonium Ionic Liquids," *Bioorganic & Medicinal Chemistry Letters*, vol. 26, no. 15, pp. 3770–3773, 2016. doi:10.1016/j.bmcl.2016.05.055

[116] A. García-Lorenzo *et al*., "Cytotoxicity of Selected Imidazolium-Derived Ionic Liquids in the Human Caco-2 Cell Line. Sub-Structural Toxicological Interpretation Through a QSAR Study," *Green chemistry*, vol. 10, no. 5, pp. 508–516, 2008. doi:10.1039/b718860a

[117] R. F. M. Frade, A. Matias, L. C. Branco, C. A. M. Afonso and C. M. M. Duarte, "Effect of Ionic Liquids on Human Colon Carcinoma HT-29 and CaCo-2 Cell Lines," *Green Chemistry*, vol. 9, no. 8, pp. 873–877, 2007. doi:10.1039/b617526k

[118] X. Li, J. Ma, C. Jing and J. Wang, "Expression Alterations of Cytochromes P4501A1, 2E1, and 3A, and Their Receptors AhR and PXR Caused by 1-Octyl-3-Methylimidazolium Chloride in Mouse Mammary Carcinoma Cells," *Chemosphere*, vol. 93, no. 10, pp. 2488–2492, 2013. doi:10.1016/j.chemosphere.2013.08.092

[119] I. Rusiecka and A. C. Składanowski, "Induction of the Multixenobiotic/Multidrug Resistance System in HeLa Cells in Response to Imidazolium Ionic Liquids," *Acta Biochimica Polonica*, vol. 58, no. 2, pp. 187–192, 2011. doi:10.18388/abp.2011_2263

[120] X. Li, J. Ma and J. Wang, "Cytotoxicity, Oxidative Stress, and Apoptosis in HepG2 Cells Induced by Ionic Liquid 1-Methyl-3-Octylimidazolium Bromide," *Ecotoxicology and Environmental Safety*, vol. 120, pp. 342–348, 2015. doi:10.1016/j.ecoenv.2015.06.018

[121] M. McLaughlin *et al*., "Cytotoxicity of 1-Alkylquinolinium Bromide Ionic Liquids in Murine Fibroblast NIH 3T3 Cells," *Green chemistry*, vol. 13, no. 10, pp. 2794–2800, 2011. doi:10.1039/c0gc00813c

[122] N. K. Kaushik, P. Attri, N. Kaushik and E. H. Choi, "Synthesis and Antiproliferative Activity of Ammonium and Imidazolium Ionic Liquids Against T98G Brain Cancer Cells," *Molecules*, vol. 17, no. 12, pp. 13727–13739, 2012. doi:10.3390/molecules171213727

[123] P. J. Carvalho *et al*., "Understanding the Impact of the Central Atom on the Ionic Liquid Behavior: Phosphonium vs Ammonium Cations," *The Journal of Chemical Physics*, vol. 140, no. 6, pp. 1–12, 2014. doi:10.1063/1.4864182

[124] A. Abbaszadegan *et al*., "The Effects of Different Ionic Liquid Coatings and the Length of Alkyl Chain on Antimicrobial and Cytotoxic Properties of Silver Nanoparticles," *Iranian Endodontic Journal*, vol. 12, no. 4, pp. 481−487, 2017. doi:10.22037/iej.v12i4.17905

[125] A. Miskiewicz, P. Ceranowicz, M. Szymczak, K. Bartuś and P. Kowalczyk, "The Use of Liquids Ionic Fluids as Pharmaceutically Active Substances Helpful in Combating Nosocomial Infections Induced by *Klebsiella pneumoniae* New Delhi Strain, *Acinetobacter baumannii* and *Enterococcus* species," *International Journal of Molecular Sciences*, vol. 19, no. 9, pp. 1−24, 2018. doi:10.3390/ijms19092779

[126] O. Forero Doria *et al*., "Novel Alkylimidazolium Ionic Liquids as an Antibacterial Alternative to Pathogens of the Skin and Soft Tissue Infections," *Molecules*, vol. 23, no. 9. pp. 1−15, 2018. doi:10.3390/molecules23092354

[127] S. P. M. Ventura *et al*., "Toxicity Assessment of Various Ionic Liquid Families Towards *Vibrio fischeri* Marine Bacteria," *Ecotoxicology and Environmental Safety*, vol. 76, pp. 162−168, 2012. doi:10.1016/j.ecoenv.2011.10.006

[128] M. Petkovic, K. R. Seddon, L. P. N. Rebelo and C. S. Pereira, "Ionic Liquids: a Pathway to Environmental Acceptability," *Chemical Society Reviews*, vol. 40, no. 3, pp. 1383−1403, 2011. doi:10.1039/c004968a

[129] J. Haldar, P. Kondaiah and S. Bhattacharya, "Synthesis and Antibacterial Properties of Novel Hydrolyzable Cationic Amphiphiles. Incorporation of Multiple Head Groups Leads to Impressive Antibacterial Activity," *Journal of Medicinal Chemistry*, vol. 48, no. 11, pp. 3823−3831, 2005. doi:10.1021/jm049106l

[130] K. R. Seddon, A. Stark and M. J. Torres, "Influence of Chloride, Water, and Organic Solvents on the Physical Properties of Ionic Liquids," *Pure and Applied Chemistry*, vol. 72, no. 12, pp. 2275−2287, 2000. doi:10.1351/pac200072122275

[131] T. E. Sintra, "Synthesis of More Benign Ionic Liquids for Specific Applications," (Doctoral dissertation, University of Aveiro, 2017).

[132] A. Mohammad, *Green Solvents II: Properties and Applications of Ionic Liquids*, vol. 2. Springer Science & Business Media, 2012.

[133] J. Teixeira *et al*., "Development of Hydroxybenzoic-Based Platforms as a Solution to Deliver Dietary Antioxidants to Mitochondria," *Scientific Reports*, vol. 7, no. 6842, pp. 1−18, 2017. doi:10.1038/s41598-017-07272-y

[134] X. Meng *et al*., "Improving Cellulose Dissolution in Ionic Liquids by Tuning the Size of the Ions: Impact of the Length of the Alkyl Chains in Tetraalkylammonium Carboxylate," *ChemSusChem*, vol. 10, no. 8, pp. 1749−1760, 2017. doi:10.1002/cssc.201601830

[135] A. Borges *et al*., "Antibacterial Activity and Mode of Action of Selected Glucosinolate Hydrolysis Products Against Bacterial Pathogens," *Journal of Food Science and Technology*, vol. 52, no. 8, pp. 4737−4748, 2015. doi:10.1007/s13197-014-1533-1

[136] A. M. Darwish, B. D. Farmer and J. P. Hawke, "Improved Method for Determining Antibiotic Susceptibility of *Flavobacterium columnare* Isolates by Broth Microdilution," *Journal of Aquatic Animal Health*, vol. 20, no. 4, pp. 185−191, 2008. doi:10.1577/H07-047.1

[137] CLSI, *Methods for Dilution Antimicrobial Susceptibility Tests for Bacteria That Grow Aerobically*; *Approved Standard—Tenth Edition*. CLSI document M07-A10, Wayne, PA: Clinical and Laboratory Standards Institute, 2015.

[138] T. L. Holland, C. W. Woods and M. Joyce, "Antibacterial Susceptibility Testing in the Clinical Laboratory," *Infectious Disease Clinics*, vol. 23, no. 4, pp. 757−790, 2009. doi:10.1016/j.idc.2009.06.001

[139] CLSI, *Methods for Determining Bactericidal Activity of Antimicrobial Agents; Approved Guideline*. CLSI document M26-A, Wayne, PA: Clinical and Laboratory Standards Institute, 1999.

[140] J. Baptista, M. Simões and A. Borges, "Effect of Plant-Based Catecholic Molecules on the Prevention and Eradication of *Escherichia coli* Biofilms: A Structure Activity Relationship Study," *International Biodeterioration & Biodegradation*, vol. 141, pp. 101−113, 2019. doi:10.1016/j.ibiod.2018.02.004

[141] J. C. Lopez-Romero, H. González-Ríos, A. Borges and M. Simões, "Antibacterial Effects and Mode of Action of Selected Essential Oils Components Against *Escherichia coli* and *Staphylococcus aureus*," *Evidence-Based Complementary and Alternative Medicine*, vol. 2015, no. 795435, pp. 1−9, 2015. doi:10.1155/2015/795435

[142] T. Moniz *et al*., "Insights on the Relationship Between Structure vs. Toxicological Activity of Antibacterial Rhodamine-Labelled 3-Hydroxy-4-Pyridinone Iron (III) Chelators in HepG2 Cells," *Interdisciplinary Toxicology*, vol. 11, no. 3, pp. 189−199, 2018. doi:10.2478/intox-2018-0016

[143] V. Y. Soldatow, E. L. LeCluyse, L. G. Griffith and I. Rusyn, "*In Vitro* Models for Liver Toxicity Testing," *Toxicology Research*, vol. 2, no. 1, pp. 23−39, 2013. doi:10.1039/c2tx20051a

[144] F. A. Barile, "Continuous Cell Lines as a Model for Drug Toxicity Assessment," in *In Vitro Methods in Pharmaceutical Research*. Academic Press, 1997, pp. 33−54.

[145] P. Bajaj, S. K. Chowdhury, R. Yucha, E. J. Kelly and G. Xiao, "Emerging Kidney Models to Investigate Metabolism, Transport, and Toxicity of Drugs and Xenobiotics," *Drug Metabolism and Disposition*, vol. 46, no. 11, pp. 1692−1702, 2018. doi:10.1124/dmd.118.082958

[146] B. George, D. You, M. S. Joy and L. M. Aleksunes, "Xenobiotic Transporters and Kidney Injury," *Advanced Drug Delivery Reviews*, vol. 116, pp. 73−91, 2017. doi:10.1016/j.addr.2017.01.005

[147] A. Jondeau, L. Dahbi, M. H. Bani-Estivals and M. C. Chagnon, "Evaluation of the Sensitivity of Three Sublethal Cytotoxicity Assays in Human HepG2 Cell Line Using Water Contaminants," *Toxicology*, vol. 226, no. 2−3, pp. 218−228, 2006. doi:10.1016/j.tox.2006.07.007

[148] L. A. Selenius, M. W. Lundgren, R. Jawad, O. Danielsson and M. Björnstedt, "The Cell Culture Medium Affects Growth, Phenotype Expression and the Response to Selenium Cytotoxicity in A549 and HepG2 Cells," *Antioxidants*, vol. 8, no. 5, pp. 1−14, 2019. doi:10.3390/antiox8050130

[149] J. E. Rodríguez, "Cytotoxicity and Effects on Cell Viability of Nickel Nanowires," (Master dissertation, King Abdullah University of Science and Technology, 2013).

[150] M. Phelan, "Unit 1.1. Basic Techniques for Mammalian Cell Tissue Culture" in *Current Protocols in Cell Biology*. J. S. Bonifacino, M. Dasso, J. B. Harford, J. Lippincott-Schwartz and K. M. Yamada eds. John Wiley & Sons, Inc, 1998.

[151] I. Zwolak, "Comparison of Three Different Cell Viability Assays for Evaluation of Vanadyl Sulphate Cytotoxicity in a Chinese Hamster Ovary K1 Cell Line," *Toxicology and Industrial Health*, vol. 32, no. 6, pp. 1013−1025, 2016. doi:10.1177/0748233714544190

[152] Cytotoxicity Assay Multiple Endpoints. [Online]. Available: www.xenometrix.ch

[153] P. Priyaja, P. Jayesh, R. Philip and I. B. Singh, "Pyocyanin Induced *In Vitro* Oxidative Damage and its Toxicity Level in Human, Fish and Insect Cell Lines for its Selective Biological Applications," *Cytotechnology*, vol. 68, no.1, pp. 143−155, 2016. doi:10.1007/s10616-014-9765-5

[154] M. V. Berridge, P. M. Herst and A. S. Tan, "Tetrazolium Dyes as Tools in Cell Biology: New Insights Into Their Cellular Reduction," *Biotechnology Annual Review*, vol. 11, pp. 127−152, 2005. doi:10.1016/S1387-2656(05)11004-7

[155] S. W. Lim, H. S. Loh, K. N. Ting, T. D. Bradshaw and Z. N. Allaudin, "Reduction of MTT to Purple Formazan by Vitamin E Isomers in the Absence of Cells," *Tropical Life Sciences Research*, vol. 26, no. 1, pp. 111−120, 2015.

[156] D. Chavarria *et al*., "Insights Into the Discovery of Novel Neuroprotective Agents: a Comparative Study Between Sulfanylcinnamic Acid Derivatives and Related Phenolic Analogues," *Molecules*, vol. 24, no. 23, pp. 1−16, 2019. doi:10.3390/molecules24234405

[157] Ö. S. Aslantürk, "*In Vitro* Cytotoxicity and Cell Viability Assays: Principles, Advantages, and Disadvantages", in *Genotoxicity: A Predictable Risk to Our Actual World*. InTech, 2018, vol. 2, p. 64.

[158] G. Repetto, A. Del Peso and J. L. Zurita, "Neutral Red Uptake Assay for the Estimation of Cell Viability/Cytotoxicity," *Nature Protocols*, vol. 3, no. 7, pp. 1125−1131, 2008. doi:10.1038/nprot.2008.75

[159] C. Fernandes *et al*., "PEGylated PLGA Nanoparticles as a Smart Carrier to Increase the Cellular Uptake of a Coumarin-Based Monoamine Oxidase B Inhibitor," *ACS Applied Materials & Interfaces*, vol. 10, no. 46, pp. 39557−39569, 2018. doi:10.1021/acsami.8b17224

[160] M. Sanaye and N. Pagare, "Evaluation of Antioxidant Effect and Anticancer Activity Against Human Glioblastoma (U373MG) Cell Lines of *Murraya Koenigii*," *Pharmacognosy Journal*, vol. 8, no. 3, pp. 220−225, 2016. doi:10.5530/pj.2016.3.7

[161] V. Vichai and K. Kirtikara, "Sulforhodamine B Colorimetric Assay for Cytotoxicity Screening," *Nature Protocols*, vol. 1, no. 3, pp. 1112−1116, 2006. doi:10.1038/nprot.2006.179

[162] E. A. Orellana and A. L. Kasinski, "Sulforhodamine B (SRB) Assay in Cell Culture to Investigate Cell Proliferation," *Bio-protocol*, vol. 6, no. 21, pp. 1−9, 2016. doi:10.21769/BioProtoc.1984

[163] C. Fernandes *et al*., "Development of a PEGylated-Based Platform for Efficient Delivery of Dietary Antioxidants Across the Blood–Brain Barrier," *Bioconjugate Chemistry*, vol. 29, no. 5, pp. 1677−1689, 2018. doi:10.1021/acs.bioconjchem.8b00151

[164] H. M. Shen, C. Y. Shi, Y. Shen and C. N. Ong, "Detection of Elevated Reactive Oxygen Species Level in Cultured Rat Hepatocytes Treated With Aflatoxin B_1," *Free Radical Biology and Medicine*, vol. 21, no. 2, pp. 139−146, 1996. doi:10.1016/0891-5849(96)00019-6

[165] S. Aula *et al*., "Biophysical, Biopharmaceutical and Toxicological Significance of Biomedical Nanoparticles," *Rsc Advances*, vol. 5, no. 59, pp. 47830−47859, 2015. doi:10.1039/c5ra05889a

[166] E. Pretsch, P. Buhlmann and M. Badertscher, *Structure Determination of Organic Compounds: Tables of Spectral Data*, Berlin Heidelberg: Springer-Verlag, 2009.

[167] V. K. R. Avula *et al*., "Synthesis, Docking, and Bioavailability of 2′-Oxo-3-phenylspiro [cyclopropane-1, 3′-indoline]-2, 2-dicarbonitriles as Antibacterial Agents In Silico," *Journal of Heterocyclic Chemistry,* vol. 56, no. 1, pp. 209−217, 2019. doi:10.1002/jhet.3396

[168] M. Andrade *et al*., "Fine-Tuning of the Hydrophobicity of Caffeic Acid: Studies on the Antimicrobial Activity Against *Staphylococcus aureus* and *Escherichia coli, RSC Advances*, vol. 5, no. 66, pp. 1−17, 2015. doi:10.1039/x0xx00000x

[169] A. Cornellas *et al*., "Self-Aggregation and Antimicrobial Activity of Imidazolium and Pyridinium Based Ionic Liquids in Aqueous Solution," *Journal of Colloid and Interface Science*, vol. 355, no. 1, pp. 164−171, 2011. doi:10.1016/j.jcis.2010.11.063

[170] G. McDonnell and A. D. Russell, "Antiseptics and Disinfectants: Activity, Action, and Resistance," *Clinical Microbiology Reviews*, vol. 12, no. 1, pp. 147−179, 1999.

[171] M. T. Garcia, I. Ribosa, L. Perez, A. Manresa and F. Comelles, "Micellization and Antimicrobial Properties of Surface-Active Ionic Liquids Containing Cleavable Carbonate Linkages," *Langmuir*, vol. 33, no. 26, pp. 6511−6520, 2017. doi:10.1021/acs.langmuir.7b00505

[172] M. T. Garcia, I. Ribosa, L. Perez, A. Manresa and F. Comelles, "Self-Assembly and Antimicrobial Activity of Long-Chain Amide-Functionalized Ionic Liquids in Aqueous Solution," *Colloids and Surfaces B: Biointerfaces*, vol. 123, pp. 318−325, 2014. doi:10.1016/j.colsurfb.2014.09.033

[173] S. Salajkova *et al*., "Wide-Antimicrobial Spectrum of Picolinium Salts," *Molecules*, vol. 25, no. 9, pp. 1−16, 2020. doi:10.3390/molecules25092254

[174] T. C. A. Pinto, A. Banerjee and P. A. Nazarov, "Triphenyl Phosphonium-Based Substances are Alternatives to Common Antibiotics," *Bulletin of Russian State Medical University*, vol. 1, pp. 16−20, 2018. doi:10.24075/brsmu.2018.003

[175] S. P. M. Ventura *et al*., "Simple Screening Method to Identify Toxic/Non-toxic Ionic Liquids: Agar Diffusion Test Adaptation, *Ecotoxicology and Environmental safety*, vol. 83, pp. 55−62, 2012. doi:10.1016/j.ecoenv.2012.06.002

[176] P. A. Lambert, "Cellular Impermeability and Uptake of Biocides and Antibiotics in Gram-Positive Bacteria and Mycobacteria, *Journal of Applied Microbiology*, vol. 92, pp. 46S−54S, 2002.

[177] M. D. Arbo *et al*., "Piperazine Designer Drugs Induce Toxicity in Cardiomyoblast h9c2 Cells Through Mitochondrial Impairment," *Toxicology letters*, vol. 229, no. 1, pp. 178−189, 2014. doi:10.1016/j.toxlet.2014.06.031

[178] J. Trnka, M. Elkalaf and M. Anděl, "Lipophilic Triphenylphosphonium Cations Inhibit Mitochondrial Electron Transport Chain and Induce Mitochondrial Proton Leak," *PloS one*, vol. 10, no. 4, pp. 1−14, 2015. doi:10.1371/journal.pone.0121837

[179] L. Y. Zakharova *et al*., "Alkyl Triphenylphosphonium Surfactants as Nucleic Acid Carriers: Complexation Efficacy Toward DNA Decamers, Interaction With Lipid Bilayers and Cytotoxicity Studies," *Physical Chemistry Chemical Physics*, vol. 21, no. 30, pp. 16706−16717, 2019. doi:10.1039/c9cp02384d

[180] S. Benfeito *et al*., "Fine-Tuning the Neuroprotective and Blood-Brain Barrier Permeability Profile of Multi-Target Agents Designed to Prevent Progressive Mitochondrial Dysfunction," *European Journal of Medicinal Chemistry*, vol. 167, pp. 525−545, 2019. doi:10.1016/j.ejmech.2019.01.055

[181] P. Silva *et al*., "Multifunctionality and Cytotoxicity of a Layered Coordination Polymer," *Dalton Transactions*, vol. 49, no. 13, pp. 3989−3998, 2020. doi:10.1039/c9dt04211c

[182] I. Pujalté *et al*., "Cytotoxicity and Oxidative Stress Induced by Different Metallic Nanoparticles on Human Kidney Cells," *Particle and Fibre Toxicology*, vol. 8, no. 10, pp. 1−16, 2011. doi:10.1186/1743-8977-8-10.

[183] H. Wang and J. A. Joseph, "Quantifying Cellular Oxidative Stress by Dichlorofluorescein Assay Using Microplate Reader," *Free Radical Biology and Medicine*, vol. 27, no. 5−6, pp. 612−616, 1999. doi:10.1016/s0891-5849(99)00107-0

[184] J. G. Sarver *et al*., "Early stage efficacy and toxicology screening for antibiotics and enzyme inhibitors," *Journal of Biomolecular Screening*, vol. 17, no. 5, pp. 673−682, 2012. doi:10.1177/1087057112438769

[185] J. Limwongyut, C. Nie, A. S. Moreland and G. C. Bazan, "Molecular Design of Antimicrobial Conjugated Oligoelectrolytes With Enhanced Selectivity Toward Bacterial Cells," *Chemical Science*, vol. 11, no. 31, pp. 8138−8144, 2020. doi:10.1039/D0SC03679J

[186] I. Y. Strobykina *et al*., "Triphenylphosphonium Cations of the Diterpenoid Isosteviol: Synthesis and Antimitotic Activity in a Sea Urchin Embryo Model," *Journal of Natural Products*, vol. 78, no. 6, pp. 1300−1308, 2015. doi:10.1021/acs.jnatprod.5b00124

[187] C. A. Reddy *et al*., "Mitochondrial-Targeted Curcuminoids: a Strategy to Enhance Bioavailability and Anticancer Efficacy of Curcumin," *Plos One*, vol. 9, no. 3, pp. 1−11, 2014. doi:10.1371/journal.pone.0089351

[188] M. Xia *et al*., "Compound Cytotoxicity Profiling Using Quantitative High-Throughput Screening," *Environmental Health Perspectives*, vol. 116, no. 3, pp. 284−291, 2008. doi:10.1289/ehp.10727

APPENDIX I – Chemical Studies

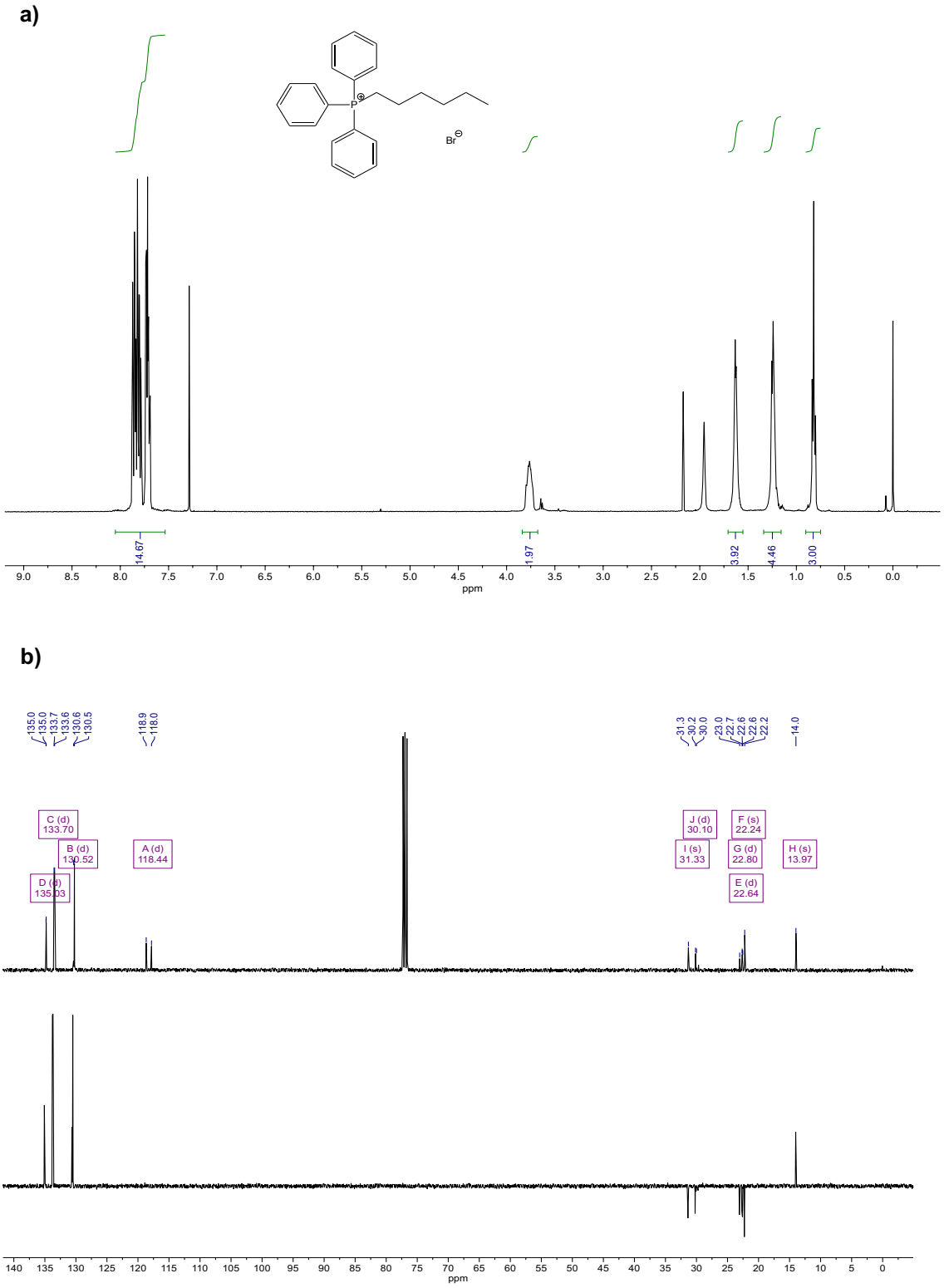

Figure 30. ^{1}H NMR **(a)**, ^{13}C NMR and DEPT135 **(b)** spectra of [C_6TPPBr].

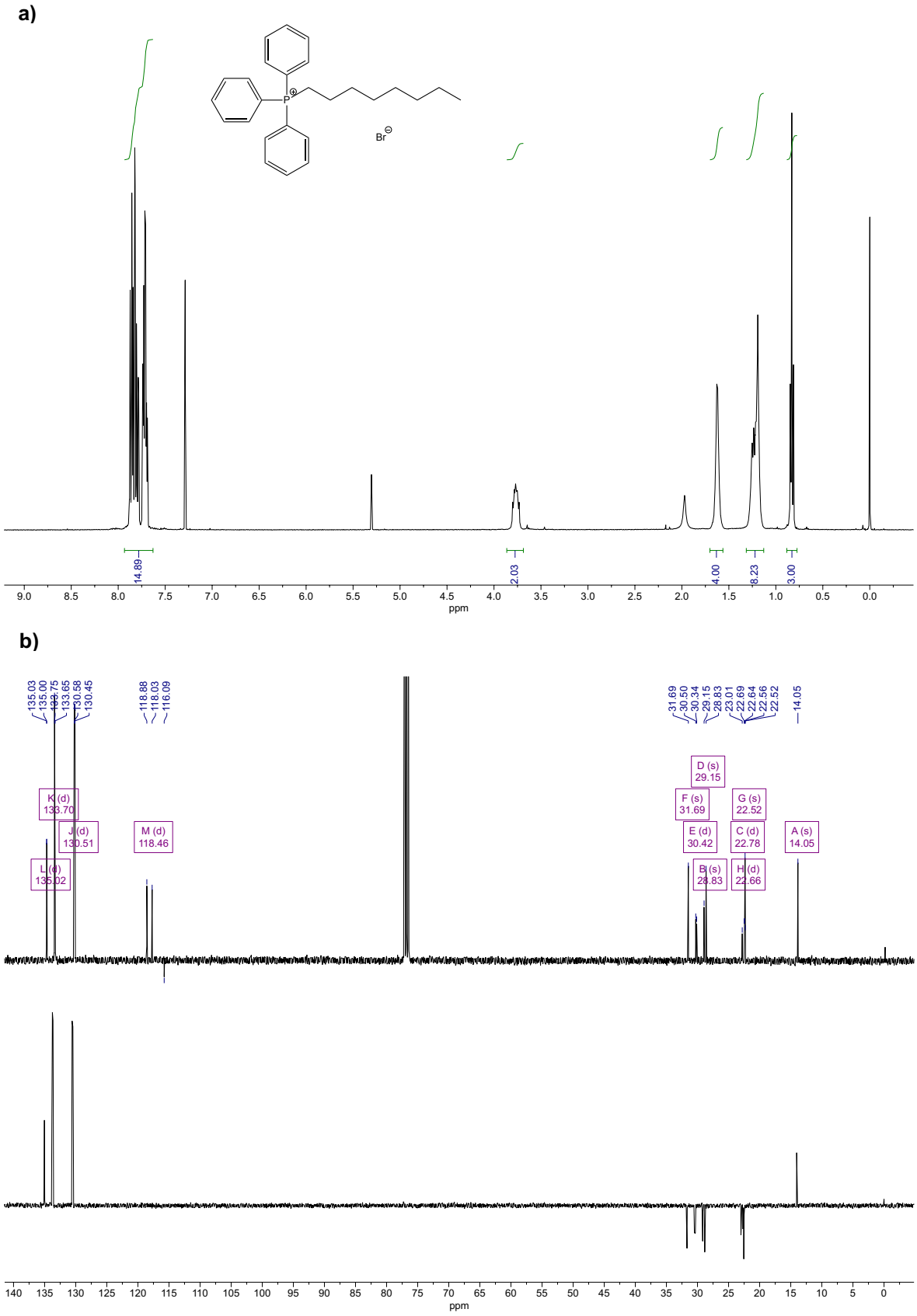

Figure 31. ^{1}H NMR **(a)**, ^{13}C NMR and DEPT135 **(b)** spectra of [C_8TPPBr].

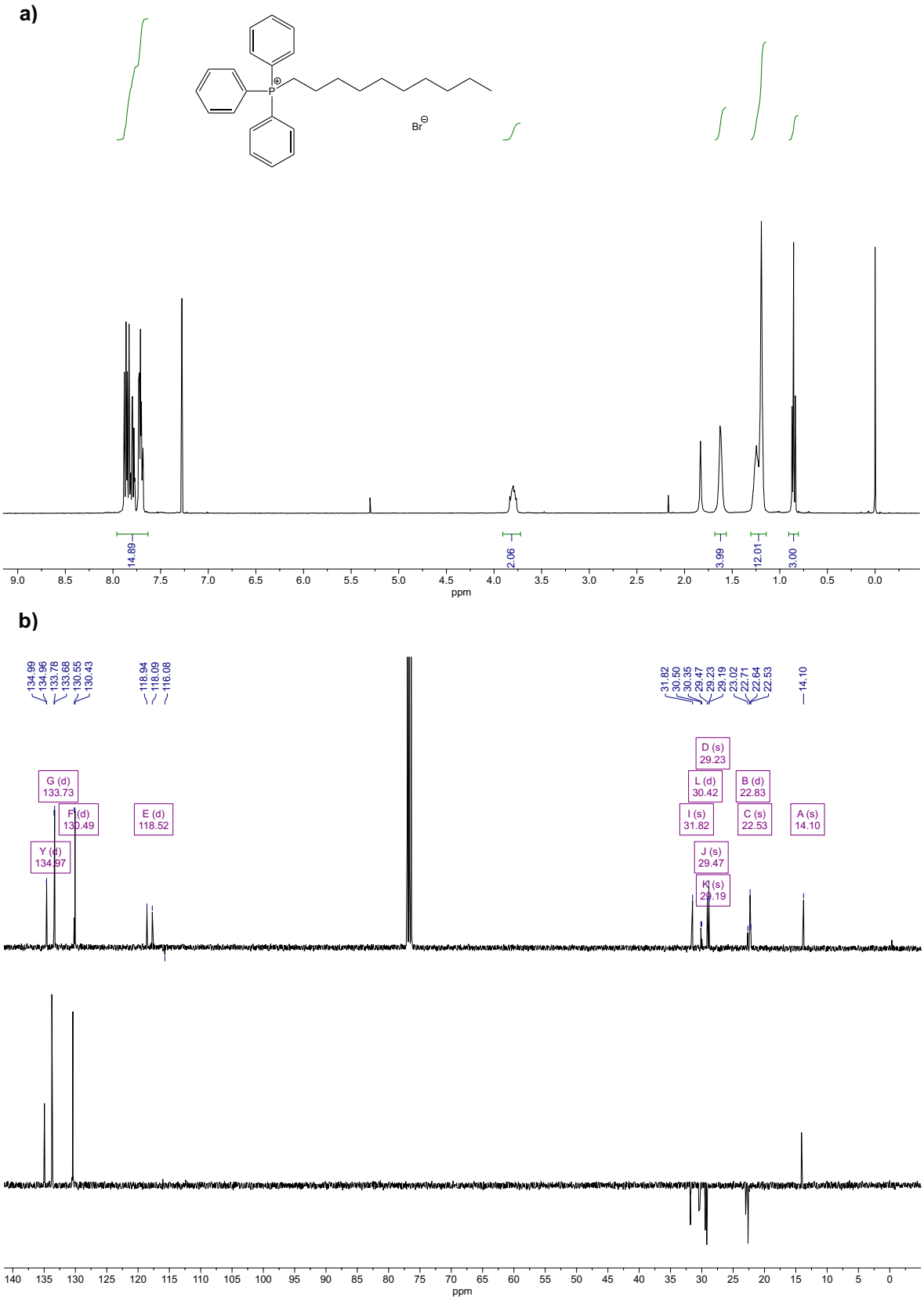

Figure 32. ^{1}H NMR **(a)**, ^{13}C NMR and DEPT135 **(b)** spectra of [C_{10}TPPBr].

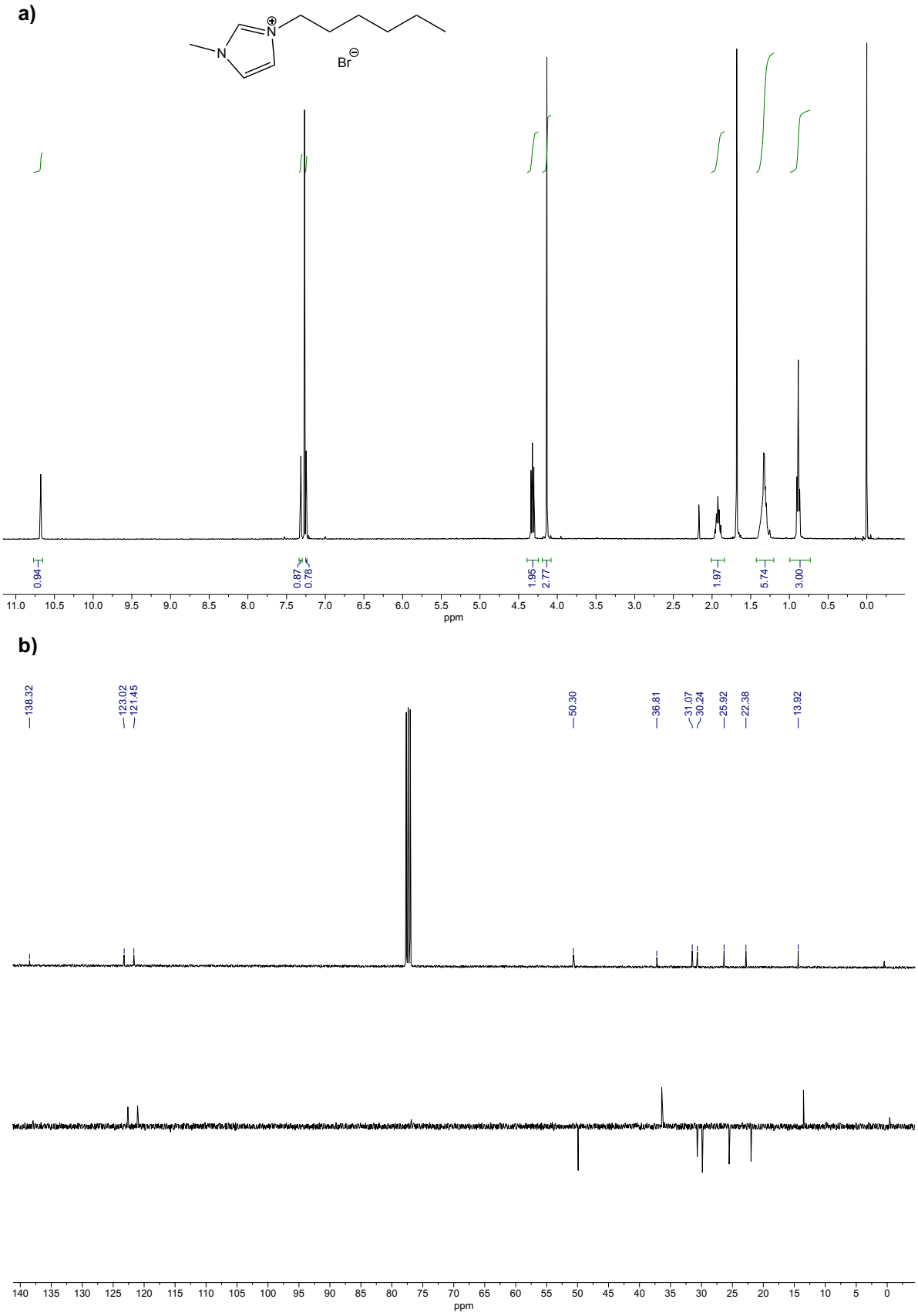

Figure 33. ^{1}H NMR **(a)**, ^{13}C NMR and DEPT135 **(b)** spectra of [C_6mimBr].

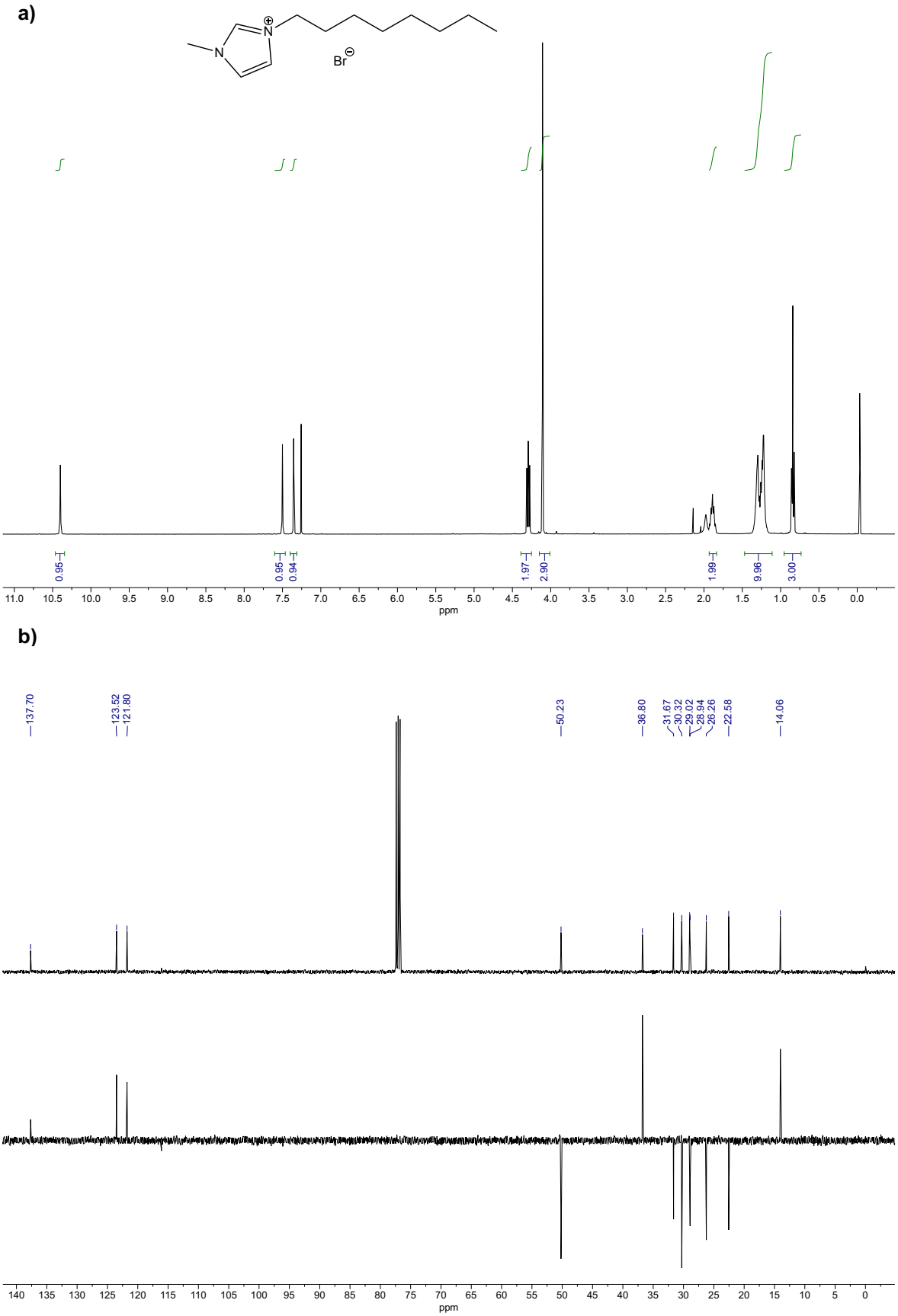

Figure 34. ^{1}H NMR **(a)**, ^{13}C NMR and DEPT135 **(b)** spectra of [C_8mimBr].

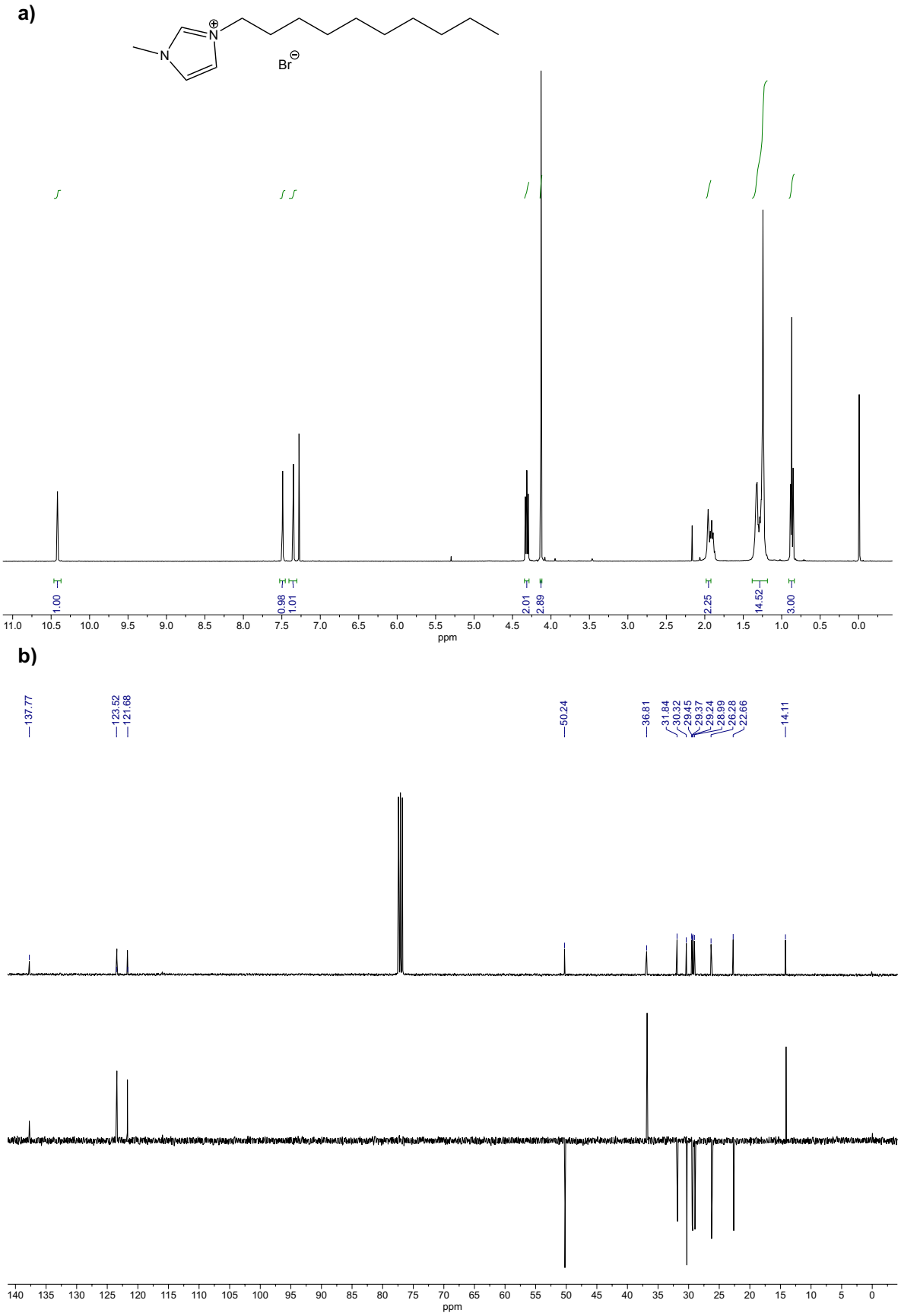

Figure 35. ^{1}H NMR **(a)**, ^{13}C NMR and DEPT135 **(b)** spectra of [C_{10}mimBr].

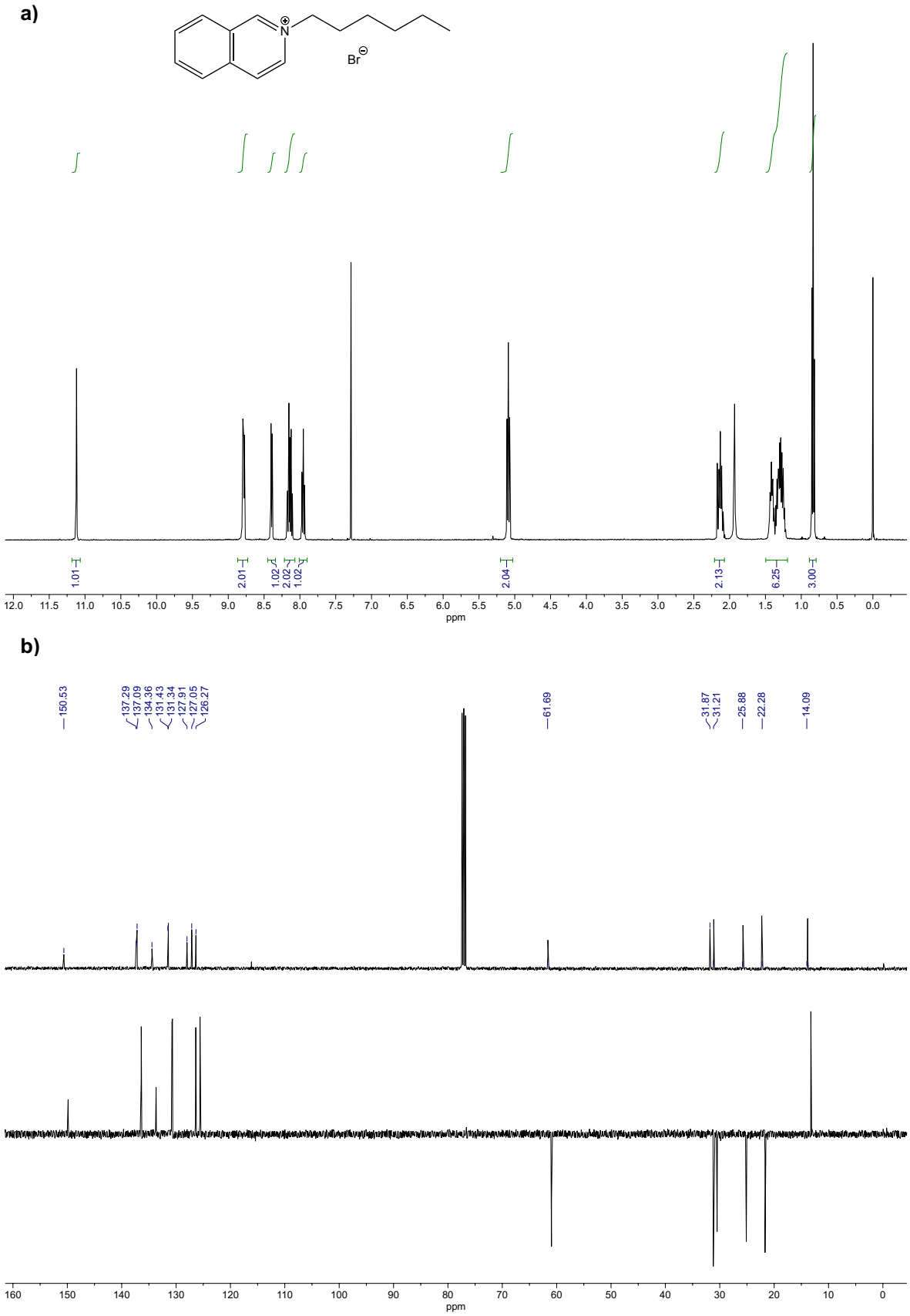

Figure 36. ^{1}H NMR **(a)**, ^{13}C NMR and DEPT135 **(b)** spectra of [C_6IQBr].

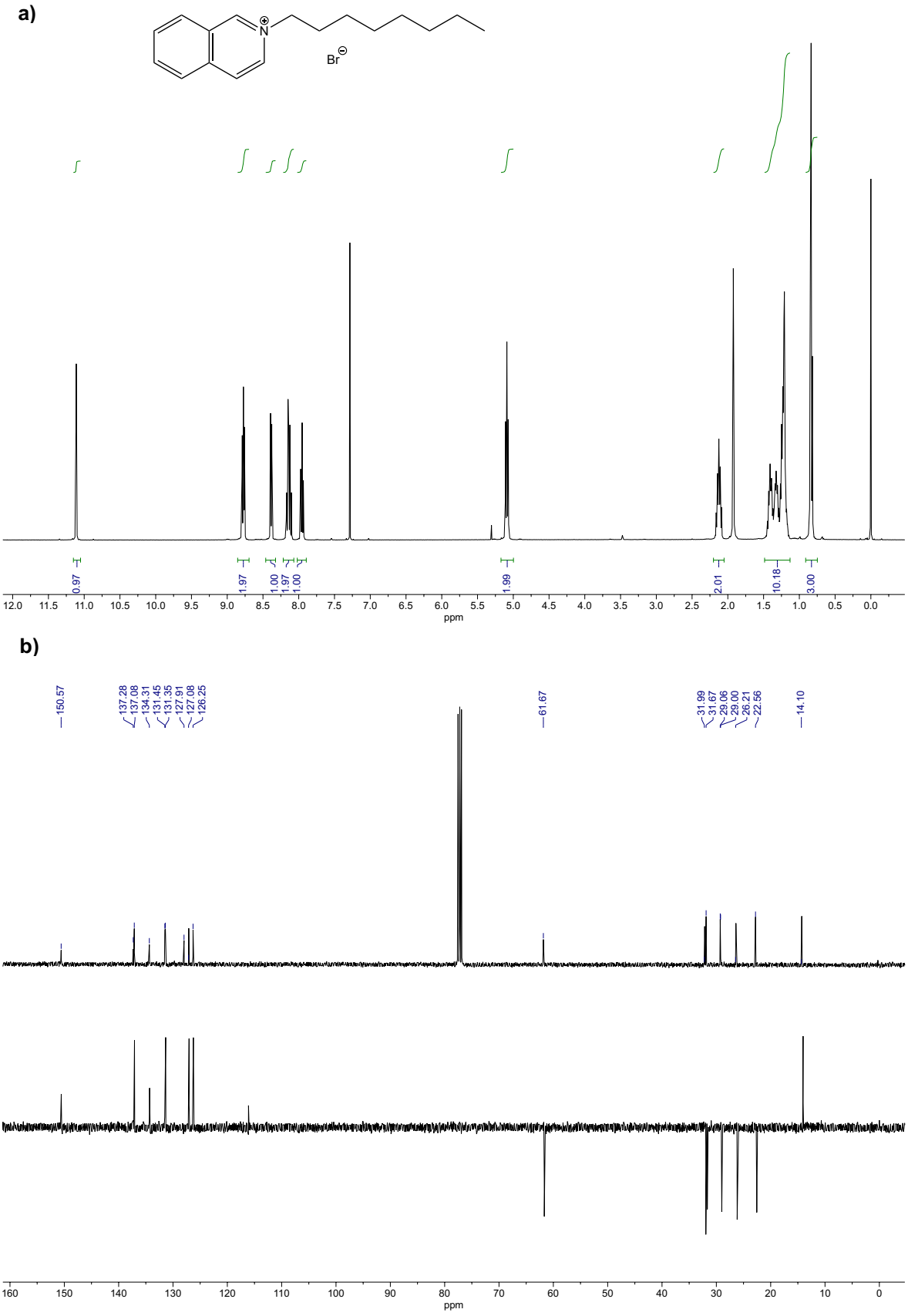

Figure 37. ^{1}H NMR **(a)**, ^{13}C NMR and DEPT135 **(b)** spectra of [C_8IQBr].

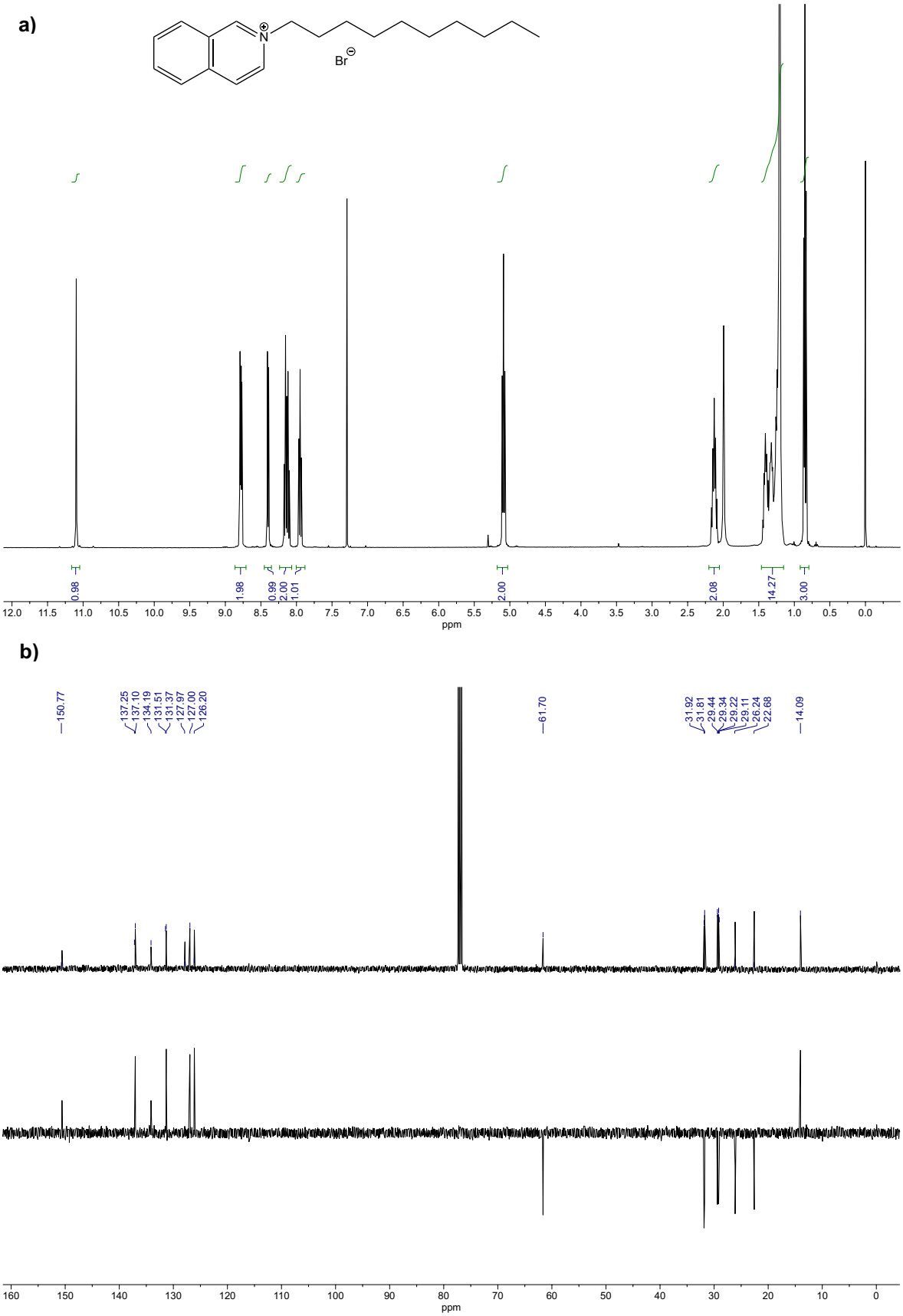

Figure 38. ^{1}H NMR **(a)**, ^{13}C NMR and DEPT135 **(b)** spectra of [C_{10}IQBr].

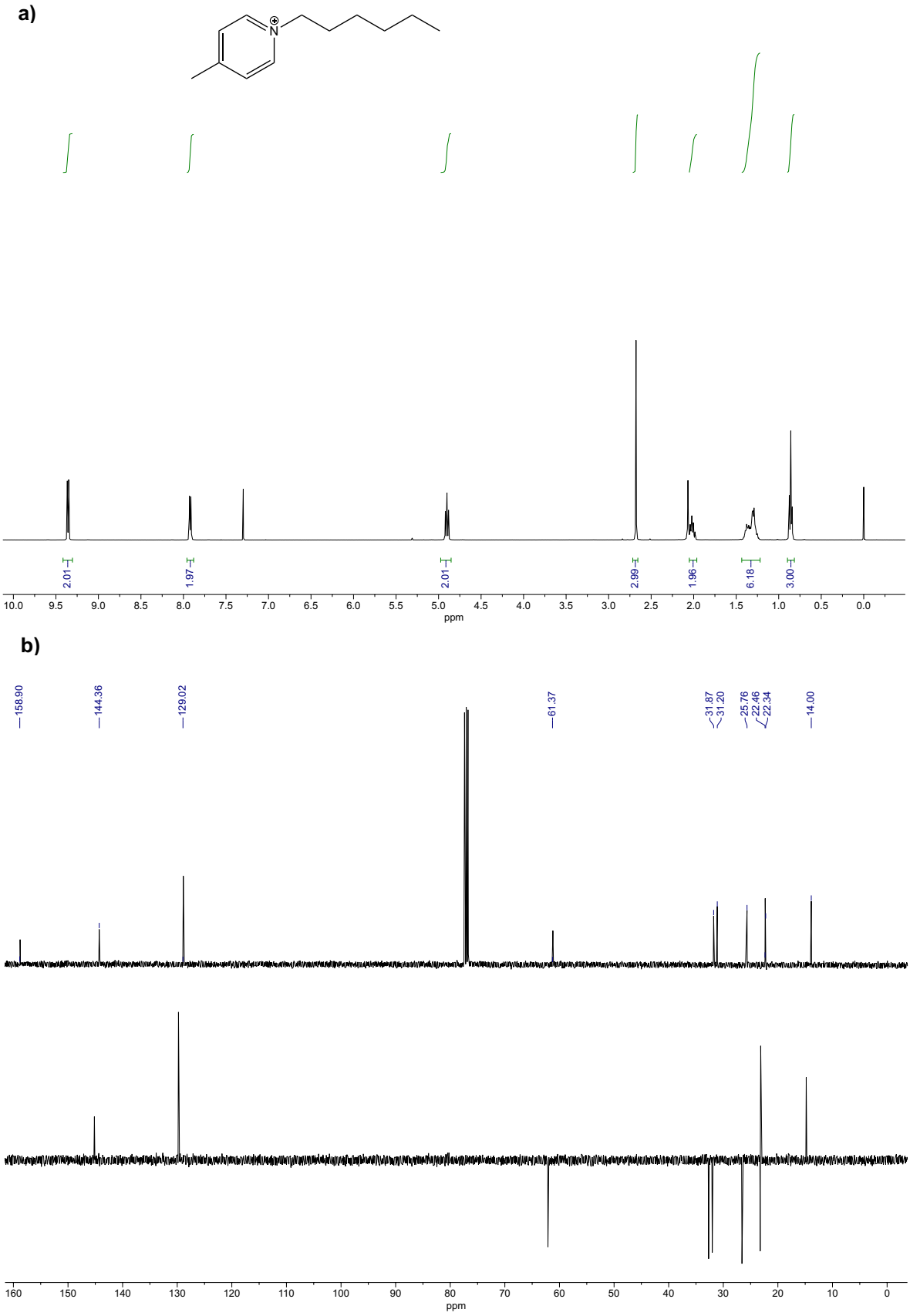

Figure 39. ^{1}H NMR **(a)**, ^{13}C NMR and DEPT135 **(b)** spectra of [C_6mPyrBr].

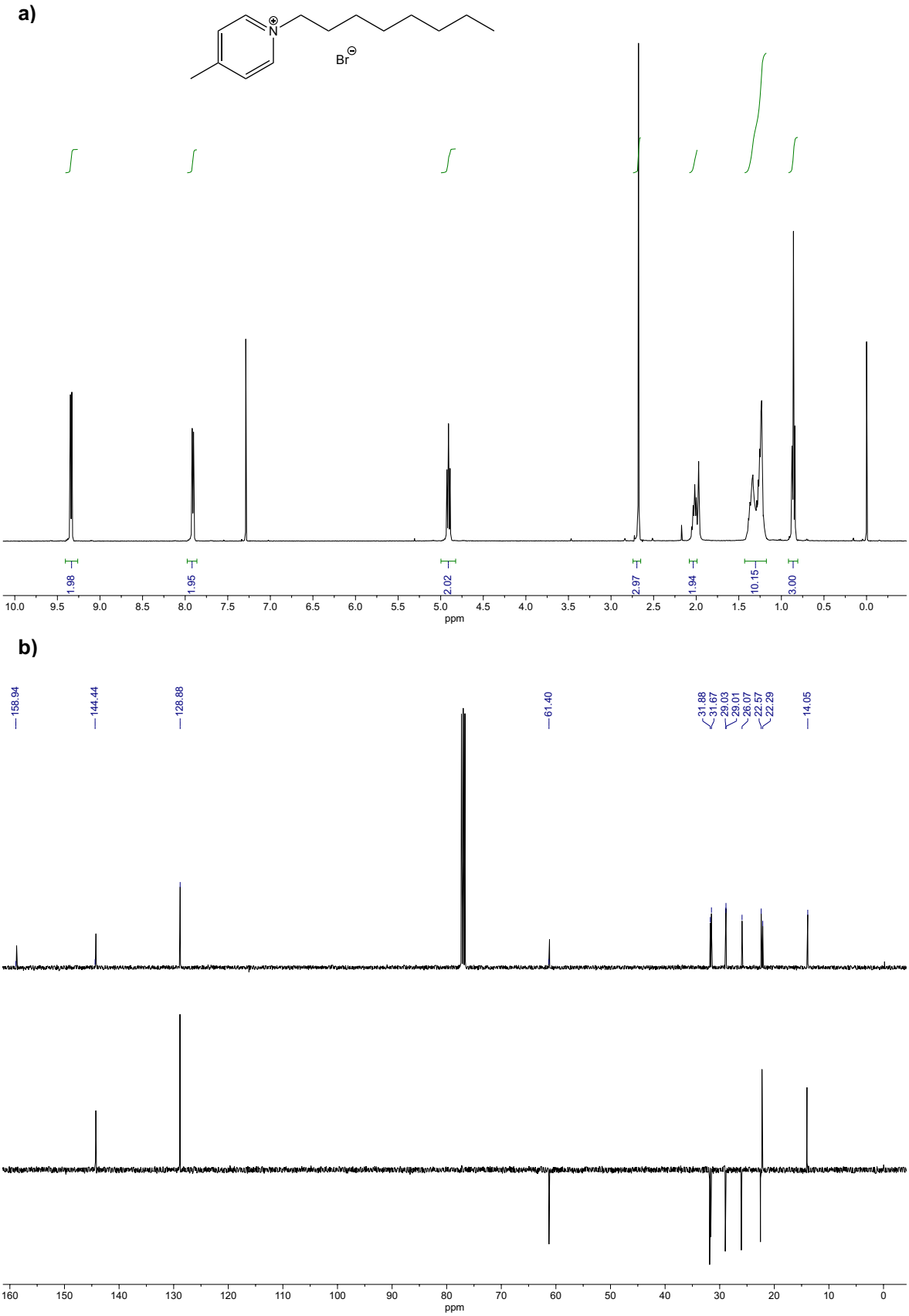

Figure 40. ^{1}H NMR **(a)**, ^{13}C NMR and DEPT135 **(b)** spectra of [C_8mPyrBr].

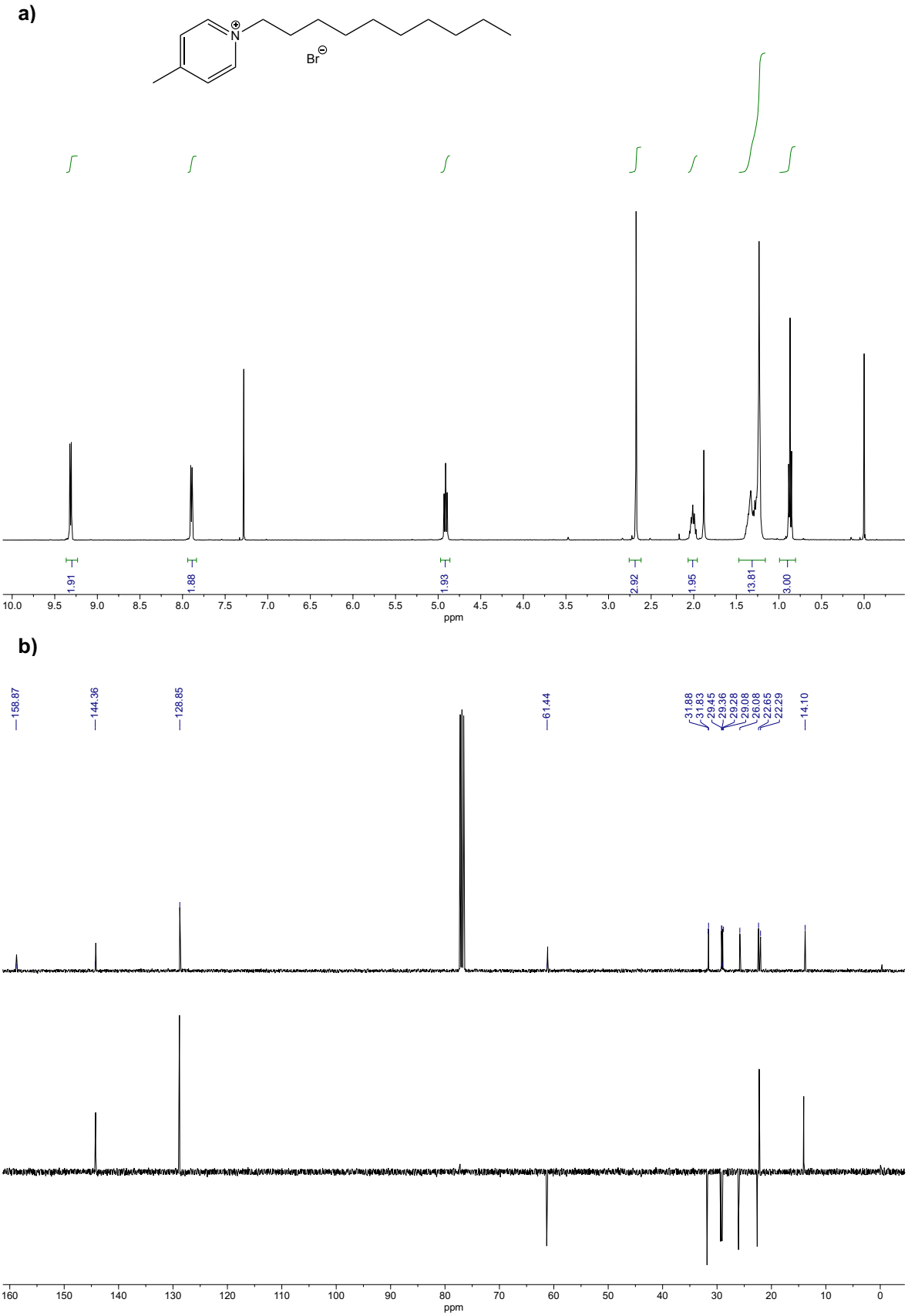

Figure 41. ^{1}H NMR **(a)**, ^{13}C NMR and DEPT135 **(b)** spectra of [C_{10}mPyrBr].

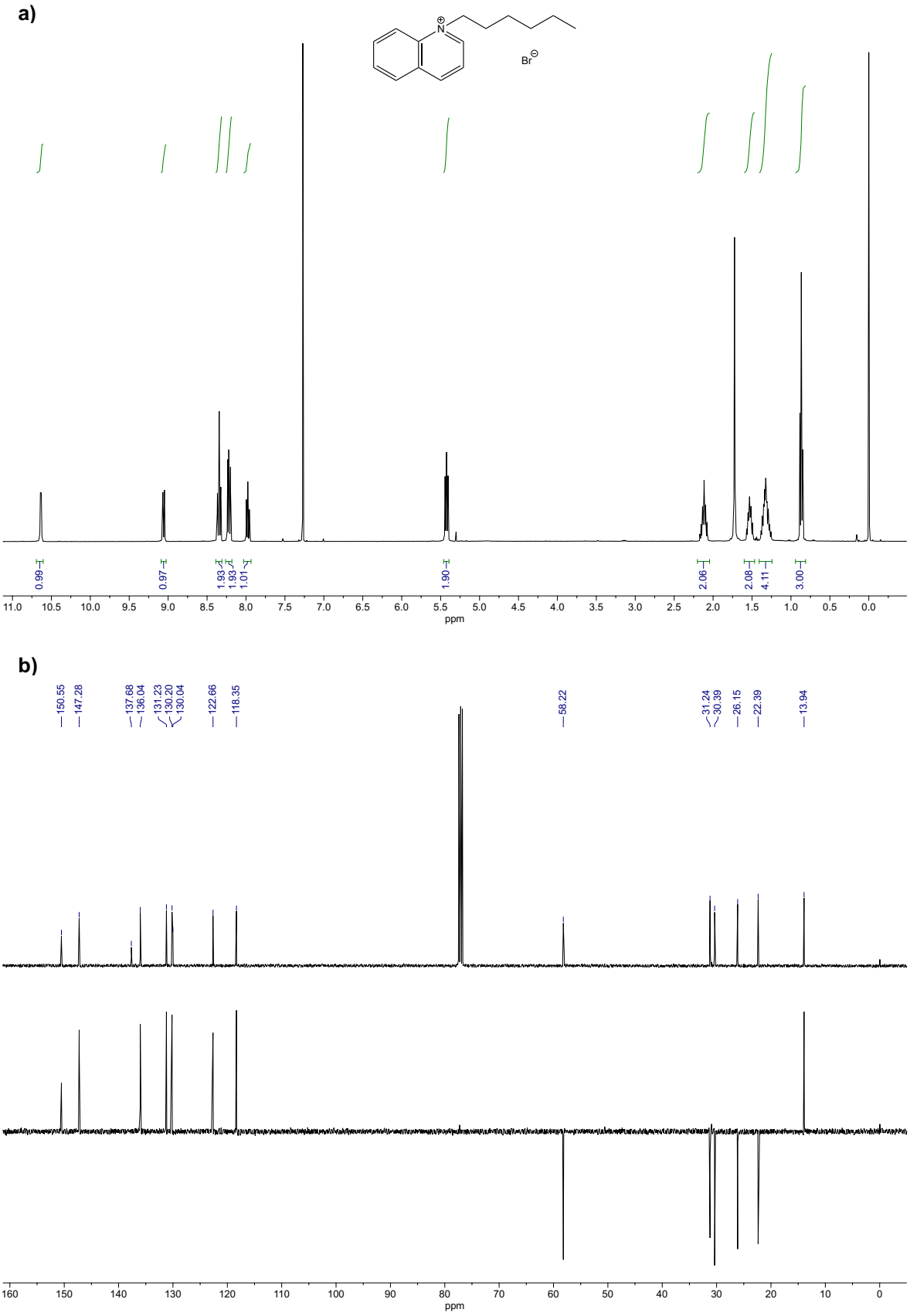

Figure 42. ^{1}H NMR **(a)**, ^{13}C NMR and DEPT135 **(b)** spectra of [C_6QBr].

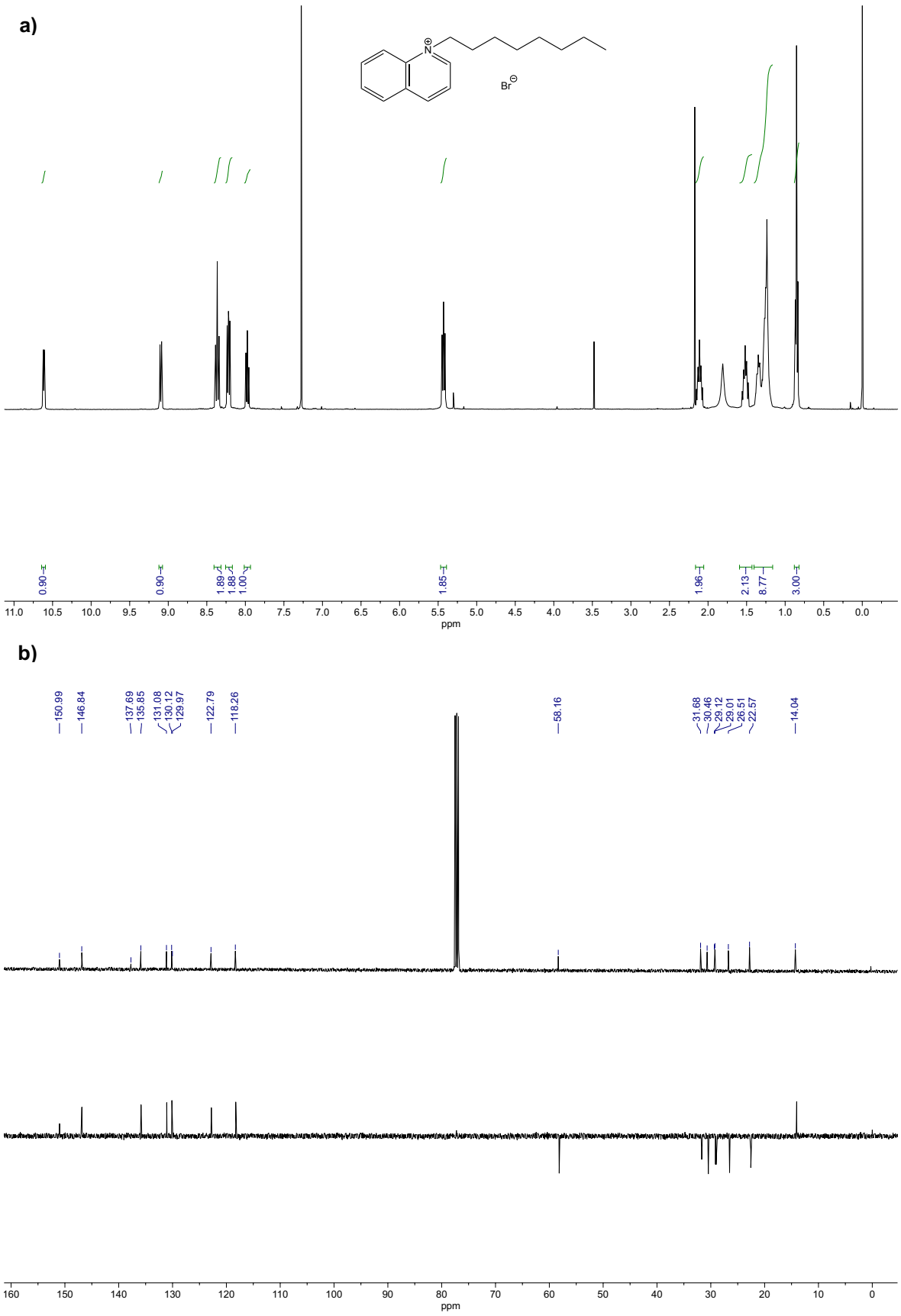

Figure 43. ^{1}H NMR **(a)**, ^{13}C NMR and DEPT135 **(b)** spectra of [C_8QBr].

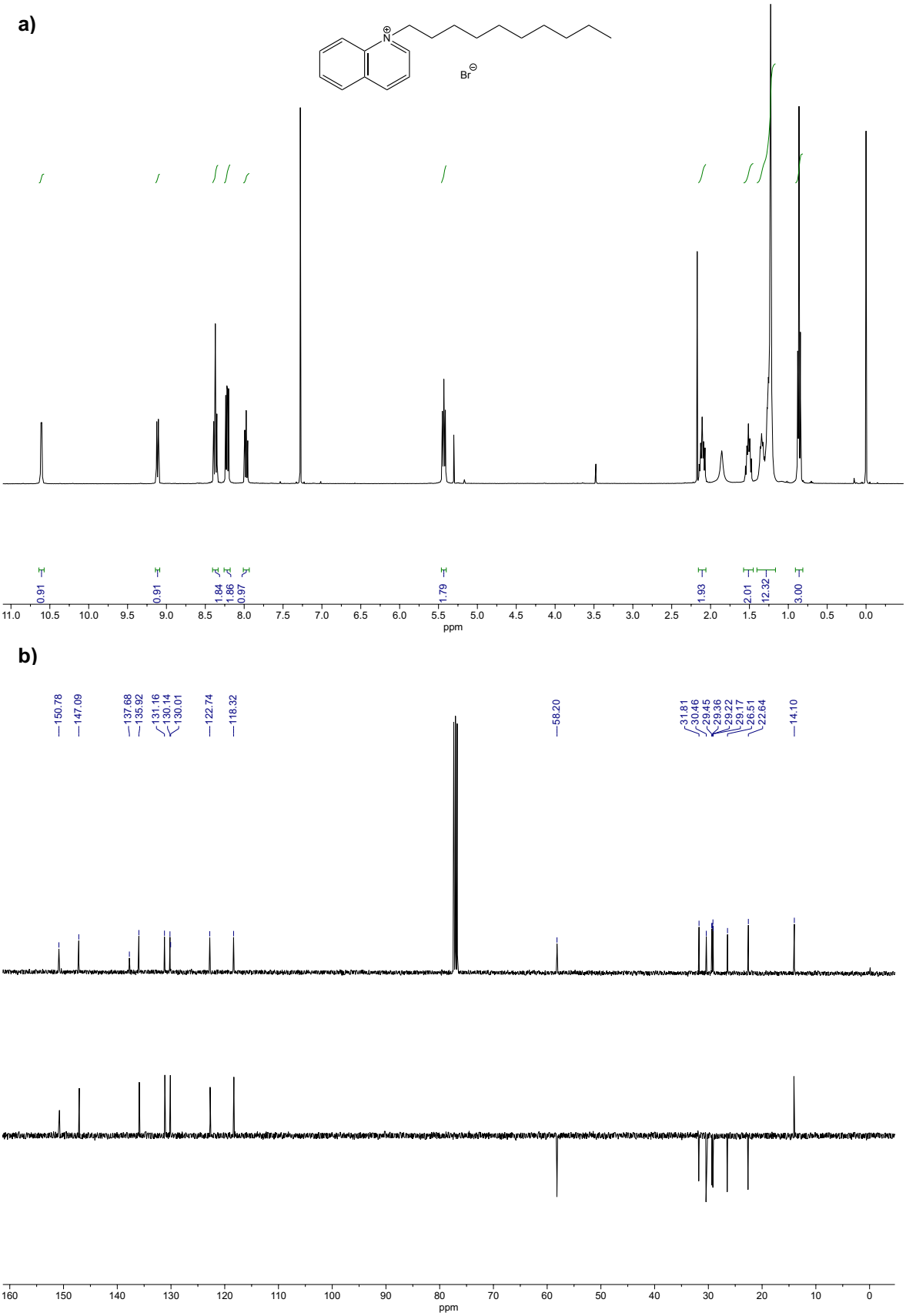

Figure 44. ^{1}H NMR **(a)**, ^{13}C NMR and DEPT135 **(b)** spectra of [C_{10}QBr].

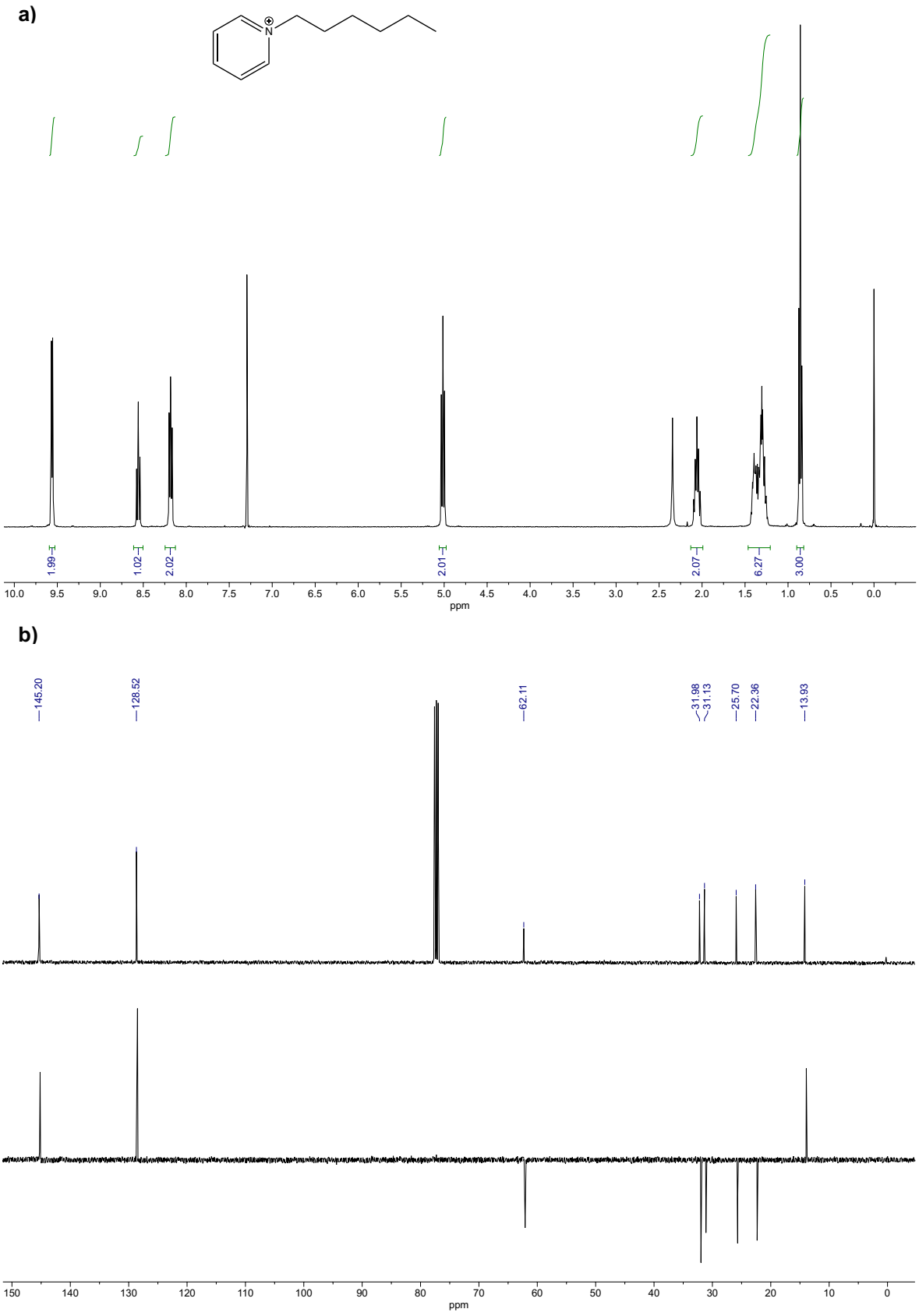

Figure 45. ^{1}H NMR **(a)**, ^{13}C NMR and DEPT135 **(b)** spectra of [C_6PyrBr].

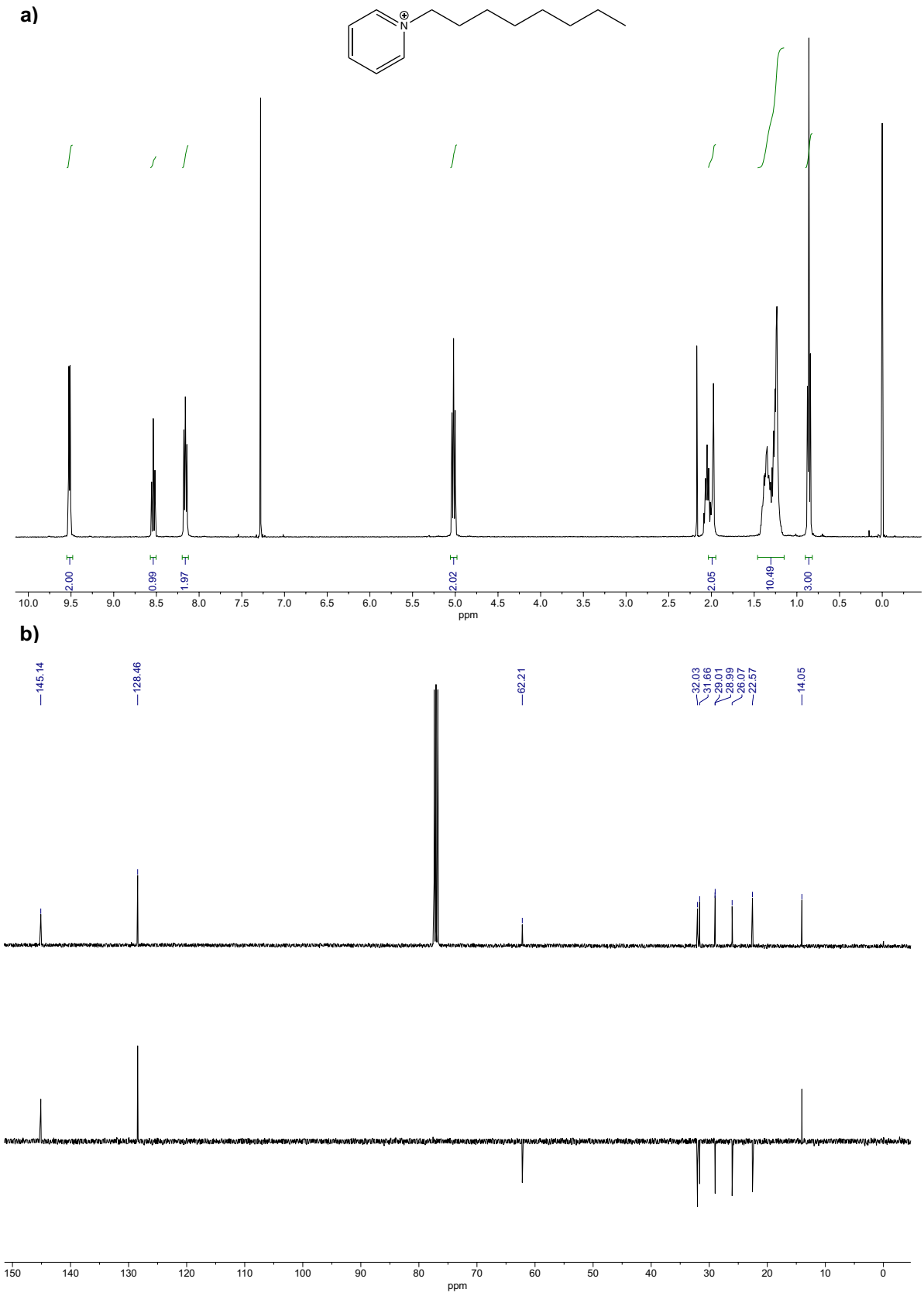

Figure 46. ^{1}H NMR **(a)**, ^{13}C NMR and DEPT135 **(b)** spectra of [C_8PyrBr].

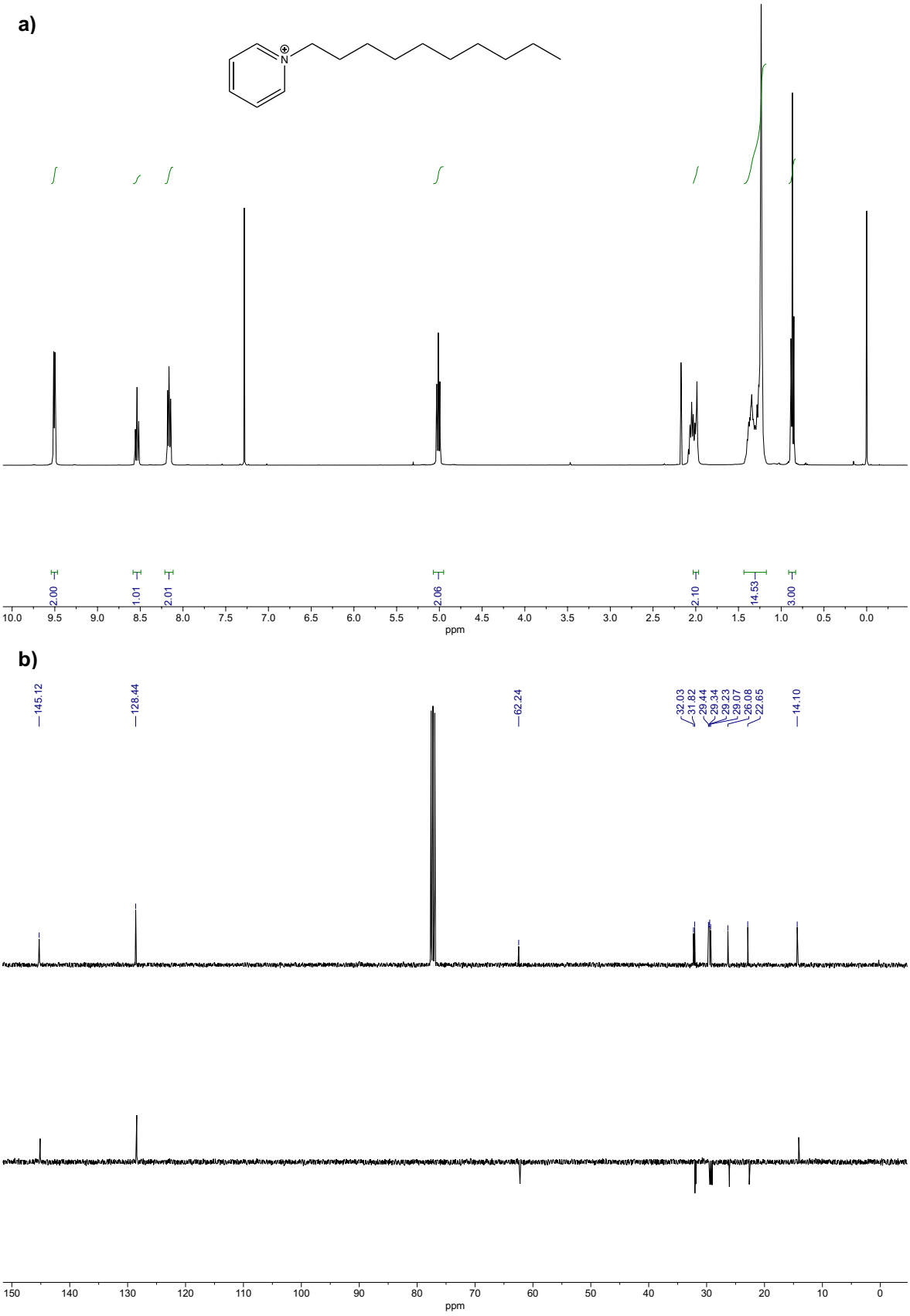

Figure 47. ^{1}H NMR **(a)**, ^{13}C NMR and DEPT135 **(b)** spectra of [C_{10}PyrBr].

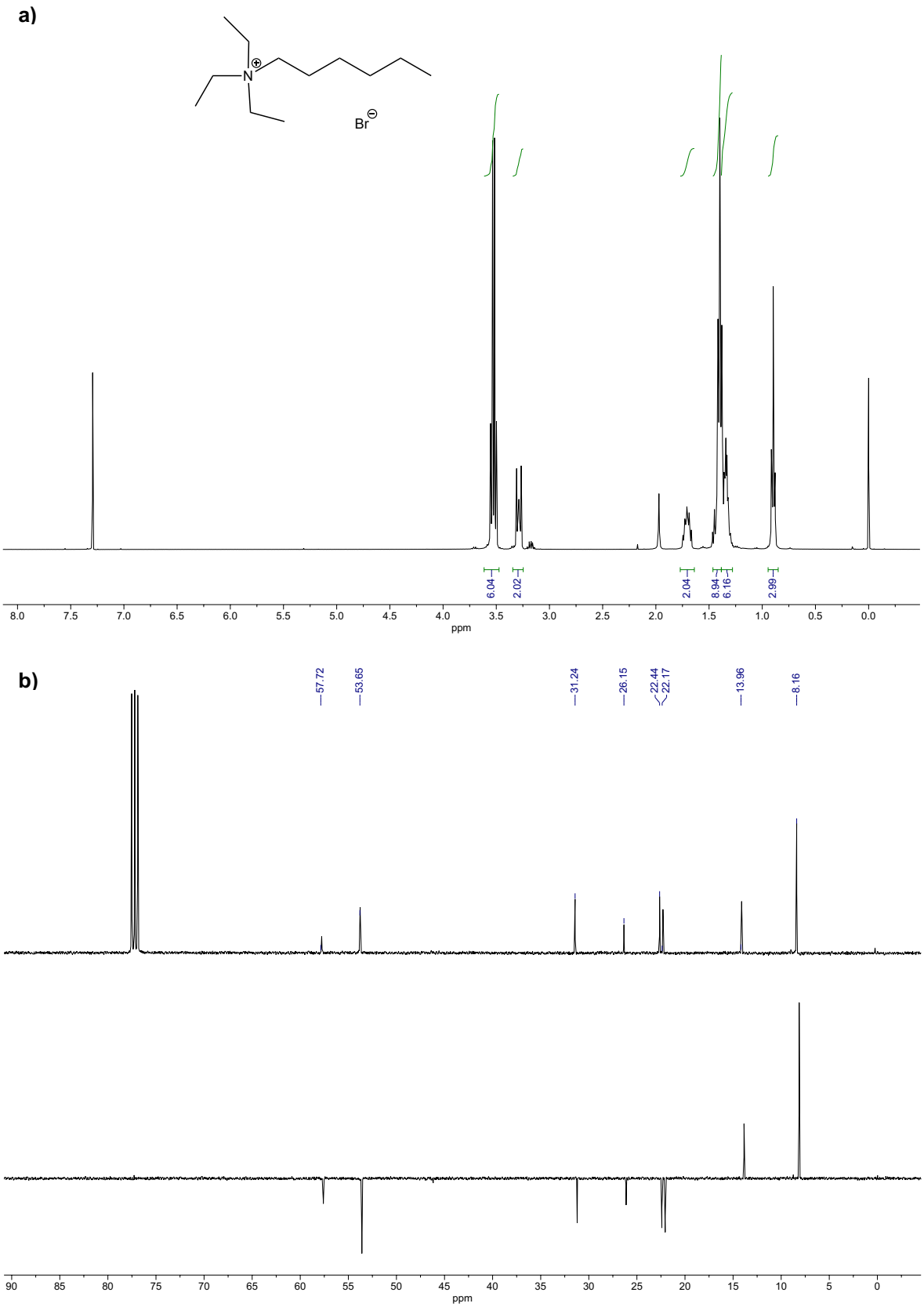

Figure 48. ^{1}H NMR **(a)**, ^{13}C NMR and DEPT135 **(b)** spectra of [C_6TEABr].

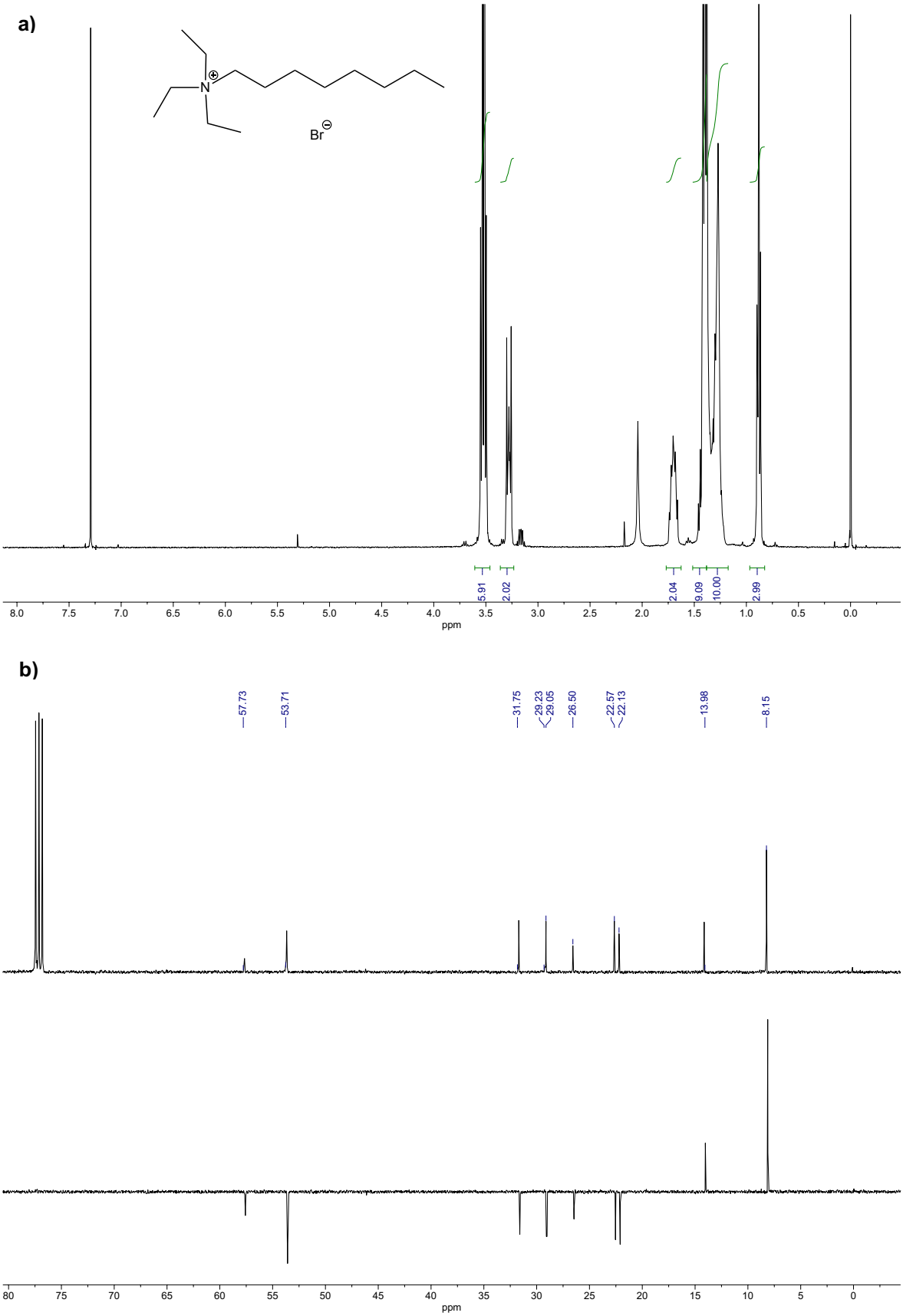

Figure 49. ^{1}H NMR **(a)**, ^{13}C NMR and DEPT135 **(b)** spectra of [C_8TEABr].

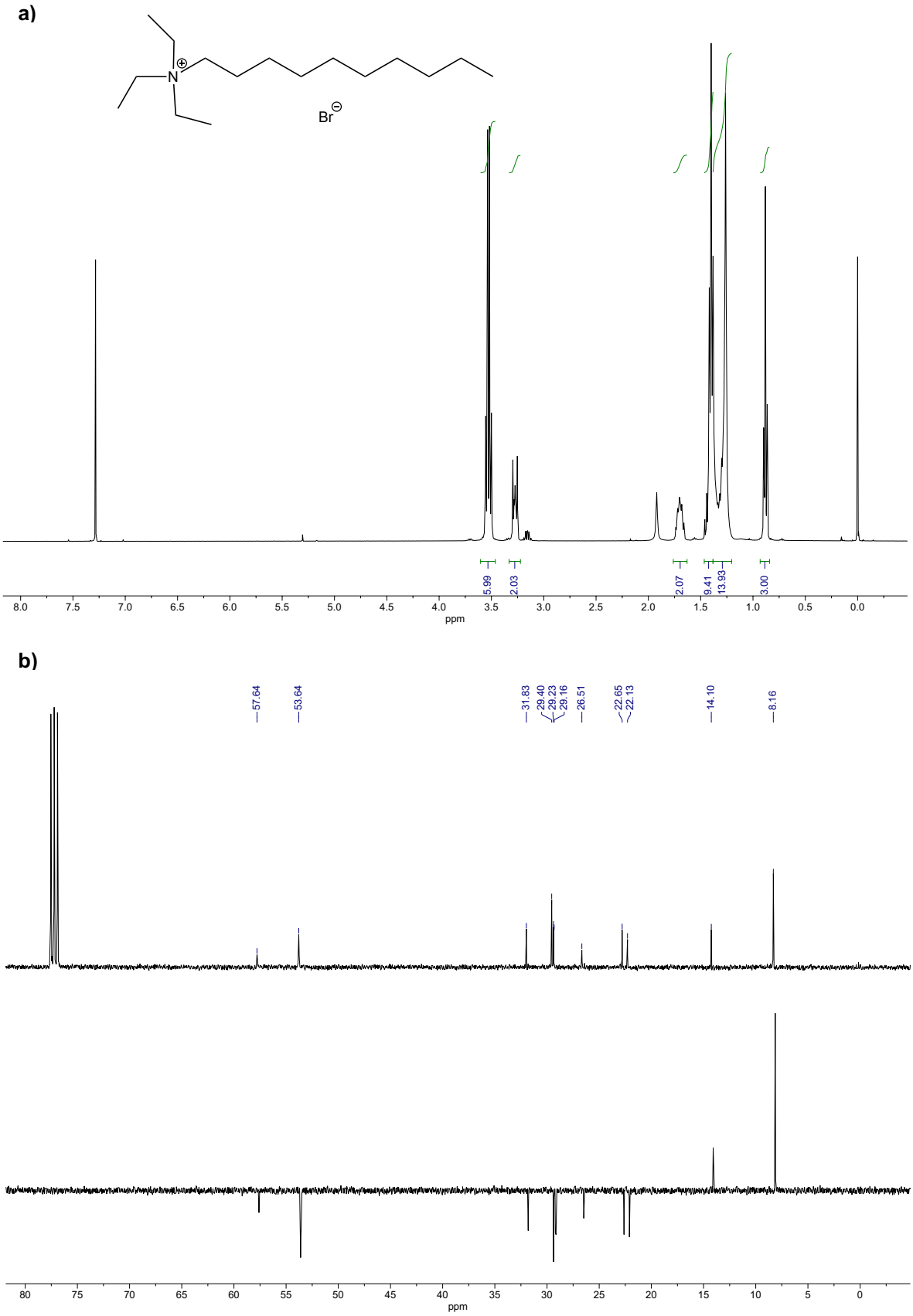

Figure 50. ^{1}H NMR **(a)**, ^{13}C NMR and DEPT135 **(b)** spectra of [C_{10}TEABr].

APPENDIX II – Human cell Studies

Table 9. Measurement of reactive species production in HK-2 cells after 24 h of exposure with the compounds [C_6TPPBr], [C_8TPPBr], [C_{10}TPPBr], [C_{10}IQBr], [C_{10}mPyrBr] and [C_{10}QBr]. Statistical comparisons were made using one-way ANOVA. In all cases, *p* values lower than 0.05 were considered significant (*p < 0.005, **p < 0.01, ***p < 0.001, ****p < 0.0001).

DCFH-DA assay						
	[C_6TPPBr]	**[C_8TPPBr]**	**[C_{10}TPPBr]**	**[C_{10}IQBr]**	**[C_{10}mPyrBr]**	**[C_{10}QBr]**
C (µg/mL)	Mean ± SD (% vs control)	Mean ± SD (% vs control)	Mean ± SD (% vs control)	Mean ± SD (% vs control)	Mean ± SD (% vs control)	Mean ± SD (% vs control)
0.00	100.00 ± 6.18 %	100.00 ± 5.01 %	100.00 ± 3.40 %	100.00 ± 4.07 %	100.00 ± 3.10 %	100.00 ± 5.46 %
2.00	98.17 ± 3.90 % (ns)	104.98 ± 8.46 % (ns)	111.69 ± 6.13 % (ns)	90.54 ± 5.01 % (ns)	94.54 ± 8.11 % (ns)	98.17 ± 6.71 % (ns)
4.00	106.42 ± 5.28 % (ns)	114.15 ± 7.90 % (*)	141.17 ± 14.23 % (****)	92.44 ± 6.24 % (ns)	101.49 ± 11.26 % (ns)	107.11 ± 8.48 % (ns)
8.00	106.82 ± 6.24 % (ns)	116.07 ± 7.29 % (**)	138.32 ± 6.65 % (****)	96.80 ± 3.42 % (ns)	103.84 ± 9.50 % (ns)	116.27 ± 10.59 % (**)
16.00	113.43 ± 8.93 % (*)	127.11 ± 10.09 % (****)	179.65 ± 17.33 % (****)	103.36 ± 16.15 % (ns)	104.10 ± 11.04 % (ns)	125.77 ± 3.00 % (****)
32.00	118.23 ± 11.73 % (***)	139.02 ± 9.58 % (****)	192.92 ± 17.72 % (****)	94.02 ± 2.76 % (ns)	104.99 ± 3.45 % (ns)	135.89 ± 4.12 % (****)
64.00	116.25 ± 8.18 % (**)	155.11 ± 6.62 % (****)	235.90 ± 19.48 % (****)	111.18 ± 15.13 % (ns)	114.43 ± 8.52 % (**)	170.43 ± 6.88 % (****)
90.00	126.36 ± 16.94 % (****)	173.30 ± 12.61 % (****)	273.26 ± 27.01 % (****)	112.81 ± 5.62 % (ns)	121.29 ± 7.48 % (****)	210.05 ± 17.77 % (****)
128.00	132.16 ± 10.73 % (****)	187.58 ± 12.70 % (****)	252.75 ± 23.63 % (****)	125.25 ± 17.77 % (****)	126.52 ± 8.39 % (****)	210.78 ± 11.84 % (****)

Table 10. Evaluation of metabolic activity of HK-2 cells after 24 h of exposure with the compounds [C_6TPPBr], [C_8TPPBr], [C_{10}TPPBr], [C_{10}IQBr], [C_{10}mPyrBr] and [C_{10}QBr]. Statistical comparisons were made using one-way ANOVA. In all cases, *p* values lower than 0.05 were considered significant (*p < 0.005, **p < 0.01, ***p < 0.001, ****p < 0.0001).

MTT assay						
	[C_6TPPBr]	**[C_8TPPBr]**	**[C_{10}TPPBr]**	**[C_{10}IQBr]**	**[C_{10}mPyrBr]**	**[C_{10}QBr]**
C (µg/mL)	Mean ± SD (% of control)	Mean ± SD (% of control)	Mean ± SD (% of control)	Mean ± SD (% of control)	Mean ± SD (% of control)	Mean ± SD (% of control)
0.00	100.00 ± 2.70 %	100.00 ± 3.44 %	100.00 ± 1.89 %	100.00 ± 3.83 %	100.00 ± 0.90 %	100.00 ± 3.75 %
2.00	76.63 ± 3.85 % (****)	59.71 ± 2.28 % (****)	45.83 ± 2.67 % (****)	72.40 ± 5.51 % (****)	68.56 ± 3.11 % (****)	86.33 ± 4.21 % (****)
4.00	70.77 ± 2.27 % (****)	50.78 ± 1.94 % (****)	26.44 ± 1.07 % (****)	55.84 ± 2.57 % (****)	54.60 ± 2.10 % (****)	76.48 ± 4.10 % (****)
8.00	63.59 ± 3.17 % (****)	33.94 ± 1.25 % (****)	16.87 ± 0.48 % (****)	35.34 ± 1.86 % (****)	36.32 ± 2.41 % (****)	64.02 ± 3.14 % (****)
16.00	56.00 ± 1.06 % (****)	14.92 ± 1.04 % (****)	17.09 ± 0.55 % (****)	19.64 ± 0.74 % (****)	19.12 ± 1.43 % (****)	40.90 ± 2.64 % (****)
32.00	44.24 ± 1.98 % (****)	14.91 ± 0.59 % (****)	16.94 ± 0.45 % (****)	16.66 ± 0.90 % (****)	16.15 ± 1.12 % (****)	22.33 ± 1.95 % (****)
64.00	21.65 ± 1.86 % (****)	15.03 ± 0.58 % (****)	18.20 ± 1.49 % (****)	16.86 ± 1.31 % (****)	16.63 ± 1.15 % (****)	16.99 ± 1.34 % (****)
90.00	16.23 ± 1.84 % (****)	15.70 ± 1.13 % (****)	18.75 ± 0.75 % (****)	17.50 ± 0.80 % (****)	18.73 ± 0.92 % (****)	16.32 ± 1.68 % (****)
128.00	15.42 ± 1.18 % (****)	15.91 ± 1.01 % (****)	18.69 ± 0.63 % (****)	17.42 ± 0.63 % (****)	19.12 ± 1.12 % (****)	16.24 ± 2.13 % (****)

Table 11. Evaluation of lysosomal activity of HK-2 cells after 24 h of exposure with the compounds [C_6TPPBr], [C_8TPPBr], [C_{10}TPPBr], [C_{10}IQBr], [C_{10}mPyrBr] and [C_{10}QBr]. Statistical comparisons were made using one-way ANOVA. In all cases, *p* values lower than 0.05 were considered significant (*p < 0.005, **p < 0.01, ***p < 0.001, ****p < 0.0001).

NR uptake assay						
	[C_6TPPBr]	**[C_8TPPBr]**	**[C_{10}TPPBr]**	**[C_{10}IQBr]**	**[C_{10}mPyrBr]**	**[C_{10}QBr]**
C (µg/mL)	Mean ± SD (% of control)	Mean ± SD (% of control)	Mean ± SD (% of control)	Mean ± SD (% of control)	Mean ± SD (% of control)	Mean ± SD (% of control)
0.00	100.00 ± 4.14 %	100.00 ± 7.63 %	100.00 ± 6.07 %	100.00 ± 5.71 %	100.00 ± 4.62 %	100.00 ± 2.62 %
2.00	67.07 ± 4.23 % (****)	65.33 ± 6.53 % (****)	56.47 ± 4.76 % (****)	35.00 ± 2.54 % (****)	78.36 ± 3.83 % (****)	45.04 ± 2.55 % (****)
4.00	67.55 ± 6.82 % (****)	66.53 ± 7.71 % (****)	26.49 ± 4.05 % (****)	18.61± 1.49 % (****)	62.55 ± 3.78 % (****)	24.06 ± 2.49 % (****)
8.00	66.01 ± 4.18 % (****)	44.73 ± 5.96 % (****)	15.74 ± 3.84 % (****)	15.55 ± 2.36 % (****)	36.32 ± 2.19 % (****)	14.96 ± 1.44 % (****)
16.00	58.07 ± 5.04 % (****)	21.06 ± 5.38 % (****)	15.50 ± 2.30 % (****)	14.07 ± 1.99 % (****)	20.81 ± 1.97 % (****)	12.25 ± 2.09 % (****)
32.00	40.86 ± 3.65 % (****)	21.92 ± 4.51 % (****)	15.78 ± 3.18 % (****)	14.16 ± 1.98 % (****)	16.56 ± 2.26 % (****)	11.18 ± 1.37 % (****)
64.00	25.68 ± 5.90 % (****)	27.14 ± 8.26 % (****)	16.20 ± 2.51 % (****)	13.64 ± 1.90 % (****)	13.25 ± 1.88 % (****)	11.29 ± 1.62 % (****)
90.00	22.80 ± 4.88 % (****)	24.62 ± 3.55 % (****)	17.29 ± 1.98 % (****)	14.29 ± 1.47 % (****)	14.76 ± 3.13 % (****)	13.24 ± 1.32 % (****)
128.00	22.00 ± 4.15 % (****)	27.14 ± 10.29 % (****)	16.34 ± 2.84 % (****)	13.69 ± 1.23 % (****)	14.07 ± 2.13 % (****)	13.63 ± 1.27 % (****)

Table 12. Evaluation of cell density of HK-2 cells after 24 h of exposure with the compounds [C_6TPPBr], [C_8TPPBr], [C_{10}TPPBr], [C_{10}IQBr], [C_{10}mPyrBr] and [C_{10}QBr]. Statistical comparisons were made using one-way ANOVA. In all cases, *p* values lower than 0.05 were considered significant (*p < 0.005, **p < 0.01, ***p < 0.001, ****p < 0.0001).

SRB assay						
	[C_6TPPBr]	**[C_8TPPBr]**	**[C_{10}TPPBr]**	**[C_{10}IQBr]**	**[C_{10}mPyrBr]**	**[C_{10}QBr]**
C (µg/mL)	Mean ± SD (% of control)	Mean ± SD (% of control)	Mean ± SD (% of control)	Mean ± SD (% of control)	Mean ± SD (% of control)	Mean ± SD (% of control)
0.00	100.00 ± 8.09 %	100.00 ± 7.94 %	100.00 ± 8.66 %	100.00 ± 6.66 %	100.00 ± 3.66 %	100.00 ± 3.38 %
2.00	69.20 ± 6.99 % (****)	61.48 ± 7.29 % (****)	49.55 ± 4.71 % (****)	52.51 ± 11.61 % (****)	76.72 ± 7.80 % (****)	52.54 ± 8.40 % (****)
4.00	66.20 ± 5.38 % (****)	58.60 ± 5.02 % (****)	33.16 ± 6.50 % (****)	37.76 ± 8.70 % (****)	63.86 ± 4.27 % (****)	37.40 ± 3.74 % (****)
8.00	61.14 ± 5.06 % (****)	41.93 ± 4.22 % (****)	24.84 ± 1.77 % (****)	35.66 ± 8.89 % (****)	43.86 ± 4.59 % (****)	35.29 ± 2.87 % (****)
16.00	53.68 ± 4.13 % (****)	25.28 ± 2.73 % (****)	25.75 ± 1.81 % (****)	33.81 ± 3.52 % (****)	33.72 ± 4.19 % (****)	34.62 ± 3.16 % (****)
32.00	41.24 ± 3.82 % (****)	23.80 ± 2.46 % (****)	25.23 ± 1.37 % (****)	32.15 ± 2.27 % (****)	30.66 ± 4.08 % (****)	33.95 ± 3.26 % (****)
64.00	26.10 ± 3.55 % (****)	23.89 ± 2.26 % (****)	25.50 ± 2.00 % (****)	33.39 ± 2.24 % (****)	29.79 ± 3.45 % (****)	34.06 ± 3.44 % (****)
90.00	24.55 ± 3.95 % (****)	26.31 ± 6.27 % (****)	26.16 ± 1.63 % (****)	33.59 ± 1.75 % (****)	30.73 ± 4.27 % (****)	39.16 ± 4.97 % (****)
128.00	22.26 ± 3.50 % (****)	23.86 ± 3.39 % (****)	25.99 ± 3.09 % (****)	31.79 ± 2.63 % (****)	33.64 ± 8.71 % (****)	37.06 ± 3.35 % (****)

Table 13. Measurement of reactive species production in HepG2 cells after 24 h of exposure with the compounds [C_6TPPBr], [C_8TPPBr], [C_{10}TPPBr], [C_{10}IQBr], [C_{10}mPyrBr] and [C_{10}QBr]. Statistical comparisons were made using one-way ANOVA. In all cases, *p* values lower than 0.05 were considered significant (**p* < 0.005, ***p* < 0.01, ****p* < 0.001, *****p* < 0.0001).

DCFH-DA assay						
	[C_6TPPBr]	**[C_8TPPBr]**	**[C_{10}TPPBr]**	**[C_{10}IQBr]**	**[C_{10}mPyrBr]**	**[C_{10}QBr]**
C (µg/mL)	Mean ± SD (% vs control)	Mean ± SD (% vs control)	Mean ± SD (% vs control)	Mean ± SD (% vs control)	Mean ± SD (% vs control)	Mean ± SD (% vs control)
0.00	100.00 ± 0.94 %	100.00 ± 1.01 %	100.00 ± 0.91 %	100.00 ± 4.23 %	100.00 ± 1.13 %	100.00 ± 1.54 %
2.00	96.27 ± 4.84 % (**)	94.08 ± 1.34 % (****)	98.45 ± 6.10 % (ns)	96.13 ± 4.07 % (ns)	101.55 ± 1.55 % (ns)	100.65 ± 2.45 % (ns)
4.00	93.90 ± 1.12 % (****)	95.45 ± 1.90 % (****)	100.33 ± 8.20 % (ns)	96.75 ± 4.93 % (ns)	102.20 ± 2.87 % (ns)	102.35 ± 2.36 % (ns)
8.00	95.61 ± 2.42 % (***)	96.14 ± 1.53 % (***)	97.29 ± 7.18 % (ns)	96.29 ± 4.81 % (ns)	103.25 ± 2.44 % (**)	104.42 ± 2.96 % (***)
16.00	94.59 ± 1.51 % (****)	94.90 ± 1.50 % (****)	99.79 ± 7.21 % (ns)	96.80 ± 5.13 % (ns)	102.52 ± 1.71 % (ns)	107.86 ± 1.92 % (****)
32.00	92.93 ± 1.64 % (****)	97.39 ± 2.33 % (*)	101.05 ± 6.39 % (ns)	95.72 ± 5.26 % (ns)	102.00 ± 1.86 % (ns)	113.69 ± 1.23 % (****)
64.00	93.94 ± 1.49 % (****)	98.73 ± 1.58 % (ns)	105.21 ± 6.23 % (ns)	97.55 ± 3.95 % (ns)	102.53 ± 1.85 % (ns)	122.97 ± 1.21 % (****)
90.00	95.02 ± 1.63 % (***)	104.32 ± 2.73 % (****)	112.77 ± 7.43 % (***)	99.72 ± 4.83 % (ns)	103.36 ± 1.42 % (**)	143.39 ± 2.45 % (****)
128.00	95.40 ± 2.51 % (***)	104.09 ± 1.66 % (****)	113.91 ± 5.74 % (***)	99.56 ± 6.19 % (ns)	104.87 ± 2.47 % (****)	138.83 ± 1.88 % (****)

Table 14. Evaluation of metabolic activity of HepG2 cells after 24 h of exposure with the compounds [C_6TPPBr], [C_8TPPBr], [C_{10}TPPBr], [C_{10}IQBr], [C_{10}mPyrBr] and [C_{10}QBr]. Statistical comparisons were made using one-way ANOVA. In all cases, *p* values lower than 0.05 were considered significant (**p* < 0.005, ***p* < 0.01, ****p* < 0.001, *****p* < 0.0001).

MTT assay						
	[C_6TPPBr]	**[C_8TPPBr]**	**[C_{10}TPPBr]**	**[C_{10}IQBr]**	**[C_{10}mPyrBr]**	**[C_{10}QBr]**
C (µg/mL)	Mean ± SD (% of control)	Mean ± SD (% of control)	Mean ± SD (% of control)	Mean ± SD (% of control)	Mean ± SD (% of control)	Mean ± SD (% of control)
0.00	100.00 ± 6.04 %	100.00 ± 5.97 %	100.00 ± 4.79 %	100.00 ± 4.83 %	100.00 ± 3.55 %	100.00 ± 5.40 %
2.00	63.97 ± 5.11 % (****)	51.53 ± 4.89 % (****)	51.34 ± 4.63 % (****)	71.06 ± 4.37 % (****)	82.49 ± 6.88 % (****)	61.49 ± 3.47 % (****)
4.00	59.60 ± 4.34 % (****)	51.26 ± 4.37 % (****)	38.53 ± 5.23 % (****)	58.15 ± 2.62 % (****)	74.30 ± 2.41 % (****)	55.75 ± 4.84 % (****)
8.00	58.67 ± 4.88 % (****)	41.49 ± 5.06 % (****)	8.65 ± 0.57 % (****)	46.58 ± 3.31 % (****)	68.01 ± 3.65 % (****)	41.32 ± 3.01 % (****)
16.00	54.91 ± 3.45 % (****)	8.21 ± 0.69 % (****)	8.61 ± 0.22 % (****)	31.25 ± 2.97 % (****)	55.71 ± 4.06 % (****)	19.44 ± 1.39 % (****)
32.00	41.90 ± 3.45 % (****)	7.81 ± 0.70 % (****)	8.33 ± 0.28 % (****)	8.57 ± 0.58 % (****)	44.93 ± 1.28 % (****)	7.98 ± 0.92 % (****)
64.00	12.85 ± 0.76 % (****)	8.00 ± 0.95 % (****)	8.31 ± 0.25 % (****)	8.05 ± 0.56 % (****)	24.12 ± 2.89 % (****)	8.01 ± 1.15 % (****)
90.00	8.20 ± 0.72 % (****)	7.70 ± 0.81 % (****)	8.42 ± 0.58 % (****)	7.78 ± 0.40 % (****)	11.96 ± 1.52 % (****)	7.55 ± 0.90 % (****)
128.00	7.82 ± 0.67 % (****)	7.29 ± 0.79 % (****)	8.95 ± 0.70 % (****)	7.46 ± 0.45 % (****)	7.82 ± 0.67 % (****)	7.92 ± 0.97 % (****)

Table 15. Evaluation of lysosomal activity of HepG2 cells after 24 h of exposure with the compounds [C_6TPPBr], [C_8TPPBr], [C_{10}TPPBr], [C_{10}IQBr], [C_{10}mPyrBr] and [C_{10}QBr]. Statistical comparisons were made using one-way ANOVA. In all cases, *p* values lower than 0.05 were considered significant (*p < 0.005, **p < 0.01, ***p < 0.001, ****p < 0.0001).

NR uptake assay						
	[C_6TPPBr]	**[C_8TPPBr]**	**[C_{10}TPPBr]**	**[C_{10}IQBr]**	**[C_{10}mPyrBr]**	**[C_{10}QBr]**
C (µg/mL)	Mean ± SD (% of control)	Mean ± SD (% of control)	Mean ± SD (% of control)	Mean ± SD (% of control)	Mean ± SD (% of control)	Mean ± SD (% of control)
0.00	100.00 ± 9.59 %	100.00 ± 4.36 %	100.00 ± 6.73 %	100.00 ± 8.99 %	100.00 ± 9.46 %	100.00 ± 8.32 %
2.00	62.05 ± 5.53 % (****)	50.04 ± 5.66 % (****)	57.13 ± 7.93 % (****)	81.79 ± 7.36 % (****)	89.73 ± 9.87 % (ns)	71.14 ± 11.52 % (****)
4.00	51.12 ± 4.29 % (****)	53.98 ± 4.21 % (****)	50.13 ± 6.89 % (****)	75.53 ± 6.14 % (****)	90.81 ± 11.51 % (ns)	71.70 ± 8.14 % (****)
8.00	52.74 ± 4.81 % (****)	42.78 ± 3.07 % (****)	27.71 ± 14.69 % (****)	68.66 ± 6.07 % (****)	80.10 ± 10.63 % (***)	72.38 ± 7.72 % (****)
16.00	51.84 ± 5.41 % (****)	11.86 ± 2.17 % (****)	36.47 ± 16.21 % (****)	64.10 ± 9.77 % (****)	89.68 ± 10.58 % (ns)	64.57 ± 4.78 % (****)
32.00	42.10 ± 6.90 % (****)	12.58 ± 2.86 % (****)	21.96 ± 6.21 % (****)	29.43 ± 8.37 % (****)	85.91 ± 7.20 % (*)	21.86 ± 7.05 % (****)
64.00	18.47 ± 6.16 % (****)	13.24 ± 1.77 % (****)	25.73 ± 13.07 % (****)	23.98 ± 4.41 % (****)	52.71 ± 6.96 % (****)	21.21 ± 5.06 % (****)
90.00	20.79 ± 10.87 % (****)	17.58 ± 14.37 % (****)	15.95 ± 4.91 % (****)	30.33 ± 8.25 % (****)	34.54 ± 8.28 % (****)	28.51 ± 7.24 % (****)
128.00	18.59 ± 8.13 % (****)	14.23 ± 5.75 % (****)	21.22 ± 5.64 % (****)	28.83 ± 6.46 % (****)	28.90 ± 7.67 % (****)	22.29 ± 4.19 % (****)

Table 16. Evaluation of cell density of HepG2 cells after 24 h of exposure with the compounds [C_6TPPBr], [C_8TPPBr], [C_{10}TPPBr], [C_{10}IQBr], [C_{10}mPyrBr] and [C_{10}QBr]. Statistical comparisons were made using one-way ANOVA. In all cases, *p* values lower than 0.05 were considered significant (*p < 0.005, **p < 0.01, ***p < 0.001, ****p < 0.0001).

SRB assay						
	[C_6TPPBr]	**[C_8TPPBr]**	**[C_{10}TPPBr]**	**[C_{10}IQBr]**	**[C_{10}mPyrBr]**	**[C_{10}QBr]**
C (µg/mL)	Mean ± SD (% of control)	Mean ± SD (% of control)	Mean ± SD (% of control)	Mean ± SD (% of control)	Mean ± SD (% of control)	Mean ± SD (% of control)
0.00	100.00 ± 12.72 %	100.00 ± 14.82 %	100.00 ± 10.31 %	100.00 ± 5.61 %	100.00 ± 5.84 %	100.00 ± 9.83 %
2.00	61.91 ± 6.00 % (****)	48.09 ± 6.72 % (****)	45.76 ± 5.65 % (****)	75.64 ± 13.14 % (****)	76.09 ± 10.92 % (****)	64.39 ± 11.90 % (****)
4.00	52.81 ± 5.55 % (****)	49.95 ± 5.07 % (****)	49.70 ± 11.16 % (****)	78.06 ± 10.64 % (***)	84.50 ± 14.14 % (*)	60.90 ± 10.17 % (****)
8.00	57.67 ± 15.51 % (****)	47.18 ± 14.85 % (****)	40.69 ± 7.39 % (****)	78.63 ± 12.58 % (***)	74.42 ± 10.48 % (****)	62.75 ± 9.22 % (****)
16.00	51.83 ± 4.62 % (****)	15.47 ± 2.31 % (****)	27.60 ± 6.77 % (****)	77.26 ± 11.68 % (***)	74.41 ± 7.62 % (****)	54.83 ± 8.93 % (****)
32.00	37.39 ± 5.79 % (****)	19.99 ± 12.18 % (****)	17.63 ± 4.42 % (****)	29.14 ± 6.25 % (****)	66.47 ± 8.63 % (****)	43.61 ± 23.12 % (****)
64.00	14.93 ± 2.20 % (****)	17.14 ± 3.24 % (****)	18.45 ± 4.49 % (****)	40.14 ± 15.18 % (****)	60.29 ± 12.26 % (****)	27.79 ± 5.64 % (****)
90.00	13.26 ± 1.96 % (****)	15.68 ± 4.73 % (****)	18.88 ± 5.34 % (****)	34.98 ± 9.86 % (****)	34.06 ± 7.61 % (****)	28.17 ± 7.94 % (****)
128.00	15.08 ± 3.33 % (****)	14.00 ± 4.06 % (****)	18.22 ± 5.93 % (****)	31.54 ± 8.05 % (****)	36.58 ± 14.98 % (****)	26.92 ± 4.17 % (****)